

RECOGNIZED BY:



HIGHER EDUCATION COMMISSION OF PAKISTAN

INDEXING




Aims and Scope

Futuristic Biotechnology (FBT) is a bi-annual journal that publishes broad-spectrum publications with close connection to experimental activity in Biological and Biotechnology fields. FBT is intended for exploring the molecular mechanisms that support key biological processes in the fields of biochemistry, cellular biosciences, molecular biology, plant biotechnology, genetic engineering, nanotechnology, and bioinformatics. Furthermore, it also covers topics related to immunology, antibody production, protein purification studies, primer synthesis, DNA sequencing, production of transgenic animal models, insect resistant crop varieties and edible and ornamental plant varieties.

Types of Articles

- Research Papers
- Short Communications
- Review and Mini-reviews
- Commentaries
- Perspectives and Opinion
- Meta Analysis
- Case Reports
- Case Studies
- Case Control Studies

Reviews on recent progress in biotechnology are commissioned by the editors. The purpose of the Futuristic Biotechnology is to publish scientific and technical research papers to bring attention of International Researchers, Scientists, Academicians, and Health Care Professionals towards recent advancements in food sciences. The articles are collected in the form of reviews, original studies, clinical studies among others. It may serve as a global platform for scientists in relevant fields to connect and share ideas mutually. This journal is open to all the research professionals whose work fall within our scope. Submissions are welcome and may be submitted here.

 editor@fbtjournal.com

Title

The title of the paper should provide a concise statement of the contents of the paper. A good title is very important and will attract readers and facilitate retrieval by online searches, thereby helping to maximize citations. The title should include topical keywords and allude to the interesting conclusions of the paper. A title that emphasizes the main conclusions, or poses a question, has more impact than one that just describes the nature of the study.

Running Head

Running head should be added in the header along with the page numbers.

Type of Article

Research Article/ Case Report/ Review Article/ Opinion/ Short Communication/ Mini Review/ Letter to Editor.

Running Title: A short version of the paper title.

Keywords: The major keywords used in the article have to be mentioned.

Authors

List here all author names, Author¹, Author² and Author³

¹Author department, University, Country

²Author department, University, Country

³Author department, University, Country

***Corresponding Author**

Author name, Affiliation, Department Name, University Name, Address, City, State, Country, E-mail.

Abstract

Abstract should include a brief content of the article. It should be structured and not more than 250 words. It should include following sub headings: Objective, Methods, Results, Conclusions.

Abbreviations

If there are any abbreviations in the article they have to be mentioned.

INTRODUCTION

Provide a context or background for the study (i.e., the nature of the problem and its significance). State the specific purpose or research objective or hypothesis tested by the study or observation; the research objective is often more sharply focused when stated as a question. Both the main and secondary objectives should be made clear, and any pre-specified subgroup analyses should be described. Give only strictly pertinent references and do not include data or conclusions from the work being reported.

METHODS

The Methods section should include only information that was available at the time the or plan of the protocol. All information gathered during the conduct of study should be included in the result section.

Study Design, Inclusion / Exclusion Criteria, Data Collection Procedure and Statistical Analysis.

RESULTS

Present your results in logical sequence in the text, tables and illustrations, giving the main or most important findings first.

Do not repeat data that is already present in tables and illustrations. emphasize or summarize only important observations. When data are summarized in the Results section, give numeric results not only as derivatives (for example, percentages) but also as the absolute numbers from which the derivatives were calculated, and specify the statistical methods used to analyze them. Table font should be 10 and caption should be above the table and below the figure.

Data should not be duplicated in both figures and tables. The maximum limit of tables and figures should not exceed more than 4. Mention the findings of the study in paragraph, while mentioning figure and table number in text in sequential order.

TABLE

Table should not be copy pasted or in picture form.

DISCUSSION

Discuss your findings by comparing your results with other literature.

REFERENCES

References should not be less than 20.

In text references should be in number style. For Example [1].

Follow the Pubmed Referencing style.

Provide the DOI link.

Example

Cook NR, Rosner BA, Hankinson SE, Colditz GA. Mammographic screening and risk factors for breast cancer. American Journal of Epidemiology. 2009 Dec;170(11):1422-32. doi: 10.1093/aje/kwp304.

If there are more than six authors, write *et al.* after the first six names.

CONCLUSION(S)

Conclusion should elucidate how the results communicate to the theory presented as the basis of the study and provide a concise explanation of the allegation of the findings.

ACKNOWLEDGEMENT

Provide the list of individuals who contributed in the work and grant details where applicable.

Plagiarism policy

Similarity index should be less than 19, and less than 5 from individual sources.

Authorship Letter

Signed authorship letter by all authors including their current department, University, City, Country, Email.

Declaration Form

Signed declaration form submit by corresponding author.

The submission of article should include: manuscript according to journal guidelines, authorship letter, declaration form. It should be submitted to the following email id: editor@fbtjournal.com



EDITORIAL BOARD

Editor-In-Chief

Prof. Dr. Riffat Mehboob

Professor/Director Research

National Heart, Lung and Blood Institute, National
Institute of Health, Bethesda, United States

Lahore Medical Research Center^{LLP}, Lahore, Pakistan

riffat.pathol@gmail.com

Editor

Prof. Dr. Fridoon Jawad Ahmed Ph.D

Professor

University of Health Sciences,
Lahore, Pakistan

Editor

Prof. Dr. Akram Tariq, Ph.D

Professor

Higher Education Department
Punjab (HED), Lahore

Managing Editor

Mr. Khurram Mehboob

Lahore Medical Research Center^{LLP},
Lahore, Pakistan

Production Editor

Mr. Zeeshan Mehboob

Lahore Medical Research Center^{LLP},
Lahore, Pakistan

Biostatistician

Mrs. Humaira Waseem

Fatima Jinnah Medical University,
Lahore, Pakistan

ADVISORY BOARD

Dr. Muhammad Ikram Ullah, Ph.D

Jouf University, Saudi Arabia

Dr. Imran Shahid, Ph.D

Umm Al-Qura University,
Makkah, Saudi Arabia

Dr. Humera Kausar, Ph.D

Kinnaird College for Women
University, Lahore, Pakistan

Dr. Nusrat Jabeen, Ph.D

University of Karachi, Karachi,
Pakistan

VOL. 04 ISSUE. 03

ISSN (E) 2959-0981
ISSN (P) 2959-0973



**FUTURISTIC
BIOTECHNOLOGY**

EDITORIAL BOARD (INTERNATIONAL)

Dr. rer. nat. Jens Peter von Kries

Leibniz-Forschungsinstitut für
Molekulare Pharmakologie (FMP),
Germany

Dr. Sulaiman Yousafzai, Ph.D

National Institute of Health, United
States of America

Dr. Muhammad Ayaz Anwar

Kyung Hee University, Yongin,
South Korea

Dr. Aditya Mojumdar, Ph.D

University of Victoria, Canada

Amber Hassan, Ph.D*

European School of Molecular
Medicine, Italy

Dr. Dinesh Velayutham, Ph.D

Hammad Bin Khalifa
University, Doha, Qatar

EDITORIAL BOARD (NATIONAL)

Dr. Sumaira Anjum, Ph.D

Kinnaird College for Women
University, Lahore, Pakistan

VOL. 04 ISSUE. 03



TABLE OF CONTENTS

Editorial

Personalized Medicine: The Dawn of a New Era in Healthcare

Fridoan Jawad Ahmed

1

Review Article

Regulation of Intestinal Iron Absorption: Balancing Supply and Demand

Shazia Yaseen, Rai Hamza Akram,
Basit Ali, Komal Zaheer,
Memoona Rafique, Pakeeza
Eman, Namal Fatima, Fazeelat
Kausar, Muhammad Luqman

2

Review Article

A Comprehensive Review of Dengue Fever: Epide- miological Trends, Diagnostic Approaches, Novel Therapeutic Strategies,

Nimra Yousaf, Ahmad Raza,
Nimra Batool, Abubakar Sheikh,
Fiza Babar, Adeeba Ali

10

Review Article

Role of Microbes in the Production of Dairy Products

Muhammad Naeem, Aatif Amin,
Joha Ejaz, Fizza Shahzad, Sehrish
Patras, Khazen Ali Aamir

17

Original Article

Insilico Insights into Resveratrol as a Potential Inhibitor of Mycobacterium Tuberculosis Enoyl-ACP Reductase (InhA) Protein

Obaid Ullah, Nimra Hanif, Ayesha,
Abdul Qayyum Mufti, Fizza Amjad,
Maleeha Manzoor, Esha Jameel,
Sana Fatima

27

Original Article

Optimization of Autosomal STR Markers for Equine Genotyping Using Multiplex PCR

Usama Mustafa, Zaroon, Sana
Shoukat, Juveria, Manzoor
Hussain

34

Original Article

Ultraviolet and Ethyl Methanesulfonate-Induced Mutagenesis in *Aspergillus niger* and *Salmonella typhi* for Enhanced Azoreductase Production in Azo Dyes Bioremediation

Faiza Tariq, Dua Batool, Huda
Rehman, Manam Walait

41

Original Article

Silver Nanoparticle-Integrated Nile Tilapia Skin Improves Healing of Skin Burn Wounds in Sprague Dawley Rats

Nadia Wajid, Sheheryar Ahmad
Khan, Amna Bibi, Sumair Raza,
Fatima Ali

56

Original Article

Antibacterial Activity of Transition Metal Complexes of 2-(2-Hydroxybenzylidene) Hydrazinecarbothioamide

Hafiz Muhammad Ghuffran Qamar,
Tehmina Bashir, Usman Ibrahim,
Adnan Mehmood, Waiza Ansar,
Noor Muhammad, Aygun
Baghirova Alazova

62

VOL. 04 ISSUE. 03

FUTURISTIC BIOTECHNOLOGY

<https://fbtjournal.com/index.php/fbt>

ISSN (E): 2959-0981, (P): 2959-0973

Volume 4, Issue 3 (July-Sep 2024)



Personalized Medicine: The Dawn of a New Era in Healthcare



Fridooun Jawad Ahmad¹

¹University of Health Sciences, Lahore, Pakistan

drfridoon@yahoo.com

ARTICLE INFO

How to Cite:

Ahmed, F. J. (2024). Personalized Medicine: The Dawn of a New Era in Healthcare. *Futuristic Biotechnology*, 4(03). <https://doi.org/10.54393/fbt.v4i03.138>

The landscape of healthcare is transforming with the advent of personalized medicine, an approach that alters medical treatment to each individual's specific characteristics. This paradigm shift is driven by advancements in genomics, molecular biology, and bioinformatics, which have developed a deeper understanding of the genetic and molecular basis of diseases. This new healthcare model is based on precision and individualization, aiming to provide customized healthcare with medical decisions and treatments by considering variability in genes, environment and lifestyle of an individual patient and offer accurate diagnosis, better treatments and prevention plans.

The accomplishment of the Human Genome Project in 2003 was a significant advancement in genomics that provided blueprints of the human genome [1]. Rapid progress in genomic sequencing technologies makes it feasible and cost effective. Advanced sequencing techniques including next-generation sequencing allow a detailed analysis of genetic makeup to locate mutations and genetic predispositions for better treatment decisions. Cancer is caused by genetic heterogeneity and has benefited greatly from genomic insights. Molecular profiling of tumor cells allows the identification of specific genetic mutations involved in cancer pathogenesis. Targeted therapies can then be designed to inhibit these specific molecular pathways, leading to more effective and less toxic treatments compared to traditional chemotherapy. For example, in breast cancer the identification of Human epidermal growth factor receptor 2 (HER2) mutations has led to the development of HER2-targeted therapies to improve treatment [2]. Besides oncology, personalized medicine is making progress in other fields. In cardiology, genetic testing allows identification of patients who are at risk of getting inherited cardiovascular diseases. In pharmacology, pharmacogenomics, the study of correlation between genes and immune response of an individual to drugs helps in designing most effective drugs with the least side effects for each patient. In infectious diseases, genomic sequencing of pathogenic microbes can lead to development of appropriate antimicrobial drugs to prevent outbreaks.

Despite its progress, the implementation of personalized medicine is facing several challenges. The utilization of genomic data in clinical workflows demands significant changes to healthcare setting and training with concerns about data privacy, equal access to diverse populations and the ethical implications of genetic information. Currently, the universal unavailability of sophisticated bioinformatics tools to interpret complex genomic data is also a challenge. Researchers and policymakers must work in to set guidelines and standards for safe use of personalized medicine.

Therefore, personalized medicine is a promising tool, which has revolutionized diagnosis, treatment, and prevention in traditional medicine. Using genomics and molecular biology, we can develop a more precise, predictive, and personalized approach to medicine. This exciting frontier must be navigated with the ultimate goal of improving patient outcomes.

REFERENCES

- [1] Powledge TM. Human genome project completed. *Genome Biology*. 2003 Apr; 4(1): spotlight-20030415. doi: 10.1186/gb-spotlight-20030415-01.
- [2] Kunte S, Abraham J, Montero AJ. Novel HER2-targeted therapies for HER2-positive metastatic breast cancer. *Cancer*. 2020 Oct; 126(19): 4278-88. doi:10.1002/cncr.33102.



FUTURISTIC BIOTECHNOLOGY

<https://fbtjournal.com/index.php/fbt>

ISSN (E): 2959-0981, (P): 2959-0973

Volume 4, Issue 3 (July-Sep 2024)



Review Article



Regulation of Intestinal Iron Absorption: Balancing Supply and Demand

Shazia Yaseen^{1*}, Rai Hamza Akram², Basit Ali³, Komal Zaheer⁴, Memoona Rafique⁵, Pakeeza Eman¹, Namal Fatima⁶, Fazeelat Kausar⁷ and Muhammad Luqman⁸

¹Department of Zoology, University of Okara, Okara, Pakistan²Services Institute of Medical Sciences, Lahore, Pakistan³Department of Chemical Engineering, University of Engineering and Technology, Peshawar, Pakistan⁴University Medical and Dental College, Faisalabad, Pakistan⁵Department of Optometry, Superior University, Lahore, Pakistan⁶Ameer-ud-Din Medical College, Lahore, Pakistan⁷Department of Molecular Biology, University of Okara, Okara, Pakistan⁸Department of Microbiology, School of Life Sciences, Nanjing Normal University, Nanjing, China

ARTICLE INFO

Keywords:

Intestinal Iron, Ferroportin, Enterocytes, Hypoxia-Inducible Factor 2(HIF-2), Ferritin, anemia

How to Cite:

Yaseen, S., Akram, R. H., Ali, B., Zaheer, K., Rafique, M., Eman, P., Fatima, N., Kausar, F., & Luqman, M. (2024). Regulation of Intestinal Iron Absorption: Balancing Supply and Demand: Regulation of Intestinal Iron Absorption. *Futuristic Biotechnology*, 4(03). <https://doi.org/10.54393/fbt.v4i03.149>

*Corresponding Author:

Shazia Yaseen

Department of Zoology, University of Okara, Okara, Pakistan

shaziayaseen871@gmail.com

Received Date: 7th August, 2024

Acceptance Date: 25th September, 2024

Published Date: 30th September, 2024

ABSTRACT

Iron, an essential micronutrient, is involved in several physiological activities, including oxygen transport, cellular respiration, and DNA synthesis. Its homeostasis is strictly controlled to avoid overload and deficiency. Ferrous iron is taken up by intestinal enterocytes through the apical membrane with the help of divalent metal transporter 1(DMT1). Iron can then be discharged into the bloodstream by ferroportin 1(FPN1) or stored intracellularly in ferritin. Hepcidin, a hormone produced in the liver, binds to FPN1 and causes its internalization and degradation, a key factor in controlling systemic iron levels. Thus, hepcidin limits the absorption and release of iron by decreasing the iron outflow from enterocytes and macrophages. Iron-responsive element/iron regulatory protein(IRE/IRP) system and hypoxia-inducible factor 2(HIF-2) are important cellular regulators of iron homeostasis. The IRE/IRP system post-transcriptionally regulates the expression of iron-related proteins in response to iron availability. At the same time, HIF-2 promotes the expression of iron transporters and metabolic enzymes under hypoxic conditions. Iron-related disorders can result from disruptions in these regulatory mechanisms; for instance, mutations in the genes encoding hepcidin, FPN1, or hereditary hemochromatosis protein (HFE) can cause iron overload disorders like hemochromatosis, while iron deficiency anemia is caused by impaired iron absorption due to genetic defects or nutritional deficiencies. A deeper understanding of these intricate mechanisms is crucial for developing effective strategies to prevent and treat iron-related disorders.

INTRODUCTION

Iron is a key nutrient that supports multiple processes in the body, especially the transportation of electrons, synthesis of DNA, and oxygen movement [1]. Cells of small intestine are essential for iron management [2]. Since excessive levels of iron and inadequate supply are responsible for several types of diseases, retaining iron homeostasis is important [3]. In the small intestine, the absorption of iron is a carefully monitored process that involves many different proteins and processes [4]. The function of the divalent metal transporter 1 (DMT1) is to transport iron across the apical membrane of enterocytes

[5]. Iron may be transported over the basolateral membrane by ferroportin as well as deposited into ferritin once it enters the enterocyte [6, 7]. Iron absorption needs to be appropriately controlled to preserve iron homeostasis. The liver's metabolic hormone hepcidin is crucial for preserving iron absorption because it binds to ferroportin and inhibits iron export [8]. Since iron is an essential ingredient, excessive intake of it will be harmful. Several systems of regulation were established to keep stability in an atmosphere full of iron. The tissue requirements for iron can be fulfilled and not increased

because of homeostatic processes. Iron deficiency may impact how efficiently various tissue iron-dependent enzymes function. Essentially, for the severe concentration of iron necessary for the synthesis of hemoglobin in developing erythroid cells, anemia is the least known indicator of iron insufficient supply. Mainly through bleeding as well as sloughing of skin and also mucosal cells, iron may escape the body; neither the liver nor the kidneys are capable of controlling the release of iron [9, 10]. Usually, hepatocytes and macrophages preserve excessive amounts of iron. Unsequestered iron produces toxic oxygenated radicals to accumulate as tissue storing capacity reaches its limit, which causes tissue fibrosis and the medical symptoms of endocrinopathies, liver failure, and cardiomyopathy to occur. Initially, iron stores are created through the process of iron transfer from the mother to the developing fetus. After birth, the duodenum's epithelial cells, or enterocytes, consume iron from the meal. It flows throughout the circulatory system linked to transferrin and gets transported to usage and preservation sites. The fundamental consumers, erythroid precursors, are entirely reliant on the receptor-mediated transferrin endocytosis by means of the transferrin cycle [11]. A few years later tissue macrophages consume red blood cells and break down hemoglobin to allow the metal again into the circulatory system to extract iron from aged and damaged erythrocytes [12]. Approximately 5% of the Earth's crust is made up of iron, making it the 2nd most abundant metal on Earth [13]. Being an essential vitamin for the survival of humanity, its significance to humankind becomes critical. It is a d-block transition metal that fluctuates between several oxidation states; it can take part in electron migration and bind to a variety of naturally occurring molecules. Trivalent ferric (Fe^{3+}) and divalent ferrous (Fe^{2+}) are the two most commonly seen iron states. Many hemoproteins and non-hemoproteins that contain iron in the human body depend on iron as a cofactor. Hemoproteins are necessary for many biological functions, such as oxygen metabolism (catalase and peroxidase), electron transport and mitochondrial respiration (cytochromes), and oxygen binding and transport (myoglobin and hemoglobin). Non-haem iron-containing proteins are also vital because they participate in the synthesis of DNA, cell division and proliferation, steroid synthesis, drug metabolism, and gene regulation. A healthy person weighing 70 kg has approximately 3500–4000 mg of iron overall, which corresponds to an average amount of 50–60 mg per kilogram of body weight. A substantial portion of the body's iron (2300 mg, or 65%) is found in the hemoglobin of erythrocytes. About 350 mg, or about a 10th of the total iron, is found in the cytochromes and enzymes

of other tissues, such as muscle myoglobin [14]. Reticuloendothelial system (RES) macrophages contain roughly 500 mg of the residual iron, hepatocytes store 200–1000 mg in the same way as ferritin, and bone marrow has 150 mg. About 15–20 mg of iron is consumed daily on average in the Western world, with 10% of this amount occurring in the haem form and the remaining 10% in the non-haem/ionic form. Only around 10% of the iron that is consumed is utilized, mainly through the duodenum as well as partially in the jejunum [15]. Because the duodenum and proximal jejunum have a significantly more acidic environment than more distal gut segments, iron absorption in the gastrointestinal tract occurs proximally. Enterocytes, or polarized intestinal epithelial cells, found in the duodenum and proximal jejunum, the upper part of the intestine, are responsible for considerable iron absorption [16]. Figure 1 illustrates the regulation of iron by enterocytes. These cells can be identified by others by having a basolateral side, which gets into touch with the blood, and an apical side, which gets into touch with the gut lumen and foodstuff. When enterocytes from developing stem cells go towards the villus every three to four days, the intestinal epithelium is completely renewed. Iron absorption may also be significantly affected by physical characteristics of the gastrointestinal system, such as the stomach's pH (low pH increases iron solubility) and the intestine's surface area, which increases under iron-deficient situations. Numerous proteins produced by differentiated duodenal enterocytes aid in iron absorption from food. The main importer of iron on the apical membrane of these cells is divalent metal transporter 1 (DMT-1) [17]. The ferrous form of dietary ferric iron, which serves as DMT-1's substrate, can be produced via ferric reductase activity on the brush boundary. While some of this reductase activity can be supplied by duodenal cytochrome B (DcytB), alternative reductases, like Steap2, might be involved [18]. It is not clear how heme and ferritin iron are absorbed. While receptor-mediated endocytosis has been shown to pick up heme, enterocytes do not yet have a verified high-affinity heme receptor. Heme carrier protein-1/proton-coupled folate transporter (HCP1/PCFT) is now known to essentially act as a folate transporter with a substantially reduced affinity for heme, despite having been discovered as an apical heme transporter [19]. Endocytosis may also be used to transfer dietary ferritin into enterocytes [20]. Iron may be deposited in endogenous ferritin or released into the bloodstream to be transferred to various bodily tissues once enterocytes have consumed it. In addition to ingested ferritin iron released from ferritin, heme oxygenase in enterocytes breaks down ingested heme iron to produce free ferric iron [16]. The makeup of this pool and the intracellular iron trafficking

pathways are poorly understood, even though dietary iron eventually enters the bloodstream linked to transferrin and seems to converge into a common cellular iron pool within enterocytes. The only known mammalian iron exporter protein, ferroportin 1 (FPN1), helps release iron from enterocytes into the blood. When FPN1 is deleted from intestinal cells, intestinal iron absorption is almost completely blocked, and iron builds up in intestinal enterocytes as a result. Since plasma transferrin (Tf) only binds to ferric iron, ferroxidases are necessary for oxidizing ferrous iron carried by FPN1. FPN1 is internalized and broken down when ferroxidase activity is absent [21, 22]. Although ceruloplasmin (CP) functions as a ferroxidase for FPN1 in various cell types, its function in intestinal iron absorption seems less important, particularly when iron needs are normal. Alternatively, intestinal cells employ hephaestin (HP), a bound by the membrane paralog of CP. Several researches have shown that there may be an interaction between HP and FPN1 [22]. The anemia-associated HP mutation results in systemic anemia and iron accumulation in intestinal enterocyte [23]. Ferroxidase, also known as amyloid precursor protein (APP), is present in intestinal enterocytes and may contribute to intestinal iron absorption [22].

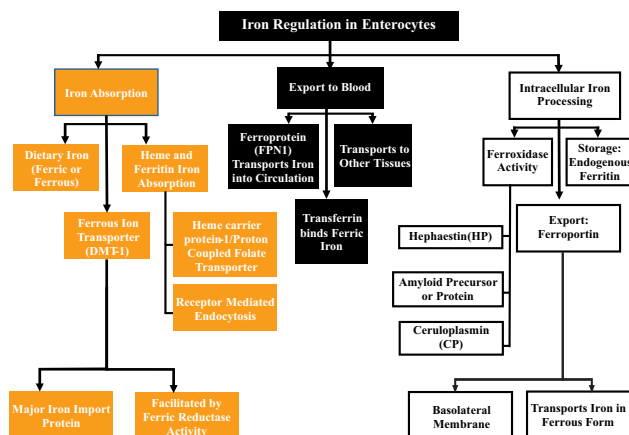


Figure 1: A Visual Representation of Enterocyte Iron Regulation

Meat proteins hemoglobin and myoglobin contain most of the ingested heme iron. These proteins are released from meat at low pH in the stomach, and free hemoglobin is then released by the stomach's and the intestines' subsequent protease activity. Hemoglobin absorption has been attributed to the Haem Carrier Protein 1 transporter (HCP1), which is present on the brush-border membrane of enterocytes. This protein was later identified as a proton-coupled folate transporter (PCFT), which is why the transporter is also referred to as PCFT/HCP1. After haem comes into the enterocyte, it can be broken down by haemoxygenase (HO-1), as shown in Figure 2 and 3, producing free iron that goes into the intracellular labile iron pool (LIP). Moreover, undamaged hemoglobin may also

be able to enter the bloodstream through two exporter proteins: the feline leukemia virus subtype C (FLVCR) and breast cancer-resistant protein (BCRP).

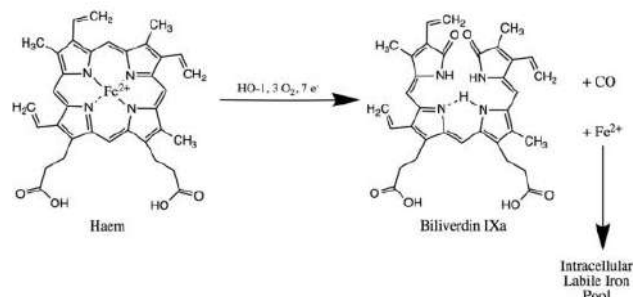


Figure 2: Haem Can Be Broken Down in Enterocytes To Release Free Iron, Which Then Joins The Intracellular Labile Iron Pool.

Steps in Heme Iron Absorption

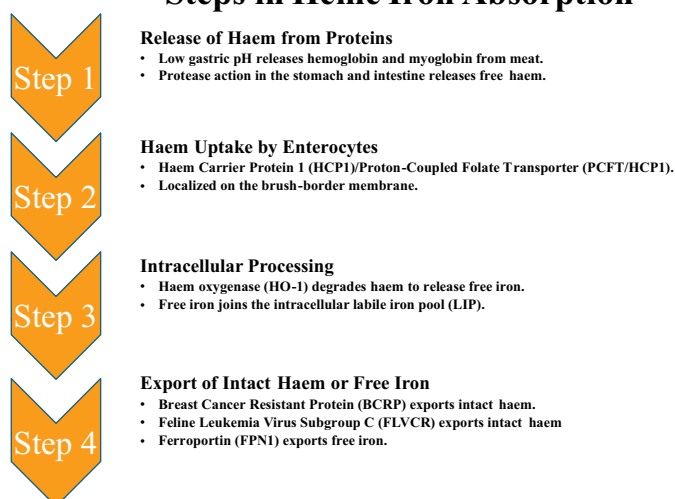


Figure 3: Steps in Heme Iron Absorption

Non-haem iron, primarily found in the ferric (Fe^{3+}) form, is found in meat and plant diets. Ferric iron, unlike ferrous (Fe^{2+}) iron, is very insoluble and challenging to absorb. The steps illustrating the regulation of non-heme iron are represented in Figure 4. Since ferrous iron is the preferred type for absorption, its reduction is crucial; it is done at low pH. Enterocytes can break down hemoglobin to liberate free iron, which moves to the intracellular labile iron pool. The stomach's low pH, and dietary ascorbic acid (vitamin C) cause Fe^{3+} ions to be converted to Fe^{2+} ions, increasing their absorption and solubility. Iron absorption in the gastrointestinal tract occurs proximally because the duodenum and proximal jejunum have a relatively more acidic environment than distal gut segments. Ferrireductase, the duodenal cytochrome b (Dcytb) protein, is found on the brush-border membrane of the enterocyte. It uses electrons from the oxidation of ascorbic acid to dehydroascorbic acid to convert ferric (Fe^{3+}) ions to ferrous (Fe^{2+}) ions as depicted in Figure 5. This process demonstrates how ascorbic acid improves iron absorption. After this reduction process, the divalent metal

transporter 1 (DMT1) then transports the divalent Fe^{2+} ions into the duodenum enterocytes. Ferrous iron, zinc (II), and copper (II) are among the divalent metal ions that are transported across the membrane by DMT1, another protein that is part of the duodenal brush-border membrane. The presence of luminal H^+ ions is necessary for this proton (H^+)-coupled transport to occur. Proton recycling across the duodenal luminal membrane is facilitated by the Sodium/Hydrogen Exchanger (NHE), another brush-border membrane transporter.

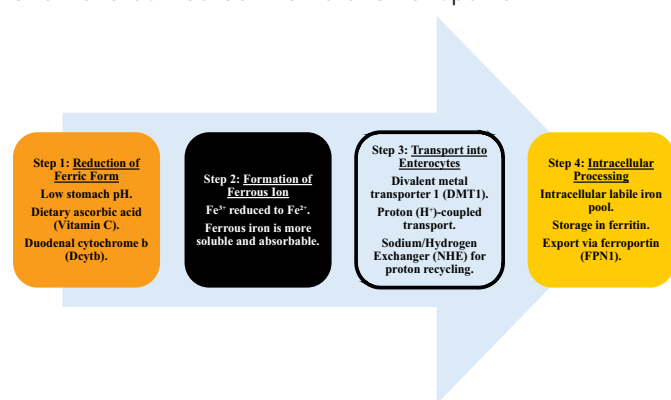


Figure 4: Steps of Non-Heme Iron Absorption

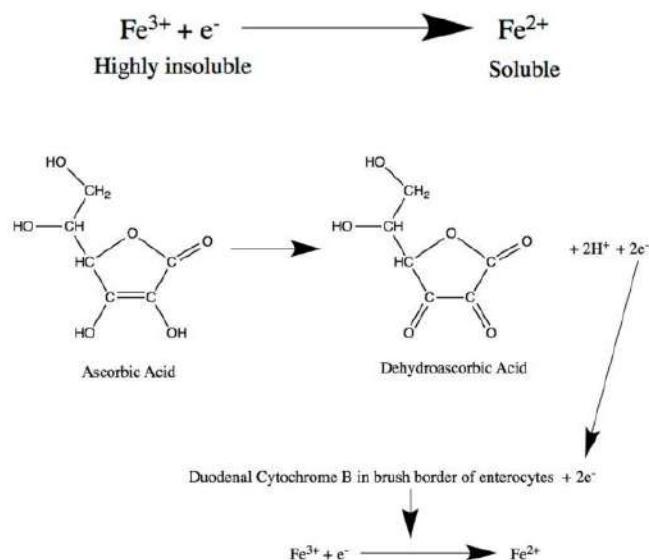


Figure 5: Dietary Ascorbic Acid and Low Stomach Ph Convert Non-Haem Iron from The Very Insoluble Fe^{3+} Form to The More Absorbable Fe^{2+} . Duodenal Cytochrome B Catalyzes the Reduction of Fe^{3+} To Fe^{2+} By Intracellularly Accepting Electrons from The Oxidation of Ascorbic Acid into Dehydroascorbic Acid.

Hepcidin, a 25-amino acid peptide hormone, regulates iron homeostasis by influencing intestinal absorption and macrophage iron release. It is one of the main indicators of anemia. Hepatocytes primarily produce hepcidin and enter the bloodstream, binding to ferroportin 1 (FPN1), an iron exporter found on the basolateral membranes of macrophages and enterocytes. Because of this binding,

FPN1 is internalized and degraded, which lowers iron efflux into the bloodstream. Human iron overload illness type IV hemochromatosis is caused by mutations in FPN1 that interfere with hepcidin binding. There are indications that hepcidin may directly affect DMT1 in enterocytes, albeit this has not been proved. Hepcidin is known to rise in reaction to infection, inflammation, and iron overload while falling in response to hypoxia, iron shortage, and elevated erythropoietic demand despite its complicated regulation. Although these processes remain unclear, hepcidin regulation has been clarified by studying animal models and human disorders involving iron imbalance. The BMP6/SMAD pathway seems essential for controlling the hepcidin response to variations in iron status. Although other members of the BMP family, such as BMP2, 6, and 9, can also affect hepcidin expression, BMP6 is significant among the BMP family because in mice, its deletion results in decreased hepcidin expression and systemic iron overload. The systemic regulation of iron is illustrated in Figure 6.

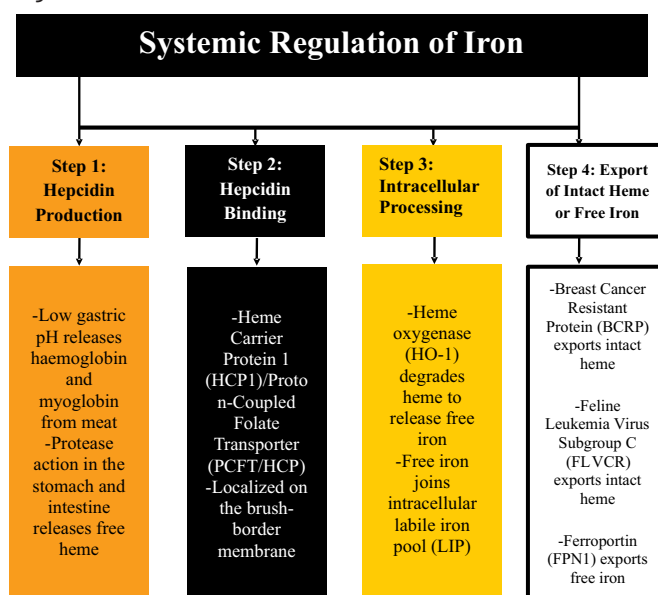


Figure 6: An Outline of The Major Processes and Elements Involved in Iron Intake, Release, and Recycling That Are Part of The Systemic Regulation of Iron.

BMP6 is produced and released by hepatocytes in response to iron load. When receptor-regulated SMADs 1, 5, and 8 bind to the BMP receptor I/II complex in hepatocytes, they become phosphorylated. By interacting with SMAD4, these phosphorylated proteins create heteromeric complexes that go into the nucleus and trigger the transcription of the HAMP gene, which codes for hepcidin. The activity of this pathway depends on hemojuvelin (HJV), a co-receptor for the BMP6 receptor complex. Hepcidin levels are extremely low in people with a congenital abnormality that prevents HJV production, and they develop juvenile

hemochromatosis, a severe iron-loading illness. Although HJV is often found attached to cell plasma membranes, the protease furin can create a soluble form of the virus. Because soluble HJV competes with membrane-bound HJV for BMP binding, it can enhance BMP/SMAD signaling. In addition to degrading HJV, the cell surface serine protease TMPRSS6 can also prevent BMP signaling. Furthermore, infection and inflammation can increase hepcidin expression by triggering inflammatory cytokines like JAK-STAT and the interleukin-6 signaling pathway. The degree of iron saturation of TF and the iron-dependent control of BMP6 are the two main pathways most likely to be engaged in transferring body iron levels to hepcidin. At the same time, the precise process is unknown. Both the membrane proteins hemochromatosis protein (HFE) and transferrin receptor 2 (TFR2) might be engaged in detecting the saturation of TF. Mutations in either protein lead to decreased production of hepcidin, increased absorption of iron, and disease due to iron overload. TFR2, an analog of TFR1, is mainly expressed in the liver and is activated by high levels of differentiating TF. Unlike TFR1, HFE can bind to TFR2, increase TFR2 stability, and attach to TFR1 in the same area as distinguishing TF. According to one theory, high levels of differentiating TF may inhibit HFE's ability to attach to TFR1, increasing HFE's binding to TFR2 and setting off a signaling cascade that would activate hepcidin. This would allow HFE and TFR2 to detect the quantity of iron in the blood [34]. Although this hasn't been proven yet, mice without both proteins show a more severe phenotype than mice with just one gene deleted, signifying that both proteins possibly will have different functions [35]. Hypoxia and cellular iron levels in intestinal enterocytes also regulate local iron absorption as explained in Figure 7. A critical regulator of this process that affects the post-transcriptional regulation of proteins engaged in iron metabolism is the iron-responsive element (IRE)/iron regulatory protein (IRP) system. In iron-deficient settings, an IRP (IRP1 or IRP2) stabilizes when it attaches to the IREs in the three UTRs of the mRNAs that produce TFR1 and two isoforms of DMT1. This stabilization lengthens the mRNA's half-life, raising the translated protein quantity. IRP1 reversibly binds iron and transitions into its RNA binding state when cellular iron levels drop. IRP2 degrades when low iron levels are low, even though it does not bind iron. APP, one isoform of FPN1, and the five UTR of ferritin all include IREs. The translation is blocked when IRP binding stabilizes the stem loop in low iron circumstances. However, the 5 IRE is absent from the predominant splice version of FPN1 seen in intestinal cells, meaning that FPN1 protein levels may be upheld even in the presence of low iron levels in the cell.

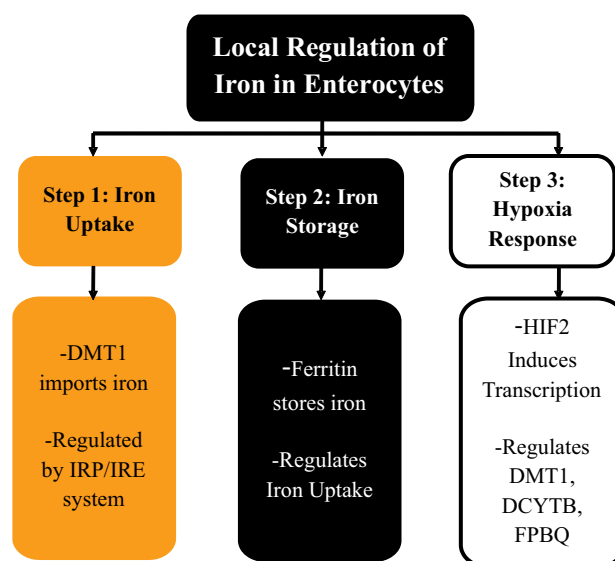


Figure 7: Illustration of the Three Main Processes Involved in Local Iron Regulation.

The body can engross iron with a low dietary iron level or systemic iron deficiency. Enterocyte ferritin, which stocks most of the iron in the enterocytes that are not present in the labile iron pool, may be essential for handling iron uptake because intestinal-specific ferritin H protein deletion causes improved iron absorption [37]. It is unknown if ferritin regulates enterocyte iron flow under typical physiological circumstances. Hypoxia-inducible factor 2 (HIF2) regulates the transcriptional levels of proteins involved in iron and oxygen status absorption because hypoxia is a potent inducer of iron absorption. A transcription factor complex comprising HIF2 attaches itself to promoters with HIF-responsive elements (HREs) to initiate transcription [38]. HREs are found in iron metabolism genes such as FPN1, DMT1, and DCYTB. HIF2 is constitutively produced by cells but is hydroxylated by iron- and oxygen-dependent prolyl hydroxylase proteins (PHDs), leading to its rapid ubiquitination and degradation in proteasomes. When oxygen and iron levels fall, HIF2 levels rise, increasing target gene transcription and limiting PHD activity. Higher production of Hif2 in the colon of genetically modified mice resulted in increased expression of DCYTB and DMT1 and improved iron absorption; however, intestinal deletion of HIF2 causes low levels of DMT1, Fpn1, and DCYTB as well as systemic iron deficit regardless of low hepcidin levels. These results imply that HIF2 is essential for the local regulation of iron absorption. It is not surprising that certain illnesses of iron homeostasis are brought on by disorders in the process of absorption of iron, which determines the body's iron concentration. Hemochromatosis and primary iron loading disorders are the most well-known; they are described by increased iron absorption even when adequate body iron stores [39, 40].

Even when the body's iron stores are sufficient or high, primary iron overload illnesses like hemochromatosis are typified by excessive iron absorption. Reduced hepcidin levels and, thus, elevated FPN1 expression on the enterocyte basolateral membrane are the causes of this enhanced absorption. One such condition is ferroportin disease, which is brought on by mutations in FPN1 [30]. FPN1 is unable to react to the body's cues to reduce iron absorption in this scenario because it is no longer sensitive to hepcidin. The high iron load linked to several other clinical disorders, particularly iron-loading anemias like thalassemia and sideroblastic anemia, is also significantly influenced by elevated iron absorption [40]. The body's natural physiological reaction to elevated erythropoiesis linked to severe diseases is to enhance iron intake. While several recognized hereditary iron-loading syndromes exist, iron refractory iron deficiency anemia (IRIDA) is a well-characterized inherited iron deficiency illness [31]. Subjects in this circumstance exhibit severe anemia that makes oral iron treatment ineffective. In most cases, the gene that is changed is hepatocyte plasma membrane protease, transmembrane serine protease 6 (TMPRSS6), which efficiently suppresses the synthesis of hepcidin and breaks down HJV. Hepcidin levels are relatively high, FPN1 expression is reduced, and body iron intake decreases when TMPRSS6 is altered. The absorption of iron in the intestine depends on several factors, some of which have been covered in detail above. The type of iron consumed plays a key role: Iron heme gotten from animal products is better absorbed in the body than non-heme iron gotten from plant products. The other factors are related to diet; vitamin C increases the absorption of non-heme iron by reducing it into a soluble ferrous form; other inhibitors include calcium, phytates (grains and legumes), polyphenols (tea and coffee) and oxalates. The absorption of iron is high in acidic environments such as the stomach hence conditions that reduce the secretion of gastric acid such as achlorhydria or the use of proton pump inhibitors are counterproductive. Again, the iron status of the body affects the extent of absorption, higher with low levels of iron in the body. Other factors include inflammation, infections particularly those affecting hepcidin pathway and hereditary disorders like hemochromatosis diseases [42]. In general, the achievement of iron balance depends on dietary intake, physiological requirement and health state.

CONCLUSIONS

Iron absorption in the intestine is a finely tuned process that ensures the body maintains iron homeostasis. This review article has explored the various proteins, hormones, and signaling pathways that work in concert to regulate iron uptake. We have highlighted the critical roles of DMT1,

FPN1, hepcidin, HIF-2, and the IRE/IRP system. Understanding the intricate interplay of these factors is crucial for developing effective strategies to prevent and treat iron overload disorders and iron deficiency anemia. Future research should focus on elucidating the precise mechanisms by which hepcidin interacts with DMT1 and FPN1 and exploring the potential therapeutic targets within the iron regulatory pathways. By continuing to unravel the complexities of intestinal iron absorption, we can strive toward a future where iron-related disorders are a thing of the past.

Authors Contribution

Conceptualization: SY, RHA, KZ, MR, PE, NF, FK

Methodology: SY, BA

Formal analysis: SY, RHA, KZ, MR, PE, NF, FK

Writing, review and editing: SY, RHA, BA, ML

All authors have read and agreed to the published version of the manuscript.

Conflicts of Interest

All the authors declare no conflict of interest.

Source of Funding

The authors received no financial support for the research, authorship and/or publication of this article.

REFERENCES

- [1] Dutt S, Hamza I, Bartnikas TB. Molecular Mechanisms of Iron and Heme Metabolism. *Annual Review of Nutrition*. 2022 Aug; 42(1): 311-35. doi:10.1146/annurev-nutr-062320-112625.
- [2] Lane DJ and Bae DH. Duodenal Cytochrome B (DCYTB) in Iron Metabolism: An Update on Function and Regulation. *Nutrients*. 2015 Mar; 7(4): 2274-96. doi: 10.3390/nu7042274.
- [3] Cappellini MD, Comin-Colet J, De Francisco A, Dignass A, Doehner W, Lam CS, et al. Iron Deficiency Across Chronic Inflammatory Conditions: International Expert Opinion on Definition, Diagnosis, and Management. *American Journal of Hematology*. 2017 Oct; 92(10): 1068-78. doi: 10.1002/ajh.24820.
- [4] Knutson MD. Iron Transport Proteins: Gateways of Cellular and Systemic Iron Homeostasis. *Journal of Biological Chemistry*. 2017 Aug; 292(31): 12735-43. doi: 10.1074/jbc.R117.786632.
- [5] Ballesteros C and Geary JF. Characterization of Divalent Metal Transporter 1 (DMT1) in *Brugia malayi* Suggests an Intestinal-Associated Pathway for Iron Absorption. *International Journal for Parasitology: Drugs and Drug Resistance*. 2018 Aug; 8(2): 341-9. doi: 10.1016/j.ijpddr.2018.06.003.
- [6] Yanatori I, Richardson DR, Imada K, Kishi F. Iron Export Through the Transporter Ferroportin 1 Is

- Modulated by the Iron Chaperone PCBP2. *Journal of Biological Chemistry*.2016 Aug; 291(33): 17303-18. doi: 10.1074/jbc.M116.721936.
- [7] La A, Nguyen T, Tran K, Sauble E, Tu D, Gonzalez A, et al. Mobilization of Iron from Ferritin: New Steps and Details. *Metallomics*.2018 Jan; 10(1): 154-68. doi: 10.1039/C7MT00284J.
- [8] Nemeth E and Ganz T. Hpcidin-Ferroportin Interaction Controls Systemic Iron Homeostasis. *International Journal of Molecular Sciences*.2021 Jun; 22(12): 6493. doi: 10.3390/ijms22126493.
- [9] Besarab A and Hemmerich S. Iron-Deficiency Anemia. Management of Anemia: A Comprehensive Guide for Clinicians.2018: 11-29. doi: 10.1007/978-1-4939-7360-6_2.
- [10] Stein J, Connor S, Virgin G, Ong DE, Pereyra L. Anemia and Iron Deficiency in Gastrointestinal and Liver Conditions. *World Journal of Gastroenterology*.2016 Sep; 22(35): 7908. doi: 10.3748/wjg.v22.i35.7908.
- [11] Kühn LC, Schulman HM, Ponka P. Iron-Transferrin Requirements and Transferrin Receptor Expression in Proliferating Cells. *Iron Transport and Storage*. 2024 Dec; 149-191. doi: 10.1201/9781003574811-14.
- [12] Nairz M, Schroll A, Demetz E, Tancevski I, Theurl I, Weiss G. 'Ride on the Ferrous Wheel'-The Cycle of Iron in Macrophages in Health and Disease. *Immunobiology*.2015 Feb; 220(2): 280-94. doi: 10.1016/j.imbio.2014.09.010.
- [13] Pushcharovsky DY. Iron and Its Compounds in the Earth's Core: New Data and Ideas. *Geochemistry International*.2019 Sep; 57: 941-55. doi: 10.1134/S016702919090088.
- [14] Saboor M, Zehra A, Hamali HA, Mobarki AA. Revisiting Iron Metabolism, Iron Homeostasis, and Iron Deficiency Anemia. *Clinical Laboratory*.2021 May; 1(3): 1. doi: 10.7754/Clin.Lab.2020.200742.
- [15] Nairz M, Theurl I, Swirski FK, Weiss G. "Pumping Iron"-How Macrophages Handle Iron at the Systemic, Microenvironmental, and Cellular Levels. *Pflügers Archiv-European Journal of Physiology*.2017 Apr; 469: 397-418. doi: 10.1007/s00424-017-1944-8.
- [16] Balusikova K, Dostalikova-Cimburova M, Tacheci I, Kovar J. Expression Profiles of Iron Transport Molecules Along the Duodenum. *Journal of Cellular and Molecular Medicine*.2022 May; 26(10): 2995-3004. doi: 10.1111/jcmm.17313.
- [17] Garrick MD. Regulation of Divalent Metal-Ion Transporter-1 Expression and Function. *Molecular, Genetic, and Nutritional Aspects of Major and Trace Minerals*. 2017 Jan; 227-238. doi: 10.1016/B978-0-12-802168-2.00019-1.
- [18] Doguer C, Ha JH, Collins JF. Intersection of Iron and Copper Metabolism in the Mammalian Intestine and Liver. *Comprehensive Physiology*.2018 Sep; 8(4): 1433. doi: 10.1002/cphy.c170045.
- [19] Donegan RK, Moore CM, Hanna DA, Reddi AR. Handling Heme: The Mechanisms Underlying the Movement of Heme Within and Between Cells. *Free Radical Biology and Medicine*.2019 Mar; 133: 88-100. doi: 10.1016/j.freeradbiomed.2018.08.005.
- [20] Esparza A, Gerdtsen ZP, Olivera-Nappa A, Salgado JC, Núñez MT. Iron-Induced Reactive Oxygen Species Mediate Transporter DMT1 Endocytosis and Iron Uptake in Intestinal Epithelial Cells. *American Journal of Physiology-Cell Physiology*.2015 Oct; 309(8): 558-67. doi: 10.1152/ajpcell.00412.2014.
- [21] Yang Q, Liu W, Zhang S, Liu S. The Cardinal Roles of Ferroportin and Its Partners in Controlling Cellular Iron In and Out. *Life Sciences*.2020 Oct; 258: 118135. doi: 10.1016/j.lfs.2020.118135.
- [22] Ji C, Steimle BL, Bailey DK, Kosman DJ. The Ferroxidase Hephaestin but Not Amyloid Precursor Protein Is Required for Ferroportin-Supported Iron Efflux in Primary Hippocampal Neurons. *Cellular and Molecular Neurobiology*.2018 Apr; 38: 941-954. doi: 10.1007/s10571-017-0568-z.
- [23] Xu E, Chen M, Zheng J, Maimaitiming Z, Zhong T, Chen H. Deletion of Hephaestin and Ceruloplasmin Induces a Serious Systemic Iron Deficiency and Disrupts Iron Homeostasis. *Biochemical and Biophysical Research Communications*.2018 May; 503(3): 1905-10. doi: 10.1016/j.bbrc.2018.07.134.
- [24] Koziolok M, Schneider F, Grimm M, Modeß C, Seekamp A, Roustom T, et al. Intragastric pH and Pressure Profiles After Intake of the High-Caloric, High-Fat Meal as Used for Food Effect Studies. *Journal of Controlled Release*.2015 Sep; 220: 71-8. doi: 10.1016/j.jconrel.2015.10.022.
- [25] Hou Z, Gangjee A, Matherly LH. The Evolving Biology of the Proton-Coupled Folate Transporter: New Insights into Regulation, Structure, and Mechanism. *The FASEB Journal*.2022 Dec; 36(2): 1. doi: 10.1096/fj.202101704R.
- [26] Kontoghiorghes GJ, Kolnagou A, Kontoghiorghes CN, Mourouzidis L, Timoshnikov VA, Polyakov NE. Trying to Solve the Puzzle of the Interaction of Ascorbic Acid and Iron: Redox, Chelation, and Therapeutic Implications. *Medicines*. 2020 Jul; 7(8): 45. doi: 10.3390/medicines7080045.
- [27] Halder S, Tripathi A, Qian J, Beserra A, Suda S, McElwee M, et al. Prion Protein Promotes Kidney Iron Uptake via Its Ferrireductase Activity. *Journal of Biological Chemistry*.2015 Feb; 290(9): 5512-22. doi:

- 10.1074/jbc.M114.607507.
- [28] Dominguez Rieg JA and Rieg T. New Functions and Roles of the Na⁺-H⁺-Exchanger NHE3. *European Journal of Physiology*. 2024 Apr; 476(4): 505-516. doi: 10.1007/s00424-024-02938-9.
- [29] Fathi ZH, Mohammad JA, Younus ZM, Mahmood SM. Hepcidin as a Potential Biomarker for the Diagnosis of Anemia. *Turkish Journal of Pharmaceutical Sciences*. 2022 Oct 19(5): 603. doi: 10.427 4/tjps.galenos.2021.29488.
- [30] Varga E, Pap R, Jánosa G, Sipos K, Pandur E. IL-6 Regulates Hepcidin Expression via the BMP/SMAD Pathway by Altering BMP6, Tmprss6, and Tfr2 Expressions at Normal and Inflammatory Conditions in BV2 Microglia. *Neurochemical Research*. 2021 May; 46(5): 1224-38. doi: 10.1007/s11064-021-03322-0.
- [31] Altamemy NN. Study the Multifaceted Roles of Bone Morphogenetic Protein (BMP) in the Regulation of Circulating Iron in Iron Deficiency Anemia Patients [dissertation]. Iraq: University of Kerbala; 2025.
- [32] Charlebois E and Pantopoulos K. Iron Overload Inhibits BMP/SMAD and IL-6/STAT3 Signaling to Hepcidin in Cultured Hepatocytes. *PLoS One*. 2021 Jun; 16(6): e0253475. doi: 10.137 1/journal. pone. 02 53475.
- [33] Pettinato M, Aghajan M, Guo S, Bavuso Volpe L, Carleo R, Nai A, *et al.* A Functional Interplay Between the Two BMP-SMAD Pathway Inhibitors Tmprss6 and Fkbp12 Regulates Hepcidin Expression In Vivo. *American Journal of Physiology-Gastrointestinal and Liver Physiology*. 2024 Mar; 326(3): 310-7. doi: 10.1152/ ajpgi .00305.2023.
- [34] Parrow NL and Fleming RE. Transferrin Receptor 1: Keeper of HFE. *Blood, The Journal of the American Society of Hematology*. 2023 Jan; 141(4): 332-3. doi: 10.1182/blood.2022018740.
- [35] Wallace DF. Combined Deletion of HFE and Transferrin Receptor 2 in Mice Leads to Marked Dysregulation of Hepcidin and Iron Overload. *Hepatology*. 2009 Apr; 50(6): 1992-2000. doi: 10.100 2/hep.23198.
- [36] Celma Nos F. Iron Regulatory Protein/Iron Responsive Element (IRP/IRE) System: Associated Diseases and New Target mRNAs (PPP1R1B) [dissertation]. Catalonia: Universitat Internacional de Catalunya; 2022.
- [37] Hanudel MR, Czaya B, Wong S, Rappaport M, Namjoshi S, Chua K, *et al.* Enteral Ferric Citrate Absorption Is Dependent on the Iron Transport Protein Ferroportin. *Kidney International*. 2022; 101(4): 711-9. doi: 10.1016/j.kint.2021.10.036.
- [38] Villar D, Ortiz-Barahona A, Gómez-Maldonado L, Pescador N, Sánchez-Cabo F, Hackl H, *et al.* Cooperativity of Stress-Responsive Transcription Factors in Core Hypoxia-Inducible Factor Binding Regions. *PLoS ONE*. 2012; 7(9): e45708. doi: 10.13 71/ journal.pone.0045708.
- [39] Schwartz AJ, Das NK, Ramakrishnan SK, Jain C, Jurkovic MT, Wu J, *et al.* Hepatic Hepcidin/Intestinal HIF-2 α Axis Maintains Iron Absorption During Iron Deficiency and Overload. *The Journal of Clinical Investigation*. 2019 Jan; 129(1): 336-48. doi: 10.11 72/J CI122359.
- [40] Corradini E, Buzzetti E, Pietrangelo A. Genetic Iron Overload Disorders. *Molecular Aspects of Medicine*. 2020 Oct; 75: 100896. doi: 10.101 6/j. mam.2020. 1008 96.
- [41] Vecchi C and Pietrangelo A. Signaling Pathways in Liver Diseases. 3rd ed. Wiley Online Library: 2015. Chapter 29, Hepcidin and Iron; 400-410. doi: 10.1002 /9781118663387.ch29.
- [42] Piskin E, Cinciosi D, Gulec S, Tomas M, Capanoglu E. Iron Absorption: Factors, Limitations, and Improvement Methods. *ACS Omega*. 2022 Jun; 7(24): 20441-56. doi: 10.1021/acsomega.2c01833.

FUTURISTIC BIOTECHNOLOGY

<https://fbtjournal.com/index.php/fbt>

ISSN (E): 2959-0981, (P): 2959-0973

Volume 4, Issue 3 (July-Sep 2024)



Review Article



A Comprehensive Review of Dengue Fever: Epidemiological Trends, Diagnostic Approaches, Novel Therapeutic Strategies, and Challenges in Vaccine Advancement over the Past Five Years in the Context of Globalization and Climatic Change

Nimra Yousaf¹, Ahmad Raza¹, Nimra Batool¹, Abubakar Sheikh¹, Fiza Babar¹ and Adeeba Ali^{1*}

¹Department of Biotechnology, University of Central Punjab, Lahore, Pakistan

ARTICLE INFO

Keywords:

Dengue fever, Epidemiological Trends, Diagnostic Approaches, Climatic Change

How to Cite:

Yousaf, N., Raza, A., Batool, N., Sheikh, A., Babar, F., & Ali, A. (2024). A Comprehensive Review of Dengue Fever: Epidemiological Trends, Diagnostic Approaches, Novel Therapeutic Strategies, and Challenges in Vaccine Advancement over the Past Five Years in the Context of Globalization and Climatic Change : Dengue Fever: Novel Therapeutic Strategies and Vaccine Advancement . Futuristic Biotechnology, 4(03), 10-16. <https://doi.org/10.54393/fbt.v4i03.154>

*Corresponding Author:

Adeeba Ali

Department of Biotechnology, University of Central Punjab, Lahore, Pakistan
adeebaali1146@gmail.com

Received date: 2nd August, 2024

Acceptance date: 24th September, 2024

Published date: 30th September, 2024

ABSTRACT

Dengue fever, which is caused by the dengue virus and primarily disseminated by Aedes mosquitoes, constitutes a significant global health issue, indicating 400 million infections and 22,000 fatalities each year. The clinical presentation of the disease varies widely, encompassing both asymptomatic manifestations and severe forms such as dengue hemorrhagic fever (DHF) and dengue shock syndrome (DSS), particularly during secondary infections attributable to antibody-dependent enhancement (ADE). The increasing incidence is influenced by several factors, including climate change, globalization, and urbanization, resulting in recurrent epidemics, particularly in Southeast Asia and the Indian subcontinent. The current diagnostic methodologies encounter difficulties, often intersecting with other medical conditions, thereby necessitating the implementation of advanced techniques for precise identification. Management predominantly entails supportive care and traditional interventions, while substantial deficiencies persist in the realm of effective therapeutic alternatives and vaccine innovation. Notwithstanding advancements with live attenuated vaccines, a universally effective vaccine has yet to be achieved. Ongoing research is imperative to confront these challenges and establish effective preventive measures against dengue fever.

INTRODUCTION

Dengue fever, which is instigated by the dengue virus (DENV), has emerged as a significant public health issue over the past several decades. Significantly, it has been classified as a neglected tropical disease. Each year, an estimated 400 million dengue cases and 22,000 fatalities are reported globally. The infection of humans by dengue is frequently asymptomatic and is universally recognized within both endemic and epidemic transmission cycles [1]. Dengue virus infection has been documented in the Americas, Africa, Southeast Asia, Europe, the Western Pacific, and Eastern Mediterranean territories. Dengue

outbreaks are the foremost contributors to the substantial rising burden of morbidity and economics in various global regions, particularly in Southeast Asia and the Indian subcontinent [2]. Dengue is a vector-borne painful viral disease. This disease is also known as Dendy fever or break bone fever due to the immense pain that occurs in humans after they get infected [3]. A single-stranded RNA-enveloped virus belongs to the flavivirus family and is transmitted by the AEDES mosquito [4]. Flaviviridae represent a family of viruses characterized by their positive-sense RNA genome, which is approximately 11

kilobases in length and contains 10,700 bases. A taxonomic genus that encompasses 53 distinct viral species [5]. The genus *Flavivirus* encloses various arthropod-borne viruses, including the yellow fever virus, West Nile virus, Zika virus, and tick-borne encephalitis virus. It is estimated to infect approximately 50 to 200 million individuals on an annual basis [6].

Epidemiology

Dengue infection was outbreak in 1944 in India, 1954 in Thailand, in 1962 in Sri Lanka, and 1964 in Bangladesh, where dengue fever is known as Dacca Fever. Moreover, 1965 in Myanmar, and 1968 in Indonesia. Furthermore, outbreaks in Maldives, Nepal, Bhutan and Timor Leste occurred in 2004 [7]. Dengue virus transmission exhibits notable periodicity, with distinct variations observed across different geographical regions. In Southeast Asia, the incidence peaks every three to five years, whereas Brazil experiences a peak approximately every four to five years. Before the year 2010, Guangzhou recognized as the epicenter of dengue outbreaks in China, also demonstrated a peak periodicity of three to five years [8]. I focus on the data of 2017 because of the high fatality rates in comparison with previous years like 2016, 2015, and 2014 (Figure 1).

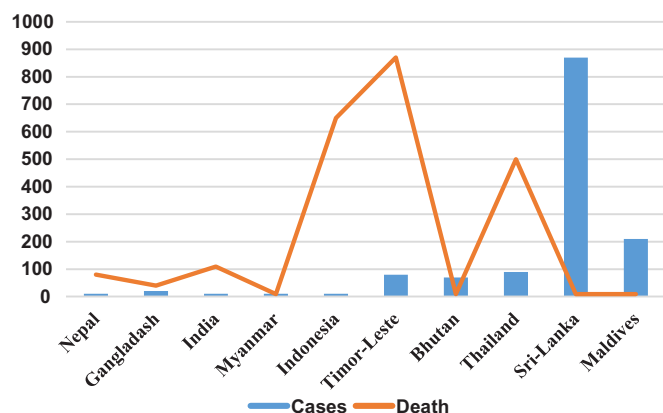


Figure 1: Dengue Incidences and Mortality Rates Among Nations in South East Asia During the Year 2017

Structure and Serotypes

The flavivirus exhibits a spherical morphology with a diameter measuring 50 nm. Mature virions are comprised of virus-encoded, membrane-associated proteins, specifically M and E. Within intracellular immature virions, the precursor protein prM is processed into M during the maturation process [9]. Moreover, Dengue virus (DENV) carries a total of 10 types of proteins of which 3 types are structural and 7 types are non-structural proteins [5, 1]. Furthermore, this virus is classified into 4 different serotypes which show approximately 65% similarity with amino acid sequence [10]. This virus consists of four serotypes. As four serotypes involved in dengue, infection from any one of these (DENV1-4) may elicit a scope of

clinical presentations, ranging from mild influenza-like symptoms to potentially fatal severe conditions recognized as dengue hemorrhagic fever (DHF) and dengue shock syndrome (DSS) in certain patients [11]. The structural and functional attributes of Dengue virus proteins exhibit considerable variability, with each protein contributing distinctively to the viral life cycle. The C protein (Capsid), consisting of 100 amino acids, forms a homodimer characterized by four α -helical regions and a disordered N-terminal segment. This protein is instrumental in the encapsulation of the viral genetic material. The E protein (Envelope), made up of 493–495 amino acids and possessing a molecular weight of 53 kDa, assembles into a class II N-glycosylated dimer. Ninety E homodimers construct a continuous shell on the surface of the virus, featuring three distinct domains (I, II, III) within each monomer, which facilitate the binding of the virus to the host cell membrane and influence host range, target cell specificity, and the severity of infection. The NS1 protein, which varies from 45 to 560 residues, participates in RNA replication while also inhibiting complement activation, thereby aiding the virus in evading immune system responses. The NS2A protein is composed of 218 amino acids (22 kDa) and facilitates RNA encapsulation and replication while simultaneously antagonizing interferon-mediated responses. The NS2B protein, a membrane-associated component comprising 130 amino acids (14 kDa), functions as a cofactor for the NS3 serine protease and is integral to the formation of the DENV protease complex. The multifunctional NS3 protein, consisting of 618 amino acids (70 kDa), encompasses a protease domain (1–180) and a helicase domain (180–618). This protein exhibits serine protease, RNA helicase, and RNA triphosphate activities, which are essential for the cleavage of the DENV polyprotein and the process of RNA replication. The NS4A and NS4B proteins are hydrophobic membrane-associated entities, with NS4A comprising 150 amino acids (16 kDa) and NS4B consisting of 245–249 amino acids (27 kDa). NS4A is involved in mediating membrane alterations necessary for viral replication, whereas NS4B interacts with NS3 and inhibits interferon signalling, thereby promoting RNA replication. Finally, the NS5 protein, recognized as the most conserved entity within DENV, comprises 900 amino acids (104 kDa). It features a methyl-transferase domain (1–269) and an RNA-dependent RNA polymerase domain (270–900), executing critical enzymatic functions requisite for viral RNA synthesis. Collectively, these proteins orchestrate the intricate processes of viral replication, host cell engagement, and immune evasion.

Transmission and Vector

In the year 2010, it was approximated that the global

incidence of dengue infections reached 390 million, of which 96 million cases presented clinically, with severe expression of dengue contributing to approximately 21,000 fatalities on a worldwide scale [12]. The proliferation of dengue fever can be ascribed to a multitude of factors, including contemporary climatic fluctuations, globalization, increased mobility, international commerce, socioeconomic variables, urbanization, and the evolutionary adaptations of the virus [13]. Non-structural genes help in the replication of viruses. The prevalence of Dengue infections varies between 2.5 and 30 percent, elevating to 40–50 in specific regions characterized by dengue hyper-endemicity [14]. Transmission of DENV virus occurred in both urban and forested areas but the transmission cycle is different because of the change in environment and evolutionary history. At 30°C transmission of the virus requires 8–10 days from the gut to the salivary gland. The temperature fluctuation between summer and winter is the main cause of seasonal transmission of the dengue virus. Moreover, the main vectors are also different in urban areas main vector is *Aedes. Aegypti* and *Ae. Albopictus* mosquito whereas in forested areas the main vector is *Ae. Luteocephalus*, *Ae. Furcifer*, *Ae. Taylori* [10]. Furthermore, rapid travel and trade are also the main factors in the expansion of the dengue virus. Indonesia has become the continuous hub of DENV transmission. Congenital dengue may manifest when there exists an inadequate duration for the transference of maternal protective antibodies to the fetus. A pregnant female has the potential to transmit the dengue virus to the fetus if she experiences a febrile condition from 10 days before delivery up until 10 hours post-delivery [15].

Pathogenesis

The pathogenesis of dengue is significantly shaped by the characteristics of the virus as well as the factors associated with the host, which are not yet fully explained. Severe manifestations of dengue may arise in individuals undergoing a secondary infection with a heterotypic strain of DENV, as well as in neonates born to mothers possessing dengue immunity characterized by primary anti-DENV antibody responses. This phenomenon, known as Antibody-Dependent Enhancement (ADE), can be explained through two simultaneous mechanisms. Initially, during the primary infection, antibodies that are cross-reactive to the serotype and exhibit sub-neutralizing properties are generated [10]. The majority of primary infections are typically asymptomatic or present as mild febrile syndrome; however, they may also lead to hemorrhagic fever in certain individuals, particularly in neonates born to mothers with pre-existing immunity to DENV [16]. Subsequently, during a secondary infection involving a heterologous serotype, the sub-neutralizing

antibodies generated from the initial infection interact with the novel Dengue virus, leading to the formation of antibody-virus complexes that are internalized into target cells through Fc gamma receptors (FcγR), thereby facilitating an augmentation of the infection [10].

Symptoms of Dengue Fever

Three phases of the dengue are recognized in the patients when they get infected with Dengue infection. Evident infections emerge as clinical cases after an incubation period of 3–15 days, succeeded by an acute onset of symptoms. It is imperative to differentiate mild illness from influenza, the common cold, and other acute febrile conditions. Classical dengue presentations generally manifest as a sudden febrile response ($\geq 38.5^\circ\text{C}$), accompanied by headache, rash, myalgia, arthralgia, thrombocytopenia, and leukopenia, which correlates with a heightened propensity for individuals to seek medical attention. These cases unfold through three distinct natural phases: febrile, critical, and recovery [17].

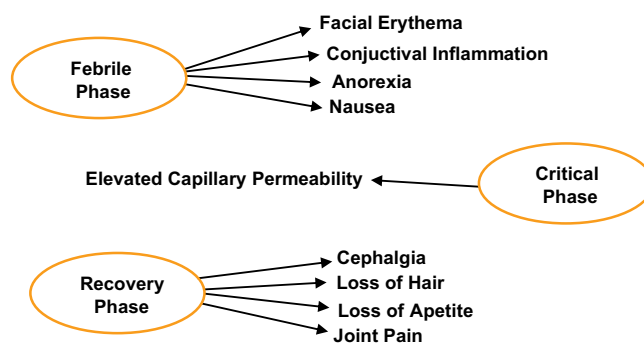


Figure 2: Three phases of Dengue

Severe Dengue and Diagnosis

Due to the fact that infection by a singular serotype confers minimal immunity against the remaining serotypes, recurrent infections involving various serotypes could play a significant role in the escalation of cases of Dengue Hemorrhagic Fever (DHF) and Dengue Shock Syndrome (DSS). For instance, preliminary investigations conducted in Thailand indicated that the incidence rates of Dengue Hemorrhagic Fever/Dengue Shock Syndrome (DHF/DSS) in the pediatric population escalated by 12.5%, with an odds ratio of 6.5 observed in individuals with a prior Dengue Virus (DENV) infection [18]. Physicians have articulated that there exists a vital impetus for the advancement of point-of-care (POC) diagnostic way specifically targeting severe dengue. The implementation of POC diagnostics is anticipated to be profoundly beneficial in rural locales characterized by inadequate laboratory infrastructure for the execution of critical serological assessments necessary for the diagnosis of severe dengue [19]. Electrochemical, optical, and piezoelectric biosensors are used in the diagnosis of dengue [20]. The specialists further articulated the perspective that the introduction of

a diagnostic assay for severe dengue would serve to mitigate expenses, given that the prevailing methodologies employed for the clinical identification of severe dengue namely, recurrent clinical evaluations, platelet quantification, and ferritin assays are characterized by both prolonged durations and substantial costs[21].

Supportive Care

Traditional medicinal practices, including the utilization of papaya leaf, guava juice, and crabmeat soup, were frequently employed by patients; notably, papaya leaf emerged as the most prevalent remedy cited. Our group of patients ingested papaya leaf predominantly in the form of juice (achieved through the infusion of boiling water with papaya leaf) or consumed tablets derived from its extract. Patients did not perceive any detrimental effects associated with the consumption of these remedies. Papaya leaf could enhance immunological responses in cases of dengue [22]. Dengue patients typically receive supportive management that encompasses bed rest, fluid rehydration therapy, analgesic medications, and antipyretic agents to reduce febrile symptoms[23].

Serological Test

Serological assays are frequently employed to identify dengue fever due to their relative cost-effectiveness and simplicity compared to molecular or culture-dependent techniques. Medical practitioners generally analyze serum (a component of blood) and cerebrospinal fluid for the presence of IgM and neutralizing antibodies; however, they may also assess plasma or whole blood in certain instances. The presence of another antibody, IgG, persists in the organism following the initial dengue infection and serves as an indicator for viral detection. Nonetheless, the presence of IgG may occasionally yield ambiguous results in cases of secondary infections or produce false positives if the individual has previously been infected or vaccinated against related viruses such as the West Nile virus, yellow fever virus, or Zika virus[24].

IgM Based Test

IgM antibodies are proteins produced by the immune system to fight infections, typically appearing five days after symptoms begin and lasting 2-3 months or longer. Due to its capacity to provoke an immune response, it is synthesized in reaction to a foreign entity referred to as an immunogenic. A particular antibody is designed to recognize exclusively one specific compound, known as an antigen [23]. The main challenge for dengue antibody detection devices is the five-day window before IgM antibodies appear. The MAC-ELISA test, developed by the Armed Forces Research Institute of Medical Sciences, is employed for the detection of IgM antibodies in dengue [24].

Plaque Reduction Neutralization Test

The Plaque Reduction Neutralization Test (PRNT) detects specific neutralizing antibodies to identify the exact origin of infection in IgM-positive individuals and is considered the gold standard for testing WHO's vaccine immunogenicity. PRNT is used to confirm cases or when detailed serological information is needed. The test involves coating cells with semi-solid media in test tubes or microtiter plates, mixing diluted serum with the virus, and counting plaques formed over a few days. It can be done at the CDC or designated labs, but lacks a global standard, making result comparisons difficult. Despite its effectiveness in identifying asymptomatic dengue infections, PRNT is time-consuming and labor-intensive [24].

Challenges in Treatment

Almost all the physicians noted that diagnosis and treatment were a great challenge. It was not feasible to discover which specific patient among the cohort may progress to severe dengue; therefore, as a precautionary measure, clinicians typically opt to admit patients to the hospital initially, primarily guided by the platelet count. In Malaysia, as well as in numerous Southeast Asian nations, there exists a variety of infectious diseases wherein the initial symptoms closely resemble those of dengue fever, including but not limited to Leptospirosis, Chikungunya, and Zika virus infections; therefore, it was essential to implement prompt diagnostic procedures. Frequently, employ the NS1 antigen assay for the diagnosis of dengue fever. An additional significant consideration highlighted by the doctors was that individuals diagnosed with DF could exhibit diminished levels of NS1, thereby presenting a risk for the occurrence of false negative results. Moreover, the concentrations of NS1 may vary among distinct patients, and it was proposed that further investigations be conducted to identify additional more indicative biomarkers, particularly for patients experiencing severe dengue, which could result in fatality if not appropriately managed [25]. In addition to that, developing drug for DF also face several challenges. Trials for dengue drugs mainly measure how quickly fever goes away and how much the virus or a specific protein (NS1) is reduced. However, these trials haven't shown significant differences between treated and untreated groups. Moreover, most of the drugs are rejected because of the toxic effects on organs like liver, kidney, heart and brain[26].

Vector Control Strategies

Its objective is to diminish or eliminate human interaction with these vectors through the implementation of chemical and non-chemical interventions. For the immature stages of vectors, such as mosquito larvae, control strategies encompass the eradication of larvae

utilizing both chemical and biological larvicides, along with the elimination of their breeding habitats. In the case of adult vectors, control methodologies comprise the lethal application of indoor residual spraying (IRS) or space spraying, as well as the minimization of human and animal exposure through the use of topical repellents, architectural barriers, insecticide-treated bed nets (ITNs), and insecticide-impregnated collars for dogs. Examples of novel vector control strategies [27].

Vaccine Development

As research showed many vaccines were developed to treat the dengue infection. There are different types of vaccines were invented like live attenuated vaccines, inactivated virus vaccines, DNA vaccines, recombinant subunit vaccines and viral vector vaccines. If we talk about live attenuated vaccine, three vaccines were developed CYD-TDV, TAK-003 and TV003/TV005. TAK-003 and TV003/TV005 are the most effective vaccines as compared to CYD-TDV [28]. In the inactivated vaccine S16803, PDK-50, R80E, and TPIV were developed and TLAV as a booster. PDK-50 and booster showed a stable response [28]. The protein is used in recombinant subunit vaccines. One monkey is immunized with E protein to boost the immune response. A vaccine called V180 was developed [28]. In the viral vector vaccine, MVA-DENV was stable because it produced good antibody levels whereas, VRP showed an effect and was not stable in comparison to MVA-DENV [29].

Research Gaps

Currently, there exists no licensed vaccine for dengue fever, and clinical trials connected to potential novel vaccines for this disease are actively underway [30]. A significant body of research has been conducted regarding this medical condition; however, there remains an absence of efficacious therapeutic drugs for this disease [31, 32]. The complex nature of the human immune response is the main cause of ineffective therapeutics because there is still a lack of research regarding the dengue mechanism interacting with the complex immune response of humans. Vector control strategies are not useful because they are ineffective and expensive [33-35].

CONCLUSIONS

It was concluded that clinical manifestations encompass a spectrum that ranges from mild clinical presentations to severe conditions such as dengue hemorrhagic fever (DHF) and dengue shock syndrome (DSS), particularly during instances of secondary infections attributable to antibody-dependent enhancement (ADE). The escalating incidence of these manifestations is influenced by factors such as climate change, globalization, and urbanization, with

Southeast Asia and the Indian subcontinent being the region's most adversely impacted. The diagnostic process presents considerable challenges, often exhibiting overlap with other medical conditions, thereby necessitating the application of advanced diagnostic methodologies. The approach to treatment is predominantly supportive, yet there are significant deficiencies in the availability of effective therapeutic interventions and vaccines. Notwithstanding advancements made with live attenuated vaccines, the pursuit of a universally effective vaccine continues to be an elusive goal. Ongoing research is imperative for the formulation of effective preventive strategies against dengue fever.

Authors Contribution

Conceptualization: NY

Methodology: NY, AR, NB, AS

Formal analysis: NY

Writing review and editing: FB, AA

All authors have read and agreed to the published version of the manuscript.

Conflicts of Interest

All the authors declare no conflict of interest.

Source of Funding

The authors received no financial support for the research, authorship and/or publication of this article.

REFERENCES

- [1] Roy SK and Bhattacharjee S. Dengue Virus: Epidemiology, Biology, and Disease Aetiology. *Canadian Journal of Microbiology*. 2021; 67(10): 687-702. doi: 10.1139/cjm-2020-0572.
- [2] Bhatt P, Sabeena SP, Varma M, Arunkumar G. Current Understanding of the Pathogenesis of Dengue Virus Infection. *Current Microbiology*. 2021 Jan; 78(1): 17-32. doi: 10.1007/s00284-020-02284-w.
- [3] Patel JP, Saiyed F, Hardaswani D. Dengue Fever Accompanied by Neurological Manifestations: Challenges and Treatment. *Cureus*. 2024 May; 16(5): e60961. doi: 10.7759/cureus.60961.
- [4] Kok BH, Lim HT, Lim CP, Lai NS, Leow CY, Leow CH. Dengue Virus Infection—A Review of Pathogenesis, Vaccines, Diagnosis and Therapy. *Virus Research*. 2023 Jan; 324: 199018. doi: 10.1016/j.virusres.2022.199018.
- [5] Faustino AF, Martins AS, Karguth N, Artileiro V, Enguita FJ, Ricardo JC et al. Structural and Functional Properties of the Capsid Protein of Dengue and Related Flavivirus. *International Journal of Molecular Sciences*. 2019 Aug; 20(16): 3870. doi: 10.3390/ijms20163870.

- [6] Kanungo S, Chatterjee A, Basak S, Sadhukhan PC, Dutta S. Global Dengue Menace: Association with Climate Change. 2024 Aug. doi: 10.5772/intechopen.1006370.
- [7] Tsheten T, Gray DJ, Clements AC, Wangdi K. Epidemiology and Challenges of Dengue Surveillance in the WHO South-East Asia Region. *Transactions of The Royal Society of Tropical Medicine and Hygiene*. 2021 Jun; 115(6): 583-99. doi: 10.1093/trstmh/traa158.
- [8] Jing Q and Wang M. Dengue Epidemiology. *Global Health Journal*. 2019 Jun; 3(2): 37-45. doi: 10.1016/j.glohj.2019.06.002.
- [9] Sabir MJ, Al-Saud NB, Hassan SM. Dengue and Human Health: A Global Scenario of Its Occurrence, Diagnosis and Therapeutics. *Saudi Journal of Biological Sciences*. 2021 Sep; 28(9): 5074-80. doi: 10.1016/j.sjbs.2021.05.023.
- [10] Harapan H, Michie A, Sasmono RT, Imrie A. Dengue: A Mini-Review. *Viruses*. 2020 Jul; 12(8): 829. doi: 10.3390/v12080829.
- [11] Anasir MI, Ramanathan B, Poh CL. Structure-Based Design of Antivirals Against Envelope Glycoprotein of Dengue Virus. *Viruses*. 2020 Mar; 12(4): 367. doi: 10.3390/v12040367.
- [12] Tsheten T, Clements AC, Gray DJ, Adhikary RK, Furuya-Kanamori L, Wangdi K. Clinical Predictors of Severe Dengue: A Systematic Review and Meta-Analysis. *Infectious Diseases of Poverty*. 2021 Dec; 10: 1-0. doi: 10.1186/s40249-021-00908-2.
- [13] Murugesan A and Manoharan M. Dengue Virus. In *Emerging and Reemerging Viral Pathogens*. 2020 Jan; 281-359. doi: 10.1016/B978-0-12-819400-3.00016-8.
- [14] Sirisena PD, Mahilkar S, Sharma C, Jain J, Sunil S. Concurrent Dengue Infections: Epidemiology and Clinical Implications. *Indian Journal of Medical Research*. 2021 Nov; 154(5): 669-79. doi: 10.4103/ijmr.IJMR_1219_18.
- [15] Mulik V, Dad N, Buhmaid S. Dengue in Pregnancy. *European Journal of Obstetrics and Gynecology and Reproductive Biology*. 2021 Jun; 261: 205-10. doi: 10.1016/j.ejogrb.2021.04.035.
- [16] Necaj L, Goxharaj A, Matkeeva A, Nikolaev E, Hartmane I. Climate Change and Vaccination Strategies: Analyzing Global Immunization Challenges. *Journal of Environmental Law and Policy*. 2024; 4: 180. doi: 10.33002/jelp040207.
- [17] Silva NM, Santos NC, Martins IC. Dengue and Zika viruses: Epidemiological History, Potential Therapies, and Promising Vaccines. *Tropical Medicine and Infectious Disease*. 2020 Sep; 5(4): 150. doi: 10.3390/tropicalmed5040150.
- [18] Rathore AP, Farouk FS, John AL. Risk Factors and Biomarkers of Severe Dengue. *Current Opinion in Virology*. 2020 Aug; 43: 1-8. doi: 10.1016/j.coviro.2020.06.008.
- [19] Trovato M, Sartorius R, D'Apice L, Manco R, De Berardinis P. Viral Emerging Diseases: Challenges in Developing Vaccination Strategies. *Frontiers in Immunology*. 2020 Sep; 11: 2130. doi: 10.3389/fimmu.2020.02130.
- [20] Hegde SS and Bhat BR. Dengue Detection: Advances and Challenges in Diagnostic Technology. *Biosensors and Bioelectronics: X*. 2022 May; 10: 100100. doi: 10.1016/j.biosx.2021.100100.
- [21] Wong PF, Wong LP, Abu-Bakar S. Diagnosis of Severe Dengue: Challenges, Needs and Opportunities. *Journal of Infection and Public Health*. 2020 Feb; 13(2): 193-8. doi: 10.1016/j.jiph.2019.07.012.
- [22] Ng WL, Toh JY, Ng CJ, Teo CH, Lee YK, Loo KK et al. Self-Care Practices and Health-Seeking Behaviours in Patients with Dengue Fever: A Qualitative Study from Patients' and Physicians' Perspectives. *PLoS Neglected Tropical Diseases*. 2023 Apr; 17(4): e0011302. doi: 10.1371/journal.pntd.0011302.
- [23] Obi JO, Gutiérrez-Barbosa H, Chua JV, Deredge DJ. Current Trends and Limitations in Dengue Antiviral Research. *Tropical Medicine and Infectious Disease*. 2021 Sep; 6(4): 180. doi: 10.3390/tropicalmed6040180.
- [24] Kabir MA, Zilouchian H, Younas MA, Asghar W. Dengue Detection: Advances in Diagnostic Tools from Conventional Technology to Point of Care. *Biosensors*. 2021 Jun; 11(7): 206. doi: 10.3390/bios11070206.
- [25] Liu Y, Wang M, Yu N, Zhao W, Wang P, Zhang H et al. Trends and Insights in Dengue Virus Research Globally: A Bibliometric Analysis(1995-2023). *Journal of Translational Medicine*. 2024 Sep; 22(1): 818. doi: 10.1186/s12967-024-05561-5.
- [26] Lim SP. Dengue Drug Discovery: Progress, Challenges and Outlook. *Antiviral Research*. 2019 Mar; 163: 156-78. doi: 10.1016/j.antiviral.2018.12.016.
- [27] Wilson AL, Courtenay O, Kelly-Hope LA, Scott TW, Takken W, Torr SJ et al. The Importance of Vector Control for the Control and Elimination of Vector-Borne Diseases. *Plos Neglected Tropical Diseases*. 2020 Jan; 14(1): e0007831. doi: 10.1371/journal.pntd.0007831.
- [28] Huang CH, Tsai YT, Wang SF, Wang WH, Chen YH. Dengue Vaccine: An Update. *Expert Review of Anti-Infective Therapy*. 2021 Dec; 19(12): 1495-502. doi: 10.1080/14787210.2021.1949983.
- [29] Deng SQ, Yang X, Wei Y, Chen JT, Wang XJ, Peng HJ. A Review On Dengue Vaccine Development. *Vaccines*.

- 2020 Feb; 8(1): 63. doi: 10.3390/vaccines8010063.
- [30] Srivastav AK and Ghosh M. Assessing the Impact of Treatment On the Dynamics of Dengue Fever: A Case Study of India. *Applied Mathematics and Computation*. 2019 Dec; 362: 124533. doi: 10.1016/j.amc.2019.06.047.
- [31] Nasar S, Rashid N, Iftikhar S. Dengue Proteins with Their Role in Pathogenesis, and Strategies for Developing an Effective Anti-Dengue Treatment: A Review. *Journal of Medical Virology*. 2020 Aug; 92(8): 941-55. doi: 10.1002/jmv.25646.
- [32] Zhang Y, Wang M, Huang M, Zhao J. Innovative Strategies and Challenges Mosquito-Borne Disease Control Amidst Climate Change. *Frontiers in Microbiology*. 2024 Nov; 15: 1488106. doi: 10.3389/fmicb.2024.1488106.
- [33] Enitan SS, Abbas KS, Elrufai RR, Umukoro S, Tsague CL, Nwafor IR *et al*. Advancing Dengue Fever Preparedness in Africa: Challenges, Resilience, and Contributions to Global Health. *Acta Elit Salutis*. 2024; 9(1). doi: 10.48075/aes.v9i1.33267.
- [34] Kanungo S, Chatterjee A, Basak S, Sadhukhan PC, Dutta S. Global Dengue Menace: Association with Climate Change. 2024 Aug. doi: 10.5772/intechopen.1006370.
- [35] Humaira HA, Iqbal T, Habib I, Aman Z. Vaccine Strategies for Dengue Fever. *Zoonosis, Unique Scientific Publishers, Faisalabad, Pakistan*. 2023; 3: 561-75. doi: 10.47278/book.zoon/2023.124.

FUTURISTIC BIOTECHNOLOGY

<https://fbtjournal.com/index.php/fbt>

ISSN (E): 2959-0981, (P): 2959-0973

Volume 4, Issue 3 (July-Sep 2024)



Review Article



Role of Microbes in the Production of Dairy Products

Muhammad Naeem¹, Aatif Amin¹, Joha Ejaz¹, Fizza Shahzad¹, Sehrish Patras¹ and Khazen Ali Aamir²

¹Department of Microbiology, University of Central Punjab, Lahore, Pakistan

²Department of Biotechnology, University of Central Punjab, Lahore, Pakistan

ARTICLE INFO

Keywords:

Lactic Acid Bacteria, Fermentation Probiotic, Dairy Products, Microbiota, Probiotic

How to Cite:

Naeem, M., Amin, A., Ejaz, J., Shahzad, F., Patras, S., & Aamir, K. A. (2024). Role of Microbes in the Production of Dairy Products: Microbes in Dairy Products. *Futuristic Biotechnology*, 4(03), 17-26. <https://doi.org/10.54393/fbt.v4i03.153>

*Corresponding Author:

Muhammad Naeem
Department of Microbiology, University of Central Punjab, Lahore, Pakistan
aminnaeem678@gmail.com

Received date: 27th July, 2024

Acceptance date: 19th September, 2024

Published date: 30th September, 2024

ABSTRACT

Microorganisms have a significant impact on the fermentation processes and health advantages of dairy products. Certain microbial strains are necessary for the fermentation, flavor, and nutritional value enhancement of traditional dairy products including kefir, cheese, and yoghurt. Yeasts, molds, and lactic acid bacteria are necessary for the transformation of lactose to lactic acid, which causes milk to coagulate and produce distinctive smells and textures. Recent developments in synthetic biology, fermentation technology, and microbial genetics have created new opportunities to improve the functioning and quality of dairy products. The present function of microbes in dairy production is examined in this review, with particular attention paid to their use in fermentation, probiotic production, and sustainability. The creation of new probiotic strains, the use of genetically modified microorganisms to produce dairy substitutes, and the application of microbes for more effective and sustainable dairy farming methods are some prospects. The future of the dairy business is expected to be significantly shaped by microbial innovation as customer demand for healthier, more sustainable dairy products increases.

INTRODUCTION

Many different types of microbiotas play an important role in dairy products. Dairy production and utilization can have negative and positive human health effects. Dairy production is a major source of high-quality protein and minerals that are accessible (e.g., Vitamin and iron. Dairy products can also play a significant role in local-regional and international-level economics and provide opportunities for employment and income generation. Different types of diseases are identified through dairy products including diet-related chronic disease, environmental change, foodborne hazards, occupational hazards and zoonotic disease (transmissible animals to humans) [1]. Microbes like Yeast, mold and bacteria have been used in fermentation. Thousands of years ago, humans used them to make food products such as bread, vinegar, beer, wine, cheese and yoghurt. Microorganisms

have also been used to ferment fish, meat, and vegetables, producing a variety of foods [2]. Microbes produce various food products through fermentation. Today, microbes are commonly used to make food or improve its quality. Biotechnologists are working on creating special food products using microbes [3]. Microbes are important in both food spoilage and food production. While they can cause bad taste, odor and texture in spoiled food, they are also essential for making many fermented foods and drinks [4]. Bread is a staple food, especially in developing countries but it loses freshness quickly due to staling and microbial contamination. Microbes are used in bread production to increase the shelf life of bread products [5]. Bakery products are an important part of a balanced and come in many types, including unsweetened (bread, rolls), sweet (cookies, doughnuts) and filled goods (pies,



sandwiches) [6]. Dairy products, like bread, biscuits and cereals are important food providing essential nutrients, including carbohydrates, proteins and vitamins. India is one of the largest food sector industries making breads and biscuits up over 80% of the total production. Common molds used in bakery products include *Rhizopus*, *Mucor*, and *Penicillium* [7]. Vinegar is a highly valued and unique fermented food product, particularly in European and Asian countries [8]. Vinegar is a liquid that contains at least 4% acetic acid and is consumed worldwide. *Aspergillus* species, lactic acid bacteria and other *Saccharomyces* and non-*Saccharomyces* yeasts are important in the fermentation of cereal vinegar. These microbes are essential for the breakdown of raw materials and the synthesis of bioactive chemicals. Vinegar is made through two types of fermentation. Such as Alcoholic fermentation (sugar to alcohol) and Acetous fermentation (alcohol to acetic acid). alcohol produced using yeast and acetic produced using acetic acid bacteria [9]. Ghee is a tasty and nutritious dairy product made by heating butter to remove water through evaporation and separating non-fat solids through sedimentation. It is also known as animal oil or milk oil [10]. Ghee is widely produced and consumed in India, Sudan, Ethiopia, Pakistan and the Middle East [11].

Ghee is utilized for culinary purposes such as dressing and frying different foods [12]. Milk and dairy products have been important components in Africa to increase the number of people living in rural as well as urban settings. Milk and dairy products have rich amounts of nutrients and are available is contain chemical hazards and contaminants mostly obtained by the environments and farm management practices [13] (Figure 1). The utilization

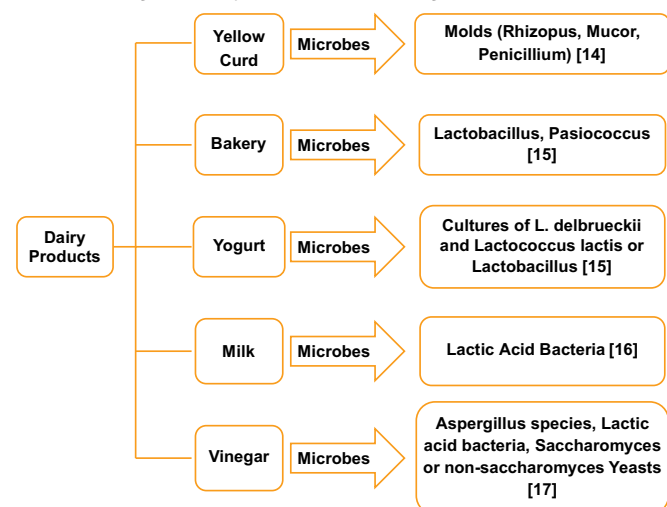


Figure 1: Different Types of Dairy Products and Microbiota Used in Dairy Production

of yoghurt increases day by day around the world. Yoghurt is the most important and popular cultured product. It contains a nutritional value and is beneficially important for

human health. It is produced by the milk through the fermentation process. Yoghurt is a nutritious food with fat (0-3.5%), proteins (4.6-5.2%), lactose, and other minerals such as calcium, phosphorus, and potassium. It is made through milk fermented with cultures of *L. delbrueckii* and *Lactococcus lactis* or *Lactobacillus plantarum* [15]. Yellow curd (YC) is a traditional Iranian food that is made from yoghurt, wheat flour, and local herbs and species. The most abundant bacteria in yellow curd were *Lactobacillus* (57%), *Pediococcus* (14%), and *Streptococcus* (12%). *Lactobacillus* plays a crucial role in traditional fermentation samples and is known for its probiotic and technological benefits [15]. Custard cream spoilage is not well studied, even though it's widely used in desserts like cream puffs and pastries. It is made from milk, sugar, eggs and sometimes vanilla or starch custard cream is a nutrient medium that can encourage bacterial growth, even when chilled. Spoilage has been linked to bacteria such as *Bacillus cereus*, *Strephlococci* lactic acid, and Psychotropic Gram-negative rods [18].

Yeast

Yeasts contribute minimally to dairy fermentations, but some fermented milk products naturally contain yeast, resulting in unique characteristics. Unlike products made solely with lactic acid bacteria, these have different physical and microbiological properties. In these products, yeast activity leads to mild alcoholic fermentation alongside the lactic acid fermentation driven by bacteria.

Non-Starter Lactic Acid Bacteria

Mesophilic lactobacilli, though overshadowed by *Lactococcus* during milk acidification, play a role in cheese ripening as secondary flora. They are especially common in raw milk cheeses but are also found in pasteurized varieties. Propionic acid bacteria are key secondary microorganisms in Swiss-type cheeses. Following lactic acid fermentation, they convert lactate into propionate, acetate, and carbon dioxide, the latter creating the characteristic holes, or "eyes," in the cheese. Recently, there has been renewed interest in their role in enhancing flavor.

Curd

Curd is a dairy product that is obtained by coagulation of milk. And the process that is used is curdling. *Lactobacillus* is the genus of bacteria and its main function is to convert sugar into lactic acid by the process of fermentation. *Lactobacillus* can convert lactose into lactic acid and provide a sour taste to curd. When acidic substances like vinegar or lemon juice are added then it will curdle the milk into two separate parts. The liquid part is known as whey and the solid part is known as curd. So, the whey contains the whey protein of milk, whereas the curd contains casein. When the milk gets older it is highly separated without

adding any citric acid. *Lactobacillus* and *Streptococcus* bacteria enhance the flavor and texture of the curd by producing volatile compounds like acetic acid, diacetyl, and acetaldehyde.

Yogurt

It is produced by the process of fermentation of milk by two specific species of bacteria *Lactococcus thermophilus* and *Lactobacillus bulgaricus* which they used as a starter culture and added to the milk. It is prepared by heating milk at about 80°C to kill any type of additional bacteria that are present in the milk. Milk is allowed to cool slowly and it is inoculated with a bacterium and then allowed to ferment at room temperature. The bacteria used in the formation of yoghurt are *Streptococcus Salivarius* subsp. *Thermophilus* and *Lactobacillus delbrueckii* subsp. Probiotic bacteria which include *Lactobacillus acidophilus*, *Bifidobacteria*, and *Streptococcus thermophilus* these species are highly used in the formation of yoghurt and it is known as bioyoghurt. As the fermentation process is used in the formation of yoghurt, then these microbes contain lactose that produces lactic acid [19]. So, lactic acid creates an acidic environment and lowers the pH of the milk. This acidic environment can cause casein milk protein to coagulate and denaturation, forming a semi-solid texture. On the other hand, it is responsible for yoghurt thickness and structure. Then, lactic acid is responsible for the tangy flavor while another bacterial activity provides a creamy texture to the yoghurt.

Cheese

Cheese is a dairy product that is formed by the process of coagulation of milk protein, and then it separates the curds (solid part) from the whey (liquid part). Curd and whey help in the ripening and ageing of cheese. The production of cheese is similar to the production of yoghurt but it contains some additional steps and other enzymes are also involved [20]. So, the coagulation depends on two methods which include acidification and proteolysis. Acidification occurs when the lactic acid bacteria ferment the lactose then they produce lactic acid. Some bacterial strains which include *Streptococcus thermophilus*, *Lactococcus lactis*, and *Lactobacillus* sp. are used in the production of cheese. The acidification causes casein to coagulate also involved in the production of cheese which includes chymosin (it is a protease enzyme that helps to break protein). In the second step, the curd which holds the casein and milk fat is separated from the whey. Depending on the variety of cheese, the curd can be heated, salted, pressed, and after all, molded into various shapes and sizes [21]. Salt is added which helps to enhance the flavor and helps in the preservation of cheese. During the stage of ageing the cheese is transformed into fresh cheese in which its flavor, texture, nature, and of cheese are highly due to the

presence of different microbes. The cheese flavor is highly associated with the catabolism of amino acids. Different amino acids are responsible for different flavors which are as follows. I-Aromatic amino acids which include (Phe, Trp, and Tyr) produce chemical, fecal flavors, and floral. I-sulfur-containing amino acids including Cys and Met) are transferred to meaty, garlic flavors and boiled cabbage. III-Branched chain amino acids including Leu, Ile, and Val) are converted into a fruity, sweaty flavor and malty [22].

Kefir

Kefir is a fermented dairy drink produced only when specific microbes act on milk. It is made up of kefir grains and some other combination of yeast, bacteria, acetic acid bacteria, and mycelial fungi. Lactic acid bacteria like *Lactobacillus acidophilus*, *Lactobacillus casei*, and *Lactobacillus kefir*, etc. On the other hand, acetic acid bacteria include *Acetobacter acetic* and yeast include *Candida*, *Saccharomyces*, and *Torula kefir*. These grains and bacteria are added to the milk and show a symbiotic relationship. Over time, typically about 12–48 hours at room temperature, yeast and bacteria in the grains start fermentation in the milk. This process produces carbon dioxide, lactic acid, and less amount of alcohol, giving a slightly tangy flavor. Accumulation of lactic acid makes the pH of the milk decrease and causes the protein to coagulate the milk to become thick. As a result, the creamy texture of kefir occurs. The last stage is after the fermentation, the kefir grains are removed and result in kefir [23].

Kumis

Kumis is also similar to the kefir but it contains liquid starter culture as compared to kefir grains which produce bactericides, antibiotics, and lactic acid. It is usually made by the process of fermentation (lactose into lactic acid and alcohol). Traditionally, mares' milk is used in Kumis because of lactose concentration. This lactose is essential for the fermentation process. As the milk is fermented, then the bacteria produce lactic acid which provides a sour flavor, while the yeast in the Kumis produce carbonation and alcohol. After ageing, kumis is aged for a few days to enhance their flavor complexity [24]. To ensure a thorough and systematic approach, this review article on the role of microbes in dairy product production was structured methodically. The initial step involved defining the scope, emphasizing prominent microbial species such as *Streptococcus*, *Lactobacillus*, and *Bifidobacterium*, which are integral to dairy fermentation processes. The review also sought to investigate their contributions to the production of various dairy products, including yoghurt, butter, cheese, kefir, and buttermilk. Additionally, it examined the impact of these microbes on the flavor, texture, nutritional profile, and shelf life of these products,

while also addressing challenges and advancements in microbial applications across traditional and industrial dairy production systems.

Literature Search Strategy

The literature search strategy for this review on the role of microbes in dairy product production was designed to be thorough and systematic, aiming to identify relevant research from various scientific sources. Key databases, including PubMed, Scopus, and Google Scholar, were searched to gather a diverse range of studies related to microbial activity in dairy production. The search used specific keywords such as "microbes," "lactic acid bacteria," "dairy production," "probiotics," "fermentation," "starter cultures," and "microbial enzymes," combined with Boolean operators to narrow and refine the results [25]. The search was limited to articles published between 2010 and 2024 ensuring that only the most up-to-date research was included. Studies were selected based on predefined criteria, focusing on peer-reviewed research that explored microbial roles in fermentation, flavor enhancement, texture changes, and preservation in dairy products [26]. Special emphasis was placed on studies discussing starter cultures, probiotics, and microbial enzymes. Articles that were non-peer-reviewed, unrelated to dairy production, or published in languages other than English were excluded. The screening process began with an assessment of titles and abstracts, followed by a full-text review of the relevant studies to assess methodological quality and relevance. Data management tools like EndNote and Excel were used to organize references and extract essential information. This strategy enabled the review to comprehensively synthesize current knowledge on the microbial role in dairy product production, emphasizing recent advancements and identifying research gaps for future exploration.

Inclusion and Exclusion Criteria

The inclusion and exclusion criteria for this review were established to ensure the selection of relevant and high-quality studies focusing on the role of microbes in dairy production. Studies eligible for inclusion specifically addressed microbial contributions to processes such as fermentation, flavor development, texture improvement, and preservation in dairy products [27]. Priority was given to research on key microbial strains such as *Lactococcus*, *Bifidobacterium*, *Streptococcus*, and *Lactobacillus* as well as their use in starter cultures, probiotics, and microbial enzymes. Only peer-reviewed original research articles, systematic reviews, and meta-analyses published between 2010 and 2024 were included to capture recent advancements in the field. Articles were required to be in English and employ either traditional microbiological methods or modern techniques like metagenomics, proteomics, and metabolomics. The review also

incorporated studies exploring a range of dairy products, including cheese, kefir, yoghurt, buttermilk, and other fermented milk products. Studies were excluded if they did not specifically address dairy production or the role of microbes in dairy-related processes. Research that concentrated on non-microbial aspects, such as chemical or mechanical methods, was not considered [28]. Non-peer-reviewed sources, including conference proceedings, promotional materials, and opinion pieces were also excluded. Articles written in languages other than English or those that lacked adequate methodological detail or clear conclusions were omitted. Additionally, research focusing on microbes in non-dairy food products or unrelated industrial applications was not included. Studies published before 2010 were excluded unless they offered significant foundational insights crucial for understanding historical progress in the field. These exclusion criteria were implemented to maintain a precise and thorough analysis of microbial contributions to dairy production [29]. Tools like EndNote and Excel were employed to effectively manage and organize the data gathered from the literature search. EndNote was mainly used to store and arrange references, ensuring accurate citation management and easy access to relevant studies. It also enabled the classification of articles based on key topics such as microbial species, fermentation processes, and types of dairy products. For data extraction and organization, Excel was used to summarize key details from each study, including the microbial strains investigated, the methodologies applied, and the results obtained. This approach facilitated an efficient comparison of findings across the studies. By leveraging these tools, the review process was made more efficient, providing a structured and organized way to synthesize the literature on microbial roles in dairy product production [30].

Quality Assessment of Studies

The quality assessment of studies was an essential part of the review process to ensure the inclusion of dependable and high-quality research [31]. Each study was examined based on several critical factors, such as the clarity and rigor of its design, the suitability of the methodologies used, and the reliability of the results. Preference was given to studies that employed robust experimental designs, including appropriate control groups, sufficient sample sizes, and reproducible outcomes [32]. The transparency of the methodology was another important consideration, with studies that provided clear protocols for microbial identification, fermentation techniques, and data analysis being favoured. Additionally, the quality of the study's reporting was evaluated, with a focus on how comprehensive the findings were, whether relevant data were included, and how well-supported the conclusions

were. Only studies demonstrating strong methodological quality and scientific rigor were included in the review, ensuring that the findings were credible and directly relevant to understanding the role of microbes in dairy product production [33]. In some fermented milk products, certain yeasts have limited roles, and that too, are not important. They release only moderate alcohols and carbonation along with the lactic acid that is formed by the bacteria. This alters the product's texture, taste, as well as the smell of the product, making the product mildly effervescent and possess a different taste. These differences make them different from products that contain only lactic acid bacteria, which give a relatively simple sour taste and rather stiff structure (Table 1).

Table 1: Yeast Involvement in Dairy Products

Aspects	Yeast-Involved Products	Lactic Acid Bacteria Products	Reference
Taste	Unique, Mildly Effervescent	Simple Sour Taste	[34]
Texture	Softer, with Slight Carbonation	Stiffer Structure	
Aroma	Distinct, Due to Alcohol Traces	Plain, Lactic Acid-Driven Aroma	

As stated in the research article, the results that we should discuss here are in Mesophilic lactobacilli though less active than *Lactococcus* in the initial periods of milk acidification they occupy an important secondary position in the cheese ripening process. These bacteria are most commonly seen in cheeses made from raw-milk cheese however this bacterium can also be found in pasteurized ones as well. They clarify it during the ripening process in that they take part in the formation of the cheese characteristics which is maturing. These bacteria not only improve the taste of cheese but also improve the texture of the cheese ultimately making the cheese more enjoyable (Table 2).

Table 2: Bacteria Used in Different Metabolism

Process Steps	Actions	Results	Reference
Lactate Metabolism	Propionic Acid Bacteria Break Down Lactate	Formation of Propionic and Acetic Acids	[35]
Carbon Dioxide Production	Byproduct of Fermentation	Creation of 'Holes' in Swiss Cheese	
Flavor Development	Fermentation Products Influence Taste	Unique Flavor Profile	
Research Focus	Study of Bacterial Roles in Cheese-Making	Diversification of Cheese Varieties	

As mentioned in the research article the results have been interpreted should become in Propionic acid bacteria are important for the formation of Swiss-type cheeses. After that, they metabolize lactate into propionic acid, acetic acid, and carbon dioxide Their fermentation products include. Carbon dioxide forms the 'holes' or eyes in the cheese. In the recent past, there has been much focus on understanding the role of these bacteria in creating flavor profiles and exponentially increasing the diversification of cheese [17]. The results we have interpreted that curd is

formed by coagulating milk where *Lactobacillus* change the lactose into lactic acid resulting in the curd having an acceptably sour taste. When a larger quantity of acid like vinegar or lemon is included in milk the milk separates into curd and whey. *Lactobacillus* and *Streptococcus* bacteria add to the flavor of curd and in the case of diacetyl the texture (Table 3).

Table 3: Different Process Used in Curd Products

Process Steps	Actions	Results	Reference
Coagulation	<i>Lactobacillus</i> Ferments Lactose To Lactic Acid	Sour Taste and Curd Formation	[36]
Acid Addition	Vinegar or Lemon Causes Curd-Whey Separation	Rapid Curdling	
Bacterial Activity	<i>Lactobacillus</i> and <i>Streptococcus</i> Enhance Flavor	Improved Taste and Texture	
Diacetyl Production	Created by Bacteria	Contributes to Smooth Texture	

Yoghurt is produced using bacteria such as *Lactococcus thermophilus* and *Lactobacillus bulgaricus* that help change lactose to lactic acid. This acid reduces the pH of milk, solidifies the proteins to a semi-solid state and imparts taste to yoghurt and the core It also imparts a tangy taste and creamy texture to yoghurt (Table 4).

Table 4: Different Processes Used in Milk

Process Steps	Actions	Results	Reference
Fermentation	Bacteria Convert Lactose into Lactic Acid	Acidification of Milk	[37]
Protein Solidification	Reduced pH Solidifies Milk Proteins	Semi-Solid Texture	
Flavor Development	Lactic Acid Activity	Tangy Taste and Creamy Consistency	

As we can consider, as the article reviewed, we researching might, Cheese is a dairy product that is produced through the process of coagulation of milk proteins. Some lactic acid bacteria are specialized in lactose to lactic acid conversion, which makes casein clump and thus form a curd while the waste material is known as whey. Such enzymes as chymosin continue the protein coagulation leading to curd formation. Those curds are subjected to heat, salt, pressure and ripening to form textures and flavors in the cheese. Microorganisms act on amino acids during ageing to create a litany of various flavors (Table 5).

Table 5: Different Process Used in Cheese Products

Process Steps	Actions	Results	Reference
Coagulation	Lactic Acid Thickens Casein	Separation of Curds and Whey	[38]
Enzymatic Breakdown	Chymosin Breaks Down Proteins	Formation of Curds	
Processing	Heating, Salting, and Pressing	Improved Texture and Preservation	
Ageing	Microbial Breakdown of Amino Acids	Development of Distinct Flavors	

when reviewing the researched article results could be, during fermentation, bacteria for example, *Lactobacillus* and *Streptococcus* and yeast by way of *Saccharomyces*

and *Candida* catalyze the change of lactose into lactic acid, alcohol and carbon dioxide. This process provides kefir with a sour flavor, mild carbonated, and smooth. Kefir can be used as a friendly bacterial culture for yoghurt making process. There are both bacteria and yeast in kefir therefore making it a good source of probiotics, which are good for the tummy. Furthermore, the process of fermentation increases the nutritional quality of the included components (Table 6).

Table 6: Different Processes Used in Kefir Products

Component	Role in Fermentation	Results	Reference
Lactic Acid Bacteria	Ferments Lactose into Lactic Acid	Tart Taste, Probiotic Benefits	[39]
Yeast (<i>Saccharomyces</i> , <i>Candida</i>)	Produces Alcohol and Carbon Dioxide	Fizz and Creamy Texture	
Combined Action	Synergistic Fermentation	Nutritional Enhancement	

Milk and milk products have been a significant part of Pakistan's agricultural and food market and the basic products in this sector include milk, cheese, yoghurt and butter. Biological technologies in the production and processing of these products have remained the key factors in improving the quality, nutritional value and shelf life of such products. Given the fact that Pakistan is among the largest producers of milk in the world, the country presents a lot of risks for industries that engage in the use of microbes in the dairy business. These are in areas such as food processing, pharmaceuticals, biotechnology and farming. Players in the dairy chains source microbes like lactic acid bacteria (LAB), probiotics and enzymes to fulfil the consumer's need for healthy, functional and sustainable products. It is only in recent times that the biopharmaceutical industry of Pakistan has begun to realize the opportunities offered by dairy-based substrates for microbial enzyme production. Some of the microorganisms with enzymes such as lactase aid in the production of lactose-free products. Moreover, certain components of dairy are employed in the subculture of microbes for antibiotic production especially *Penicillium* strains [40]. Even though this industry is not fully developed in Pakistan, dairy products are easily available and relatively low-cost inputs are required for microbial boosters in pharmaceutical production. Biofuels and bioplastics that are developed industries also often use microbes farmed on dairy leftovers. Cheese manufacture results in whey, and because of the nutritional value of this product, microbial fermentation is highly recommended [17]. In Pakistan, research is being conducted and attempted on the usage of whey for the generation of bioethanol and several other biofuels. Likewise, some bacterium transforms the waste generated by the use of milk into poly-hydroxy-alkanoates (PHAs), a kind of bioplastic. In addition, these applications help to put value in dairy waste, solve environmental issues, and produce a

circular model [41]. This food and beverage sector in Pakistan incorporates high ingredients of dairy products for microbial fermentation. Examples of foods that use bacterial cultures include yoghurt which uses *Lactobacillus* and *Streptococcus* bacteria, cheese and kefir. Currently, the demand for probiotic-containing dairy products is on the rise and therefore; food manufacturing firms both domestic and international players in Pakistan have been directing their investments on these products. Beneficial microbes dominate dairy substrates where milk is converted into functional foods in accordance to the health-conscience market. The increasing understanding of gut health has introduced an opportunity that calls for integration between the dairy industry and microbial research facilities. This sector employs agents such as Rennet through microbial fermentation in the preparation of cheese. Lactose is also excluded through microbial enzymes to meet the lactose-sensitive market demand. In Pakistan, the biotechnology industry has also started implementing these processes to exploit its home and export markets [42]. The cosmetics industry is using microbes cultured in a dairy substrate to develop bioactive chemicals. Microbial fermentation-based compounds for instance hyaluronic acid and peptides are used in cosmetics [43]. This industry in Pakistan is inclined towards these natural and environmentally friendly approaches and can fulfil international customer demands for organic makeup [44]. In the dairy sector, microbes are very useful for the preparation of cultures that are used to support products such as cheese and yoghurt. Pakistan's dairy businesses are now exploring microbial technology to enhance fermentation operations product quality and shelf life [45]. In their internal application, these microbes encourage local manufacturing and lower reliance on imported cultures. Waste from the dairy industry including whey and spoilt milk can be converted to biofuels and fertilizer through the use of microbes. Sewage waste such as such waste is today finding its way into Pakistan's biogas plants with microbes decomposing it into methane and carbon dioxide. This approach of taking time to implement energy solutions fits well with the country's strategy to embrace sustainable energy solutions [46].

Future Perspective

Although microbes have played a vital part in dairy production for centuries, their significance is only expected to grow in the upcoming decades as a result of developments in biotechnology, rising consumer demand for environmentally friendly and healthier food products, and a better understanding of microbial ecosystems. Some of the future perspectives are mentioned. The market for dairy products, notably kefir and yoghurt that contain bacteria that are beneficial to health when ingested in sufficient quantities is already expanding. Probiotic dairy

products will proliferate in the future, with a wider variety of strains designed to enhance immune function, improve gut health, or treat certain medical issues like lactose intolerance or even mental health [47]. Also, by improving the beneficial microbial populations in the gut or producing strains that are resistant to pathogens, advanced genetic engineering may enable the creation of personalized probiotics that can more successfully target illnesses. While current technological advances allow for more control over microbial activity, traditional fermentation techniques have relied on naturally occurring microbial populations. By altering their genetic composition, scientists will be able to create microorganisms with extremely precise characteristics, such as the capacity to manufacture specific tastes, vitamins, or bioactive peptides, because of the development of synthetic biology. This will make it possible to produce dairy products with even more accuracy, enhancing their texture, flavor profiles, and nutritional value. Furthermore, dairy proteins like casein or whey can be produced using precision fermentation instead of animal milk, resulting in completely new kinds of dairy-like products that may help satisfy consumer desire for plant-based or lab-grown substitutes [48]. Dairy production is probably going to be significantly impacted by personalized nutrition. Developments in microbiome science may make it possible to produce dairy products that are especially suited to a person's genetics, gut microbiota, and medical requirements [49]. To maximize the health advantages for every customer, this might involve developing customized probiotic strains, prebiotics, or even particular kinds of dairy proteins. There is growing pressure on the dairy business to adopt a more sustainable practice. Improved feed digestibility and lower methane emissions from dairy cows are a couple of demonstrations of how microbial technologies may help dairy farmers adopt more environmentally friendly methods [50]. To reduce waste and increase resource efficiency, microbes may also be utilized to upcycle dairy waste, such as whey, into useful goods like protein isolates or bioactive compounds. There will probably be a big change in the dairy industry in the future toward functional meals. Dairy products will be more often designed to provide particular health advantages, such as reduced inflammation, better digestion, or boost immunity, as scientific understanding of the microbiome and gut health improves [51]. Synthetic biology-created microbial cell factories can produce dairy proteins like whey and casein for use in plant-based or allergy-free substitutes that replicate the flavors and textures of traditional dairy products [52]. Probiotic strains that can tolerate environmental stressors like heat and acidic pH are being found and improved using genomic methods. These resistant strains increase the probiotics' stability

and effectiveness in dairy products, guaranteeing that their health benefits continue even after processing and storage. NGPs are modified strains created to offer improved advantages such as customized medicinal effects, targeted delivery, and gut microbiota manipulation. They might be significant in creating dairy products that are enhanced with bioactive substances for therapeutic and individualized nutrition. This invention is the result of developments in bioinformatics and synthetic biology, which enable accurate strain engineering and selection [53]. The use of microbial fermentation to produce non-dairy functional foods that replicate the nutritional profile and sensory qualities of conventional dairy products is becoming more popular as lactose sensitivity and veganism increase. This includes goods like probiotic-fermented plant-based cheeses and yoghurts, which broaden the range of dairy-like uses while preserving health advantages [54-57]. AI and machine learning are becoming more and more useful technologies for improving fermentation and microbial strain selection. These technologies can improve flavor profiles, anticipate microbial behaviour, and maximize the nutritional content of dairy products by evaluating massive databases [58-60].

CONCLUSIONS

It was concluded that as customers look for more creative, sustainable, and nutrient-dense food options, microbes will become more and more significant in the manufacture of dairy products. Microbes will increasingly shape the future of dairy products as a result of developments in fermentation technology, synthetic biology, and microbial genomics. The future of dairy is probably going to be impacted by the untapped potential of microbial innovation, whether it is through the development of novel probiotic strains, the application of microbes in environmentally friendly production methods, or the creation of entirely new dairy-like products. By enabling customized and regionalized flavor profiles that satisfy a range of customer tastes, microbial collaborations could be used to improve the taste, texture, and shelf life of products. Additionally, combining artificial intelligence with microbial fermentation systems could optimize industrial procedures, lowering expenses and increasing productivity.

Authors Contribution

Conceptualization: MN

Methodology: MN, AA, JE, FS

Formal analysis: MN

Writing review and editing: SP, KAK

All authors have read and agreed to the published version of the manuscript.

Conflicts of Interest

All the authors declare no conflict of interest.

Source of Funding

The authors received no financial support for the research, authorship and/or publication of this article.

REFERENCES

- [1] Grout L, Baker MG, French N, Hales S. A Review of Potential Public Health Impacts Associated with the Global Dairy Sector. *Geo-Health*. 2020 Feb; 4(2): e2019GH000213. doi: 10.1029/2019GH000213.
- [2] Kalsoom, M., Rehman, F. U., Shafique, T., Junaid, S., Khalid et al.. Biological Importance of Microbes in Agriculture, Food and Pharmaceutical Industry: A Review. *Innovare Journal of Life Sciences*. 2020 8(6): 1-4. doi: 10.22159/ijls.2020.v8i6.39845.
- [3] Gholami-Shabani M, Shams-Ghahfarokhi M, Razzaghi-Abyaneh M. Food Microbiology: Application of Microorganisms in Food Industry. 2023. doi: 10.5772/intechopen.109729.
- [4] Nain N, Kumari KG, Haridasan H, Sharma SG. Microbes in the Food and Beverage Industry. Microbial Diversity, Interventions and Scope. 2020: 249-58. doi: 10.1007/978-981-15-4099-8_15.
- [5] Noshirvani N, Abolghasemi Fakhri L. Advances in Extending the Microbial Shelf-Life of Bread and Bakery Products Using Different Technologies: A Review. *Food Reviews International*. 2024 Aug; 1-26. doi: 10.1080/87559129.2024.2386029.
- [6] Smith JP, Daifas DP, El-Khoury W, Koukoutsis J, El-Khoury A. Shelf Life and Safety Concerns of Bakery Products—A Review. *Critical Reviews in Food Science and Nutrition*. 2004 Jan; 44(1): 19-55. doi: 10.1080/10408690490263774.
- [7] Saranraj P and Geetha M. Microbial Spoilage of Bakery Products and Its Control by Preservatives. *International Journal of Pharmaceutical and Biological Archives*. 2012 Jan; 3(1): 38-48.
- [8] Román-Camacho JJ, Mauricio JC, Santos-Dueñas IM, García-Martínez T, García-García I. Recent Advances in Applying Omic Technologies for Studying Acetic Acid Bacteria in Industrial Vinegar Production: A Comprehensive Review. *Biotechnology Journal*. 2024 Feb; 19(2): 2300566. doi: 10.1002/biot.202300566.
- [9] Abid J, Padmapriya G, Thakur D, Balaji J, Chauhan AS, Shah MA. Acetic Fermentation and Health Effects: An In-Depth Examination of Grain Vinegars and Their Production Technologies: A Review. *CyTA—Journal of Food*. 2024 Dec; 22(1): 2393758. doi: 10.1080/19476337.2024.2393758.
- [10] Nezhad Razmjoui Akhgar R, Shaviklo A. Investigating the Chemical and Microbial Characteristics of Kermanshahi Ghee and Azerbaijan Yellow Ghee During the Storage Period. *Food Research Journal*. 2024 Sep; 34(3): 53-68.
- [11] Pena-Serna C and Restrepo-Betancur LF. Chemical, Physicochemical, Microbiological and Sensory. *Food Science and Technology*. 2020 Jun; 40: 444-50.
- [12] Kirazci A and Javidipour I. Some Chemical and Microbiological Properties of Ghee Produced in Eastern Anatolia. *International Journal of Dairy Technology*. 2008 Aug; 61(3): 300-6. doi: 10.1111/j.1471-0307.2008.00402.x.
- [13] Owusu-Kwarteng J, Akabanda F, Agyei D, Jespersen L. Microbial Safety of Milk Production and Fermented Dairy Products in Africa. *Microorganisms*. 2020 May; 8(5): 752. doi: 10.3390/microorganisms8050752.
- [14] Bhatia SK, Otari SV, Jeon JM, Gurav R, Choi YK, Bhatia RK et al. Biowaste-to-Bioplastic (Polyhydroxyalkanoates): Conversion Technologies, Strategies, Challenges, and Perspective. *Bioresource Technology*. 2021 Apr; 326: 124733. doi: 10.1016/j.biortech.2021.124733.
- [15] Dan T, Hu H, Tian J, He B, Tai J, He Y. Influence of Different Ratios of *Lactobacillus Delbrueckii* Subsp. *Bulgaricus* and *Streptococcus Thermophilus* on Fermentation Characteristics of Yogurt. *Molecules*. 2023 Feb; 28(5): 2123. doi: 10.3390/molecules28052123.
- [16] Yu J, Mo L, Pan L, Yao C, Ren D, An X et al. Bacterial Microbiota and Metabolic Character of Traditional Sour Cream and Butter in Buryatia, Russia. *Frontiers in Microbiology*. 2018 Oct; 9: 2496. doi: 10.3389/fmicb.2018.02496.
- [17] Bücher C, Burtcher J, Domig KJ. Propionic Acid Bacteria in the Food Industry: An Update on Essential Traits and Detection Methods. *Comprehensive Reviews in Food Science and Food Safety*. 2021 Sep; 20(5): 4299-323. doi: 10.1111/1541-4337.12804.
- [18] Techer C, Jan S, Thierry A, Maillard MB, Grosset N, Galet O et al. Identification of the Bacteria and their Metabolic Activities Associated with the Microbial Spoilage of Custard Cream Desserts. *Food microbiology*. 2020 Apr; 86: 103317. doi: 10.1016/j.fm.2019.103317.
- [19] García-Burgos M, Moreno-Fernández J, Alférez MJ, Díaz-Castro J, López-Aliaga I. New Perspectives in Fermented Dairy Products and their Health Relevance. *Journal of Functional Foods*. 2020 Sep; 72: 104059. doi: 10.1016/j.jff.2020.104059.
- [20] Gänzle M and Gobbetti M. Physiology and Biochemistry of Lactic Acid Bacteria. In *Handbook on Sourdough Biotechnology*. 2012 Oct: 183-216. doi:

- 10.1007/978-1-4614-5425-0_7.
- [21] Singh TK, Drake MA, Cadwallader KR. Flavor of Cheddar Cheese: A Chemical and Sensory Perspective. *Comprehensive Reviews in Food Science and Food Safety*. 2003 Oct; 2(4): 166-89. doi: 10.1111/j.1541-4337.2003.tb00021.
 - [22] Zheng X, Shi X, Wang B. A Review on the General Cheese Processing Technology, Flavor Biochemical Pathways and the Influence of Yeasts in Cheese. *Frontiers in Microbiology*. 2021 Jul; 12: 703284. doi: 10.3389/fmicb.2021.703284.
 - [23] Egea MB, Santos DC, Oliveira Filho JG, Ores JD, Takeuchi KP, Lemes AC. A Review of Nondairy Kefir Products: Their Characteristics and Potential Human Health Benefits. *Critical Reviews in Food Science and Nutrition*. 2022 Feb; 62(6): 1536-52. doi: 10.1080/10408398.2020.1844140.
 - [24] Bajaj A, Sharma S, Regassa H, Ameen F, Gudeta K. Bio-Production of Fermented Dairy Products and Health Benefits: A Review of the Current Scenario and Prospects. 2023 Jul.
 - [25] Sharma BR, Halami PM, Tamang JP. Novel Pathways in Bacteriocin Synthesis by Lactic Acid Bacteria with Special Reference to Ethnic Fermented Foods. *Food Science and Biotechnology*. 2021 Oct; 1-6. doi: 10.1007/s10068-021-00986-w.
 - [26] Stegmayer MÁ, Sirini N, Frizzo LS, Fernández-López J, Álvarez JÁ, Rosmini MR *et al.* Enrichment of Foods with Prebiotics. In *Strategies to Improve the Quality of Foods*. 2024 Jan: 171-201. doi: 10.1016/B978-0-443-15346-4.00007-0
 - [27] Liberati A, Altman DG, Tetzlaff J, Mulrow C, Gøtzsche PC, Ioannidis JP *et al.* The PRISMA Statement for Reporting Systematic Reviews and Meta-Analyses of Studies That Evaluate Health Care Interventions: Explanation and Elaboration. *Annals of Internal Medicine*. 2009 Aug; 151(4): W-65. doi: 10.7326/0003-4819-151-4-200908180-00136.
 - [28] Jpt H. *Cochrane Handbook for Systematic Reviews of Interventions*. 2008.
 - [29] Moher D, Liberati A, Tetzlaff J, Altman DG, PRISMA Group* T. Preferred Reporting Items for Systematic Reviews and Meta-Analyses: The PRISMA Statement. *Annals of Internal Medicine*. 2009 Aug; 151(4): 264-9. doi: 10.7326/0003-4819-151-4-200908180-00135.
 - [30] Ouzzani M, Hammady H, Fedorowicz Z, Elmagarmid A. Rayyan—A Web and Mobile App for Systematic Reviews. *Systematic Reviews*. 2016 Dec; 5: 1-0. doi: 10.1186/s13643-016-0384-4.
 - [31] Salameh JP, Bossuyt PM, McGrath TA, Thombs BD, Hyde CJ, Macaskill P *et al.* Preferred Reporting Items for Systematic Review and Meta-Analysis of Diagnostic Test Accuracy Studies (PRISMA-DTA): Explanation, Elaboration, and Checklist. *British Medical Journal*. 2020 Aug; 370. doi: 10.1136/bmj.m2632.
 - [32] Chandler J, Cumpston M, Li T, Page MJ, Welch VJ. *Cochrane Handbook for Systematic Reviews of Interventions*. Hoboken: Wiley. 2019.
 - [33] Sterne JA, Egger M, Moher D. Addressing Reporting Biases. *Cochrane Handbook for Systematic Reviews of Interventions: Cochrane Book Series*. 2008 Sep: 297-333. doi: 10.1002/9780470712184.ch10.
 - [34] Li Y, Wang C, Wang J. Establishment of a Rapid Counting Method for Lactic Acid Bacteria and Yeast in Dairy Products. *International Journal of Dairy Technology*. 2024 May; 77(2): 415-26. doi: 10.1111/1471-0307.13063.
 - [35] Serrazanetti DI, Gottardi D, Montanari C, Gianotti A. Dynamic Stresses of Lactic Acid Bacteria Associated to Fermentation Processes. In *Lactic Acid Bacteria—R and D for Food, Health and Livestock Purposes*. IntechOpen. 2013 Jan.
 - [36] Kandasamy S, Park WS, Bae IS, Yoo J, Yun J, Hoa VB *et al.* HRMAS-NMR-Based Metabolomics Approach to Discover Key Differences in Cow and Goat Milk Yoghurt Metabolomes. *Foods*. 2024 13(21), 3483. doi: 10.3390/foods13213483.
 - [37] Dias PG, Sajiwan JW, Rathnayaka RM. Consumer Perception and Sensory Profile of Probiotic Yogurt with Added Sugar and Reduced Milk Fat. *Heliyon*. 2020 Jul; 6(7). doi: 10.1016/j.heliyon.2020.e04328.
 - [38] Foegeding EA, Brown J, Drake M, Daubert CR. Sensory and Mechanical Aspects of Cheese Texture. *International Dairy Journal*. 2003 Jan; 13(8): 585-91. doi: 10.1016/S0958-6946(03)00094-3.
 - [39] Marsh AJ, O'Sullivan O, Hill C, Ross RP, Cotter PD. Sequencing-Based Analysis of the Bacterial and Fungal Composition of Kefir Grains and Milks from Multiple Sources. *PloS one*. 2013 Jul; 8(7): e69371. doi: 10.1371/journal.pone.0069371.
 - [40] Alzahrani F, Akanbi TO, Scarlett CJ, Aryee AN. The Use of Immobilised Enzymes for Lipid and Dairy Processing and their Waste Products: A Review of Current Progress. *Processes*. 2024 Mar; 12(4): 634. doi: 10.3390/pr12040634.
 - [41] Rana A, Kumar V, Dhewa T, Taneja NK. Bioplastic Production Using Whey (Polyhydroxyalkanoates and Polyhydroxybutyrates). In *Whey Valorization: Innovations, Technological Advancements and Sustainable Exploitation*. Singapore: Springer Nature Singapore. 2023 Oct: 103-113. doi: 10.1007/978-981-99-5459-9_6.
 - [42] Sahu DK, Kashyap LL. Future of Food Industry Sustainability Using Biotechnological Interventions in The Dairy Sector. *Agricultural Biotechnology*

- Journal. 2024 Jan1;16(1).
- [43] Bae SE, Bae S, Park SJ, Lee P, Hyun CG. Microbial Consortium of Jeju Traditional Fermented Foods and Their Cosmetic Ingredient Potential. *Fermentation*. 2024 Jul; 10(7): 345. doi: 10.3390/fermentation10070345.
- [44] Krzyżostan M, Wawrzyńczak A, Nowak I. Use of Waste From the Food Industry and Applications of the Fermentation Process to Create Sustainable Cosmetic Products: A Review. *Sustainability*. 2024 Mar; 16(7): 2757. doi: 10.3390/su16072757.
- [45] Buldo P, Sokolowsky M, Hoegholm T. The Role of Starter Cultures on Oral Processing Properties of Different Fermented Milk Products. *Food Hydrocolloids*. 2021 May; 114: 106571. doi: 10.1016/j.foodhyd.2020.106571.
- [46] El-Aidie SA and Khalifa GS. Innovative Applications of Whey Protein for Sustainable Dairy Industry: Environmental and Technological Perspectives—A Comprehensive Review. *Comprehensive Reviews in Food Science and Food Safety*. 2024 Mar; 23(2): e13319. doi: 10.1111/1541-4337.13319.
- [47] Sharma V, Sharma N, Sheikh I, Kumar V, Sehrawat N, Yadav M et al. Probiotics and Prebiotics Having Broad Spectrum Anticancer Therapeutic Potential: Recent Trends and Future Perspectives. *Current Pharmacology Reports*. 2021 Apr; 7(2): 67-79. doi: 10.1007/s40495-021-00252-x.
- [48] Tamime AY, Saarela MA, Sondergaard AK, Mistry VV, Shah NP. Production and Maintenance of Viability of Probiotic Microorganisms in Dairy Products. *Probiotic dairy products*. 2005; 3: 39-63. doi: 10.1002/9780470995785.ch3
- [49] Kumar R., and Puniya AK. Probiotics in Dairy Products: A Review on the Mechanisms and Health Benefits. *Dairy Science and Technology*. 2016 96(5): 579-597.
- [50] Verma DK, Patel AR, Billoria S, Kaushik G, Kaur M, Editors. *Microbial Biotechnology in Food Processing and Health: Advances, Challenges, and Potential*. Chemical Rubber Company Press. 2022 Oct.
- [51] Agyei D, Owusu-Kwarteng J, Akabanda F, Akomea-Frempong S. Indigenous African Fermented Dairy Products: Processing Technology, Microbiology and Health Benefits. *Critical reviews in food science and nutrition*. 2020 Mar; 60(6): 991-1006. doi: 10.1080/10408398.2018.1555133.
- [52] Khalil AS, Collins JJ. Synthetic Biology: Applications Come of Age. *Nature Reviews Genetics*. 2010 May; 11(5): 367-79. doi: 10.1038/nrg2775.
- [53] Abouelela ME and Helmy YA. Next-Generation Probiotics as Novel Therapeutics for Improving Human Health: Current Trends and Future Perspectives. *Microorganisms*. 2024 Feb; 12(3): 430. doi: 10.3390/microorganisms12030430.
- [54] Papadopoulou OS, Doulgeraki A, Panagou E, Argyri AA. Recent Advances and Future Perspective in Probiotics Isolated from Fermented Foods: From Quality Assessment to Novel Products. *Frontiers in Microbiology*. 2023 Feb; 14: 1150175. doi: 10.3389/fmicb.2023.1150175.
- [55] Xia Y, Zeng Z, López Contreras A, Cui C. Innovative Microbial Technologies for Future and Sustainable Food Science. *Frontiers in Microbiology*. 2023 Jun; 14: 1215775. doi: 10.3389/fmicb.2023.1215775.
- [56] Techer C, Jan S, Thierry A, Maillard MB, Grosset N, Galet O et al. Identification of the Bacteria and their Metabolic Activities Associated with the Microbial Spoilage of Custard Cream Desserts. *Food Microbiology*. 2020 Apr; 86: 103317. doi: 10.1016/j.fm.2019.103317.
- [57] Bae SE, Bae S, Park SJ, Lee P, Hyun CG. Microbial Consortium of Jeju Traditional Fermented Foods and Their Cosmetic Ingredient Potential. *Fermentation*. 2024 Jul; 10(7): 345. doi: 10.3390/fermentation10070345.
- [58] Shamseer, L., Moher, D., Clarke, M., Ghersi, D., Liberati, A., Petticrew, M et al. Preferred Reporting Items for Systematic Review and Meta-Analysis Protocols (PRISMA-P) 2015: Elaboration And Explanation. *PLOS Medicine*. 2015; 12(3): e1001819. doi: 10.1136/bmj.g7647.
- [59] Verma DK, Patel AR, Billoria S, Kaushik G, Kaur M, Editors. *Microbial Biotechnology in Food Processing and Health: Advances, Challenges, And Potential*. Chemical Rubber Company Press. 2022 Oct.
- [60] Liberati A, Altman DG, Tetzlaff J, Mulrow C, Gøtzsche PC, Ioannidis JP et al. The PRISMA Statement for Reporting Systematic Reviews and Meta-Analyses of Studies that Evaluate Health Care Interventions: Explanation and Elaboration. *Annals of Internal Medicine*. 2009 Aug; 151(4): W-65. doi:10.7326/0003-4819-151-4-200908180-00136.

FUTURISTIC BIOTECHNOLOGY

<https://fbtjournal.com/index.php/fbt>

ISSN (E): 2959-0981, (P): 2959-0973

Volume 4, Issue 3 (July-Sep 2024)



Original Article



Insilico Insights into Resveratrol as a Potential Inhibitor of Mycobacterium Tuberculosis Enoyl-ACP Reductase (InhA) Protein

Obaid Ullah¹, Nimra Hanif², Ayesha², Abdul Qayyum Mufti², Fizza Amjad², Maleeha Manzoor³, Esha Jameel² and Sana Fatima⁴

¹Department of Computer Science, University of Agriculture, Faisalabad, Pakistan

²Department of Biotechnology, University of Central Punjab, Lahore, Pakistan

³Department of Basic and Applied Chemistry, University of Central Punjab, Lahore, Pakistan

⁴Department of Biological Sciences, Superior University, Lahore, Pakistan

ARTICLE INFO

Keywords:

Mycobacterium Tuberculosis, Resveratrol, Insilico, Drug, Enoyl-ACP Reductase

How to Cite:

Ullah, O., Hanif, N., Ayesha, ., Mufti, A. Q., Amjad, F., Manzoor, M., Jameel, E., & Fatima, S. (2024). Insilico Insights into Resveratrol as a Potential Inhibitor of Mycobacterium Tuberculosis Enoyl-ACP Reductase (InhA) Protein: Insilico Insights into Mycobacterium Tuberculosis Enoyl-ACP Reductase. *Futuristic Biotechnology*, 4(03), 27-33. <https://doi.org/10.54393/fbt.v4i03.134>

*Corresponding Author:

Obaid Ullah

Department of Computer Science, University of Agriculture, Faisalabad, Pakistan
obaidualahrana2@gmail.com

Received Date: 12th August, 2024

Acceptance Date: 23th September, 2024

Published Date: 30th September, 2024

ABSTRACT

Mycobacterium tuberculosis, the causative agent of tuberculosis, is a global cause of death. Thus, the development of innovative treatment strategies is required. **Objective:** To develop insilico drugs by phytochemicals to inhibit the Enoyl-ACP reductase (InhA) protein, which is essential for synthesizing mycobacterial cell walls. **Methods:** The 3D structure of InhA was taken from the Protein Data Bank. The Ramachandran plot validated the model with a score of 98.7% from the favoured Ramachandran plot. Computed Atlas of Surface Topography of Proteins was used to detect the active sites for ligand interaction. Resveratrol were selected based on existing studies and further listed for drug-likeness. Absorption, Distribution, Metabolism, Excretion, and Toxicity analysis showed the possibility of resveratrol as a drug candidate, with no violation of Lipinski rules and excellent absorption in the Gastrointestinal Tract. **Results:** The boiled egg model confirmed the ability of ligands to go through the blood-brain barrier. Toxicity predictions of resveratrol indicated low risks with several other systems of organs. Molecular docking with CB-Dock2 showed the strong binding of Resveratrol to InhA, with a Vina score equal to -8.8 kcal/mol. Further exploration of the docking complex by molecular docking simulation using the Integrated Management of the Public Distribution System was carried out, and the trajectory confirmed stable interaction and protein flexibility. **Conclusions:** It was concluded that resveratrol acts as a potent, non-toxic candidate for tuberculosis treatment and highlights its inhibition capacity of InhA. Results need future vitro and in vivo validation to develop this highly reliable therapeutic alternative for combating tuberculosis.

INTRODUCTION

Tuberculosis (TB) is an infectious disease caused by Mycobacterium tuberculosis that most often affects the lungs. It spreads through the air when an active TB infectious patient coughs, sneezes, or spits, and someone else inhales that air containing TB bacteria [1]. About 10 million people are infected due to Mycobacterium tuberculosis, and 5-10% of people will eventually get symptoms and develop TB disease [2]. While some tuberculosis patients struggle with treatment adherence, the implementation of Directly Observed Therapy (DOT) programs has been a significant success. These programs ensure compliance through supervised doses, either in

clinics or communities, and have proven cost-effective in reducing tuberculosis cases [3]. The emergence of drug-resistant tuberculosis strains underscores the need for advancements in treatment research [4]. Promising avenues include fluoroquinolones and alternative pharmaceutical categories such as oxazolidinones (like linezolid). Additionally, investigations into immune system-targeted therapies, such as enhancing Bacillus Calmette-Guérin (BCG) or Mycobacterium vaccae vaccines, and sterilization via the citrate lyase pathway, show promise [5]. InhA, also known as Enoyl-ACP reductase, is involved in the fatty acid synthesis pathway of



Mycobacterium tuberculosis, the causative agent of tuberculosis. This enzyme reduces enoyl-ACP to acyl-ACP, an essential step in elongating fatty acids required for mycolic acid biosynthesis [6]. Mycolic acids are long-chain fatty acids incorporated into the mycobacterial cell wall structure and provide the cell wall with its hydrophobic nature and resistance to most antibiotics [7]. The repression of *InhA* prevents the synthesis of mycolic acids and weakens the bacteria's cell wall, resulting in cell death. As a result, *InhA* is an attractive target for antitubercular agents, including isoniazid, which acts by blocking this enzyme to fight *Mycobacterium tuberculosis* infection [8]. Resveratrol is a phenolic compound in the stilbene family of bioactive agents identified primarily in grapes, berries, peanuts, and red wine. This, in turn, has generated much interest because of the interconnected multiple health uses and a highly effective antibacterial nature. Based on the information mentioned above, it can be concluded that Resveratrol acts against various bacteria, viruses, and fungi by affecting their cell walls and restricting their ability to synthesize their genetic material and essential metabolites [9]. This substance can also suppress the immune response and decrease inflammation, contributing to its excellent antimicrobial activity, thus pointing towards the need to use it in developing drugs for treating various infections. This distribution, combined with a broad-spectrum antimicrobial characteristic, stresses the possible use of Resveratrol in prevention and treatment [10]. The main objective of this study is to successfully design a phytochemical-based drug, employing computational approaches for treating Tuberculosis caused by *Mycobacterium tuberculosis*. The method used, namely silicon drug designing, is a relatively well-known method used for analyzing biological components with the help of computers. As a result, we gain suitable drug candidates and similar structural compounds that are promising and relatively economical compared to traditional drug designing methods. This study includes the analysis of virulent proteins produced by the mycobacterium and employs phytochemicals to help degrade the proteins. With the help of computational methods, current work was to analyze the drug interactions within the body through simulation, cutting down the time and resources required to produce successful drug candidates.

This study aims to construct befitting therapeutic molecules for treating Tuberculosis, simultaneously testing any toxic or otherwise adverse effects the drug may have.

METHODS

The tertiary structure for *InhA* (Enoyl-ACP reductase) was obtained from Research Collaboratory for Structural

Bioinformatics (RSCB) Protein Data Bank (PDB ID: 2NSD), where 3D structures of various proteins, found experimentally through X-ray crystallography, are submitted [11]. The tertiary structure of Enoyl-ACP reductase (also known as Enoyl-acyl carrier protein reductase) retrieved through the Research Collaboratory for Structural Bioinformatics Protein Data Bank (RSCB-PDB) was validated through PROCHECK Ramachandran Plot [12]. PROCHECK predicts the stereochemical quality of a protein by analyzing the torsion angle distribution of various protein residues on a 2D plane. The binding sites of the Enoyl-ACP reductase protein were identified from the Computed Atlas of Surface Topography of Proteins (CASTp). These binding sites are the protein's active site where ligands will interact with the protein [13]. Resveratrol from grapes (*Vitis vinifera*) was chosen based on its antimicrobial properties based on existing literature. The Signed Distance Fields (SDF) formatted 3D models were downloaded from PubChem [14]. Pharmacokinetic properties consist of ADMET, which is an acronym for Absorption, Distribution, Metabolism, Excretion, and Toxicity, meaning how the body absorbs the drug, how it is distributed across the body systems, what metabolic reactions become part of, after how long it is excreted from the body and if it imposes any toxic effects on the body. Absorption, Distribution, Metabolism, Excretion, and Toxicity (ADMET) analysis monitors the properties of any ligand selected as a drug candidate. The ADME were analyzed using the Swiss ADME tool [15], whereas the toxicity analysis was conducted using the Pro Tox II Server [16]. Docking is the interaction study between the ligand and the target protein; CB-Dock2 was used to analyze the docking patterns of Resveratrol with the target protein [17]. The results from CB-Dock2 provide five cavities by default and docking possibilities in each. To simulate the molecular docking interactions between ligand and protein, Integrated Management of Public Distribution System (iMODS) software was operated with default parameters for the most appropriate dock complex selected [18].

RESULTS

This method predicts a protein's structure by comparing it to a previously known structure. These known structures are frequently determined using techniques like X-ray crystallography, nuclear magnetic resonance (NMR) spectroscopy, and cryo-electron microscopy. Protein 3D structure is downloaded in the Protein Data Bank (PDB) file and after that Discovery Studio tool was employed for protein purification to remove water molecules and ligands attached to the protein to avoid any hindrance for further analysis. The Ramachandran Plot showed a quality score, with most favoured Rama score of 98.7 including both the favourable and most favourable regions. In the

Ramachandran Plot, the red colour represents the most favoured region, while the yellow colour indicates the favored region. The majority of protein residues fall within the red region, suggesting that the protein structure has high quality. The 3D structure of InhA protein taken from PDB is seen in Figure 1a. The Expasy ProtParam Tool helps analyze numerous characteristics depicting the physical and chemical properties of InhA. Physiochemical properties showed that protein is stable as its instability index is below 40, if this value was above 40 then protein would be unstable. The aliphatic index showed how many aliphatic amino acids are present in the protein primary sequence and its predicted value is 99.85. The Grand Average of Hydropathicity (GRAVY) indicates that the protein is hydrophobic, as its value is 0.152, if the GRAVY value were negative, it would suggest that the protein is hydrophilic. The Ramachandran Plot is seen in figure 1b.

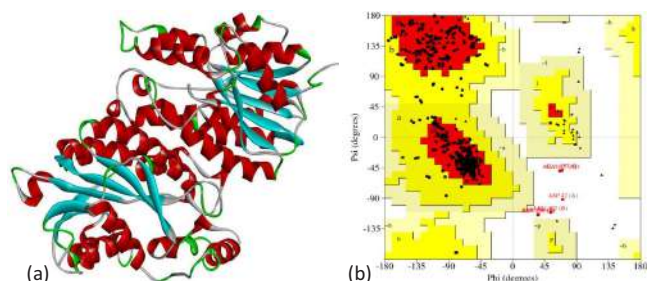


Figure 1: (a) 3D structure of InhA Protein, (b) Ramachandran of Plot Protein Validation

Details extracted from the ProtParam results page are shown in table 1.

Table 1: Physiochemical Properties of InhA

Physiochemical Properties InhA Protein	InhA Protein
No. of Amino Acids	269
Molecular Weight	28527.84
Theoretical pI	5.73
Total No. of Negatively Charged Residues	26
Total No. of Positively Charged Residues	22
Formula	$C_{1269}H_{2029}N_{349}O_{375}S_{11}$
Total No. of Atoms	4033
Extinction Coefficient	$30940 \text{ M}^{-1} \text{ cm}^{-1}$
Estimated Half-life	30 hours (mammalian reticulocytes, in vitro) >20 hours (yeast, in vivo) >10 hours (Escherichia coli)
Instability Index	39.29 (Stable)

STRING results provide protein-protein interactions based on which gene ontology functions are determined. Each of the nodes (circles) is coloured which means the particular protein of interest (InhA) has a first shell or level of interaction with all the other proteins. InhA interacts with 10 different proteins by being involved in various biological processes such as fatty acid elongation, mycolic acid biosynthesis process, fatty acid biosynthesis process and

response to antibiotics and these results are shown in figure 2.

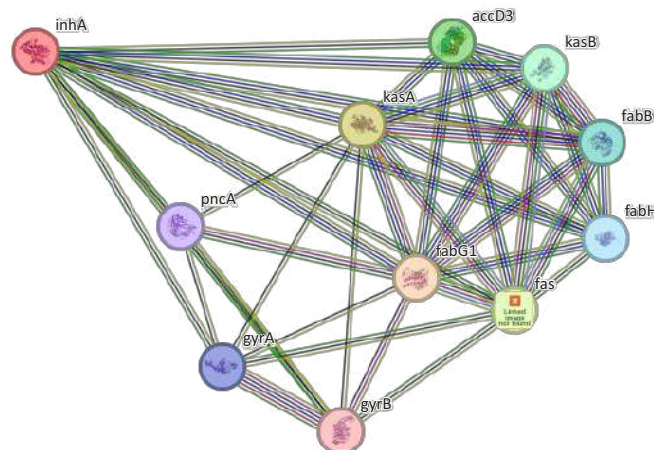


Figure 2: STRING Analysis of the Protein InhA (Enoyl-ACP Reductase)

In the case of InhA, Richards' and Connolly's surfaces are visibly marked red where the ligands can interact with the protein pockets. The residues in pocket are as follows: SER13, GLY14, ILE15, ILE16, THR17, SER19, SER20, ILE21, ALA22, THR39, GLY40, PHE41, ASP42, ARG43, ILE47, LEU63, ASP64, VAL65, GLN66, HIS93, SER94, ILE95, GLY96, PHE97, MET98, PRO99, GLN100, MET103, GLY104, LYS118, ILE122, SER123, MET147, ASP148, PHE149, MET155, PRO156, ALA157, TYR158, MET161, LYS165, LEU168, ALA191, GLY192, PRO193, ILE194, THR196, LEU197, ALA198, MET199, ALA201, ILE202, VAL203, GLY205, ALA206, LEU207, ILE215, LEU218, GLU219, TRP222, MET232. Binding site identification results are indicated in figure 3.

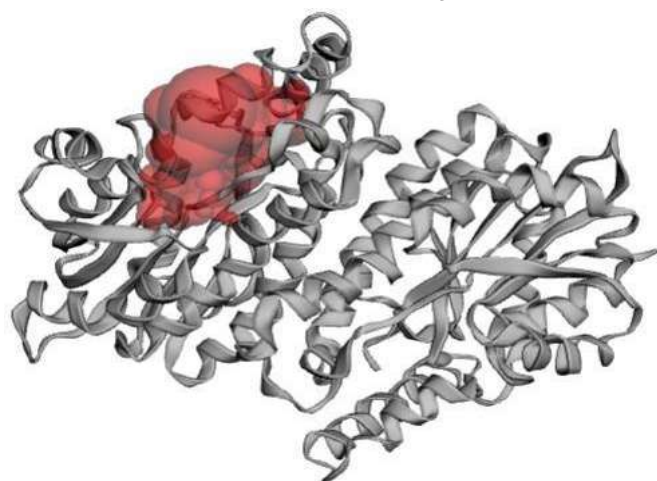


Figure 3: Active Site Identification by Castp. Highlighted Regions in Red Are the Active Sites

Resveratrol had the best Vina Score, -8.8 kcal/mol. The docking interaction of top ligand Resveratrol with targeted protein is represented in Figure 4a. A 2D visualization of docking is shown in figure 4b.

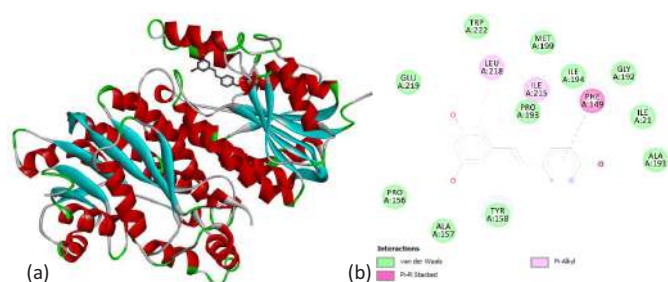


Figure 4: (a) 3D Visualization of Docking Interaction of Top Ligand Resveratrol with InhA, and (b) 3D Visualization of Docking Interaction

Various physiochemical parameters including GI absorption, bioavailability score and water solubility was analyzed using ADMET. No violation of Lipinski's rule was demonstrated by Resveratrol. Four ligands, e.g., epigallocatechin gallate (ECG), curcumin, berberine, and resveratrol, were selected and further listed for their drug-likeness. ADMET analysis showed the possibility of resveratrol as a drug candidate, with no violation of Lipinski rules and excellent absorption in the Gastrointestinal Tract. The list of physiochemical parameters for Resveratrol is seen in table 2.

Table 2: ADMET Properties for Resveratrol

Category	Property	Value
Physicochemical Properties	Formula	C ₁₄ H ₁₂ O ₃
	Molecular weight	228.24 g/mol
	Num. heavy atoms	17
	Num. arom. heavy atoms	12
	Fraction Csp ³	0.00
	Num. rotatable bonds	2
	Num. H-bond acceptors	3
	Num. H-bond donors	3
	Molar Refractivity	67.88
	TPSA	60.69 Å ²
Lipophilicity	Log Po/w (iLOGP)	1.71
	Log Po/w (XLOGP3)	3.13
	Log Po/w (WLOGP)	2.76
	Log Po/w (MLOGP)	2.26
	Log Po/w (SILICOS-IT)	2.57
	Consensus Log Po/w	2.48
Water Solubility	Log S (ESOL)	-3.62
	Solubility (ESOL)	5.51e-02 mg/ml ; 2.41e-04 mol/l
	Class (ESOL)	Soluble
	Log S (Ali)	-4.07
	Solubility (Ali)	1.93e-02 mg/ml ; 8.44e-05 mol/l
	Class (Ali)	Moderately soluble
	Log S (SILICOS-IT)	-3.29
	Solubility (SILICOS-IT)	1.18e-01 mg/ml ; 5.16e-04 mol/l
	Class (SILICOS-IT)	Soluble
	GI absorption	High
	BBB permeant	Yes

Pharmacokinetics	P-gp substrate	No
	CYP1A2 inhibitor	Yes
	CYP2C19 inhibitor	No
	CYP2C9 inhibitor	Yes
	CYP2D6 inhibitor	No
	CYP3A4 inhibitor	Yes
	Log Kp (skin permeation)	-5.47 cm/s
Drug likeness	Lipinski	Yes; 0 violation
	Ghose	Yes
	Veber	Yes
	Egan	Yes
	Muegge	Yes
	Bioavailability Score	0.55
Medicinal Chemistry	PAINS	0 alert
	Brenk	1 alert: stilbene
	Leadlikeness	No; 1 violation: MW<250
	Synthetic accessibility	2.02
Toxicity	Hepatotoxicity	Inactive
	Neurotoxicity	Inactive
	Nephrotoxicity	Active
	Respiratory toxicity	Inactive
	Cardiotoxicity	Active
	Carcinogenicity	Inactive
	Immunotoxicity	Inactive
	Mutagenicity	Inactive
	Cytotoxicity	Inactive
	BBB-barrier	Inactive
	Ecotoxicity	Inactive
	Clinical toxicity	Inactive
	Nutritional toxicity	Inactive

Figure 5a shows that the lower modes are associated with lower eigenvalues suggesting that; they are easier to deform than higher modes that are associated with higher eigenvalues and therefore need more energy to deform. This is a general behaviour and implies that the results obtained from the simulation are in line with the expected physical response. Higher modes (Mode 1 and Mode 2) have higher variances as indicated in Figure 5b. Also, the total variance rises gradually with the number of modes, indicating the gradual addition of motion. These trends indicate the simulation is valid and by the existing theories. Figure 5c indicates the deformability of atoms in a simulation. The peaks indicate varying levels of deformability among the atoms, with some atoms showing high deformability close to 1, and others much lower, closer to 0. This variability suggests differences in the flexibility or structural properties of the atoms within the simulated molecular system. Figure 5d indicates the B-factor value, the red line representing the Normal Mode Analysis (NMA) closely follows the trend of the grey bars from the Protein Data Bank (PDB) data, indicating that the simulation accurately captures the atomic mobility compared to the experimental data. This alignment suggests that the

simulation results are reliable. Figure 5e represents an elastic network model, showing which pairs of atoms are connected by springs. The dots indicate the stiffness of these springs, with darker greys representing stiffer springs. Based on the heat map, the results appear to be good. Figure 5f shows the strong red diagonal line indicates consistent and strong interactions between residues, which is generally a positive sign in protein simulations. This suggests that the simulation has captured the expected residue-residue interactions accurately.

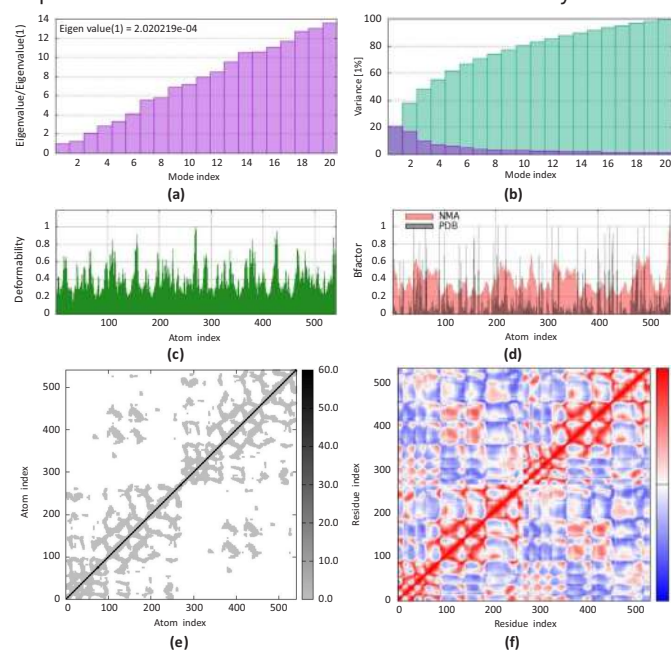


Figure 5: Results of MD simulation by iMODS. (a) Eigenvalues representing stiffness of the protein, (b) Variance of the protein structure, (c) Graphs represent deformability, (d) Graphs representing B-factor, (e) Elastic network also provides information on protein strength and stiffness, and (f) Covariance depicts the motion of pairs and groups of residues.

DISCUSSION

The computational method applied in this research was quite helpful in identifying resveratrol as a possible drug for the treatment of TB. The high score from the Ramachandran plot that was used to analyze the quality of the structural model of the target protein InhA proves that the method used to model the protein's three-dimensional structure is accurate. It is crucial to validate the structure because it means that the interactions that will be studied will be grounded in a proper and correct model [19]. The binding sites of the InhA protein were predicted and estimated using the CASTp tool and were entirely accurate. These are the regions of the protein that the ligand, the compound used in this case, resveratrol, can interact with to affect the protein [20]. More elaborative analysis of this interaction was done with the help of CB-Dock2, and the findings indicated that resveratrol has a high affinity for these active sites on InhA. The Vina score of the given

structure is -8.8 kcal/mol. Thus, these docking studies imply a good firm and stable interaction between resveratrol and InhA protein, which is a favourable implication for its therapeutic value [21]. When ADMET was carried out in more detail, this was even more positive for using resveratrol as a drug. Based on the ADMET analysis, it was observed that the compound has good permeability, especially across the gastrointestinal tract; besides, it does not violate any of Lipinski's rule of five. Toxicity analysis revealed that this drug candidate does not cause significant harm to any body organs, except for minor toxicity in the heart and kidneys, which is considered negligible. This, therefore, means that resveratrol has properties that are suitable as far as the bioavailability and solubility of the compound, which are factors that determine the effectiveness of any drug. Moreover, the acute and sub-chronic toxicity predictions demonstrated that the risks associated with the potential adverse effects are pretty low, which is beneficial since the use of supplements in therapeutic regimens is of great concern [22]. The molecular dynamics simulations performed in this study using the iMODS provided more details on the dynamic behaviour of the resveratrol-InhA complex in a physiological environment. Furthermore, these simulations have helped substantiate the assumption that the interaction between the resveratrol and InhA is both essential and temporal. It was concluded from the analysis of the simulations that resveratrol can interact with the target protein and will not lead to the disruption of the docking complex. This stability is essential for the compound to work in a biological system; thus, resveratrol can continue to inhibit in the long run [23]. The study conducted by Singh and Pandey reveals Gravacridone diol from the Rutaceae family with the best binding affinity of -10.80 kcal/mol is better than the known inhibitor triclosan (-7.33 kcal/mol) [24]. The current study focuses on Resveratrol as a possible inhibitor, and the docking score is -8.8 kcal/mol, describing the different physicochemical properties and the interaction residues. Both studies use ADMET profiling and molecular dynamics simulations to assess the compounds' stability and drug-likeness. However, study shows that Gravacridonediol has a higher binding energy and better pharmacokinetic profile than the first compound. Both research studies are based on identifying inhibitors for the InhA protein in Mycobacterium tuberculosis [24]. Thus, based on results, resveratrol can be a potential anti-TB drug. However, to prove the efficiency and reliability of the method, it is necessary to pass to the computational level. Further diagnostic and research studies, including clinical experiments (in vitro and in vivo), are needed to support these findings. These experimental validations will help confirm that resveratrol can inhibit InhA in a living organism and check the side effects of resveratrol. Moving from in-silico to in-vitro and then to in-vivo is a giant leap in the drug development

process to come up with a new treatment for tuberculosis.

CONCLUSIONS

It was concluded that TB remains a global health challenge because the FDA has endorsed no medications for concomitant therapy, and the InhA protein plays a significant role in the disease. In our study, Resveratrol was considered an antioxidant polyphenol with antimicrobial characteristics. These digital simulations showed that it has a tight binding affinity for the active site of InhA and forms a complex that inhibits the proper function of InhA and, hence, the growth of *Mycobacterium tuberculosis*. Similarly, Resveratrol was endowed with good pharmacodynamics, such as not being toxic, crossing the blood-brain barrier, and good GI absorption; thus, it remains one of the best for optimization. Consequently, in light of this study, using Resveratrol as a new treatment for TB can help improve the patient's health status and lessen the infection rate.

Authors Contribution

Conceptualization: OU, NH

Methodology: OU, NH, A

Formal analysis: OU, NH, AQM,

Writing review and editing: FA, MM, EJ, SF

All authors have read and agreed to the published version of the manuscript.

Conflicts of Interest

The authors declare no conflict of interest.

Source of Funding

The authors received no financial support for the research, authorship and/or publication of this article.

REFERENCES

- [1] Swalehe HM and Obeagu EI. Tuberculosis: Current Diagnosis and Management. *Elite Journal of Public Health*. 2024; 2(1): 23-33.
- [2] Daley CL. The Global Fight Against Tuberculosis. *Surgery for Pulmonary Mycobacterial Disease, An Issue of Thoracic Surgery Clinics*. 2018 Nov 21; 29(1): 19-25. doi: 10.1016/j.thorsurg.2018.09.010.
- [3] Stillo J. Connecting the DOTS: Should We Still Be Doing Directly Observed Therapy?. *Human Organization*. 2024 Jan; 83(1): 18-30. doi: 10.1080/00187259.2023.2286173.
- [4] Fu L, Deng G, Lu H. Faster, Higher, Stronger: The Evolution of Clinical Perspectives on Pan-TB. *One Health & Implementation Research*. 2024 Jun; 4(2): 38-52. doi: 10.20517/ohir.2024.03.
- [5] Ebenhan T, Lazzeri E, Gheysens O. Imaging of Bacteria: Is There Any Hope for The Future Based On Past Experience? *Current Pharmaceutical Design*. 2018 Feb; 24(7): 772-86. doi: 10.2174/1381612823666171122111558.
- [6] Prasad MS, Bhole RP, Khedekar PB, Chikhale RV. Mycobacterium Enoyl Acyl Carrier Protein Reductase (InhA): A Key Target for Antitubercular Drug Discovery. *Bioorganic Chemistry*. 2021 Oct; 115: 105242. doi: 10.1016/j.bioorg.2021.105242.
- [7] Singh S, Singh D, Hameed S, Fatima Z. An Overview of Mycolic Acids: Structure-Function-Classification, Biosynthesis, and Beyond. *Biology of Mycobacterial Lipids*. 2022 Jan: 1-25. doi: 10.1016/B978-0-323-91948-7.00016-6.
- [8] Belete TM. Recent Progress in The Development of Novel Mycobacterium Cell Wall Inhibitor to Combat Drug-Resistant Tuberculosis. *Microbiology Insights*. 2022 May; 15: 11786361221099878. doi: 10.1177/11786361221099878.
- [9] Ferraz da Costa DC, Pereira Rangel L, Quarti J, Santos RA, Silva JL, Fialho E. Bioactive Compounds and Metabolites from Grapes and Red Wine in Breast Cancer Chemoprevention and Therapy. *Molecules*. 2020 Aug; 25(15): 3531. doi: 10.3390/molecules25153531.
- [10] Abedini E, Khodadadi E, Zeinalzadeh E, Moaddab SR, Asgharzadeh M, Mehramouz B et al. A Comprehensive Study On the Antimicrobial Properties of Resveratrol as an Alternative Therapy. *Evidence-Based Complementary and Alternative Medicine*. 2021 Mar; 2021(1): 8866311. doi: 10.1155/2021/8866311.
- [11] Naveed M, Ali N, Aziz T, Hanif N, Fatima M, Ali I et al. The Natural Breakthrough: Phytochemicals as Potent Therapeutic Agents Against Spinocerebellar Ataxia Type 3. *Scientific Reports*. 2024 Jan; 14(1): 1529. doi: 10.1038/s41598-024-51954-3.
- [12] Sawal HA, Nighat S, Safdar T, Anees L. Comparative in Silico Analysis and Functional Characterization of TANK-Binding Kinase 1-Binding Protein 1. *Bioinformatics and Biology Insights*. 2023 Apr; 17: 11779322231164828. doi: 10.1177/11779322231164828.
- [13] Dariya B, Muppala S, Srivani G, Momin S, Alam A, Saddala MS. Targeting STAT Proteins Via Computational Analysis in Colorectal Cancer. *Molecular and Cellular Biochemistry*. 2021 Jan; 476: 165-74. doi: 10.1007/s11010-020-03893-6.
- [14] Mitra D and Mohapatra PK. Effect of Natural Compounds to Inhibit Human Respiratory Syncytial Virus. *Smart Environmental Science, Technology and Management*. 2022; 1: 97-101. doi: 10.36647/978-93-92106-02-6.18.
- [15] Mohamed HS, El-Serwy WS, El-Serwy WS. Synthesis, Molecular Docking, In Silico ADME Predictions, and Toxicity Studies of N-Substituted-5-(4-Chloroquinolin-2-Yl)-1, 3, 4-Thiadiazol-2-Amine Derivatives as COVID-19 Inhibitors. *Russian Journal*

- of Bioorganic Chemistry. 2021 Jan; 47: 158-65. doi: 10.1134/S1068162021010155.
- [16] Naveed M, Abid A, Aziz T, Saleem A, Hanif N, Ali I et al. Comparative Toxicity Assessment of Fisetin-Aided Artificial Intelligence-Assisted Drug Design Targeting Epibulbar Dermoid Through Phytochemicals. Open Chemistry. 2024 May; 22(1): 20230197. doi: 10.1515/chem-2023-0197.
- [17] Liu Y and Cao Y. Protein-Ligand Blind Docking Using CB-Dock2. In Computational Drug Discovery and Design. 2023 Sep; 113-125. New York, NY: Springer US. doi: 10.1007/978-1-0716-3441-7_6.
- [18] Braz JD and Batista MV. Immunoinformatics-Based Design of Multi-epitope DNA and mRNA Vaccines Against Zika Virus. Bioinformatics and Biology Insights. 2024 May; 18: 11779322241257037. doi: 10.1177/11779322241257037.
- [19] Mohinani T, Saxena A, Singh SV. Computational Analysis to Predict Drug Targets for the Therapeutic Management of Mycobacterium avium sub. Paratuberculosis. Current Drug Discovery Technologies. 2023 Jul; 20(4): 73-88. doi: 10.2174/1570163820666230310140613.
- [20] Medha, Joshi H, Sharma S, Sharma M. Elucidating the Function of Hypothetical PE_PGRS45 Protein of Mycobacterium Tuberculosis as an Oxidoreductase: A Potential Target for Drug Repurposing for the Treatment of Tuberculosis. Journal of Biomolecular Structure and Dynamics. 2023 Nov; 41(19): 10009-25. doi: 10.1080/07391102.2022.2151514.
- [21] Ibitoye O, Ibrahim MA, Soliman ME. Exploring the Composition of Protein-Ligand Binding Sites for Cancerous Inhibitor of PP2A (CIP2A) By Inhibitor Guided Binding Analysis: Paving A New Way for The Discovery of Drug Candidates Against Triple Negative Breast Cancer (TNBC). Journal of Receptors and Signal Transduction. 2023 Nov; 43(6): 133-43. doi: 10.1080/10799893.2023.2298903.
- [22] Pavlović N, Đanić M, Stanimirov B, Goločorbin-Kon S, Stankov K, Lalić-Popović M et al. In Silico Discovery of Resveratrol Analogues as Potential Agents in Treatment of Metabolic Disorders. Current Pharmaceutical Design. 2019 Oct; 25(35): 3776-83. doi: 10.2174/1381612825666191029095252.
- [23] Santra D and Maiti S. Molecular Dynamic Simulation Suggests Stronger Interaction of Omicron-Spike with ACE2 Than Wild but Weaker Than Delta SARS-Cov-2 Can Be Blocked by Engineered S1-RBD Fraction. Structural Chemistry. 2022 Oct; 33(5): 1755-69. doi: 10.1007/s11224-022-02022-x.
- [24] Singh K, Pandey N, Ahmad F, Upadhyay TK, Islam MH, Alshammari N et al. Identification of Novel Inhibitor Of

Enoyl-Acyl Carrier Protein Reductase (Inha) Enzyme In Mycobacterium Tuberculosis From Plant-Derived Metabolites: an in Silico Study. Antibiotics. 2022 Aug; 11(8): 1038. doi: 10.3390/antibiotics11081038.

FUTURISTIC BIOTECHNOLOGY

<https://fbtjournal.com/index.php/fbt>

ISSN (E): 2959-0981, (P): 2959-0973

Volume 4, Issue 3 (July-Sep 2024)



Original Article



Optimization of Autosomal STR Markers for Equine Genotyping Using Multiplex PCR

Usama Mustafa¹, Zaroon¹, Sana Shoukat¹, Juveria¹ and Manzoor Hussain¹

¹Department of Applied Molecular Biology, University of the Punjab, Lahore, Pakistan

ARTICLE INFO

Keywords:

Microsatellites, Polymorphism, Genotyping, Capillary Electrophoresis

How to Cite:

Mustafa, U., Zaroon, ., Shoukat, S., Juveria, ., & Hussain, M. (2024). Optimization of Autosomal STR Markers for Equine Genotyping Using Multiplex PCR: Optimizing Markers for Equine Genotyping. *Futuristic Biotechnology*, 4(03), 34-40. <https://doi.org/10.54393/fbt.v4i03.128>

*Corresponding Author:

Zaroon
Department of Applied Molecular Biology, University of the Punjab, Lahore, Pakistan
zaroonigill37@gmail.com

Received Date: 13th August, 2024

Acceptance Date: 26th September, 2024

Published Date: 30th September, 2024

ABSTRACT

The investigation of horse lineage was of paramount importance in the registration of different breeds, trade, and formulation of studbooks. The pioneering technique of DNA fingerprinting emerged as the first highly responsive method reliant on DNA for individual identification and the examination of genetic affiliations. Microsatellites were a valuable tool for analyzing the genetic variations present among different horse breeds. The International Society for Animal Genetics (ISAG) has endorsed a set of 17 specific Short Tandem Repeats (STRs) for the equine identification, although these can be quite expensive to obtain through commercially available multiplex kits. **Objective:** To determine five autosomal STR markers (HMS6, HMS7, ASB23, VHL20, and LEX14) were optimized using multiplex PCR for equine genotyping. **Methods:** DNA was extracted from a Thoroughbred horse blood sample via an organic extraction method. Sensitivity analysis determined the optimal PCR concentration. Genotyping was performed on the ABI PRISM® 3100XL, and data were processed with Gene Mapper ID 3.2v software. **Results:** The optimal conditions for multiplex PCR of HMS6, HMS7, ASB23, VHL20, and LEX14 primers were 60°C annealing temperature, 3ng DNA concentration and 6μM primer concentration. A 12.5μL PCR reaction volume was recommended for cost efficiency. **Conclusions:** The results of this research have the potential to create a cost-effective, regionally produced multiplex PCR kit. This kit would be designed for analyzing parentage lineage within the Equine family in Pakistan, incorporating ISAG-recommended markers: VHL20, HMS6, HMS7, ASB23, and additionally LEX14. It could significantly streamline the import and export of horses in Pakistan.

INTRODUCTION

Horses are truly remarkable beings, acclaimed for their unparalleled fusion of speed and potency. Horses (*Equus caballus*) hold the distinction of being the most ancient animals intertwined with human civilization, exerting a profound influence on human culture. The earliest evidence of the pivotal role of horses in human culture within the Eurasian context dates back around 15,000 years ago and originates from the southern region of France and adjacent areas. This evidence is manifested through archaeological findings, including faunal remains and cave paintings [1]. The classification of horses was established based on criteria encompassing their size, body morphology, physiology, and anatomical features. Among horse breeds the Thoroughbred is the valuable breed of light horses. The equestrian industry supports this breed because of its great physiological qualities i.e. in racing,

jumping, fox hunting and steeplechase [2]. The process of breeding involved the introduction of Arabian, Barb, or Turk stallions to mate with indigenous. English horse mares, resulting in the creation of the Thoroughbred horse breed [3]. Thoroughbred was originally a crossbred breed so it is necessary to record back to its ancestry. For around 200 years, a stud book has been used to keep track of the family history of this breed and to make sure the breed stays pure and healthy [4]. The inaugural publication of the Thoroughbred Stud Book took place in England in the year 1791 [5]. When horses are imported and exported, a parentage analysis is necessary. At the outset in 1960, the verification of equine parentage relied on blood typing antigens like EAC, EAA, EAD, AIB, and PGD [6]. Nevertheless, with the progression of molecular technology, a shift occurred towards utilizing STR markers

instead of blood typing antigens. Presently, the examination of genetic variance in horse parentage is conducted through STR genotyping, offering both precision and efficiency in performing parentage analysis as well as assessing genetic diversity. Short Tandem Repeats (STRs) are sequences of DNA consisting of 2 to 6 base pairs, which are dispersed across the genome and varies from person to person [7]. This advancement has led to improved precision in confirming parentage. Microsatellite genotyping is widely employed in forensic applications and parentage investigations, as well as in clinical settings, agriculture, animal breeding, and the food industry [8]. From 2001, Genetic testing facilities were required to conduct testing on TB horses using autosomal DNA STR loci by following the guidelines established by the International Society for Animal Genetics and (ISBC). The PCR molecular technique is employed to amplify STR markers, facilitating parentage verification [9]. Subsequently, the amplified PCR product undergoes genotyping, resulting in data that is presented in the form of peaks [10]. In Korea, the parentage verification of Thoroughbred (TB) horses was carried out utilizing a set of 14 microsatellites, which are part of the ISAG panel [11]. To evaluate phylogenetic relationships and genomic variability in horses, ten microsatellite markers (HTG10, ASB2, ASB17, HMS3, AHT4, HMS7, VHL20, AHT05, HTG4, and HMS6) were examined in Pakistan [12]. In Colombia certification and filiation tests were accurately performed by utilizing 17 STRs markers recommended by ISAG [13]. Meanwhile in Syria, an assessment of the genetic diversity and lineage of horses was conducted using 16 STR markers as suggested by ISAG [14]. This study has been done to develop multiplex PCR of five Thoroughbred horses STR markers (VHL20, HMS6, HMS7, ASB23 and LEX14). Because commercially available kits are expensive, it's really important to create a cheaper local kit for accurately testing horse's parentage. To address, this study has meticulously adjusted several critical factors in a multiplex PCR setup for the recommended ISAG STR markers. These factors include the annealing temperature, minimum template DNA and primer concentrations, as well as the optimal PCR volume. This study will provide a platform to establish a mega multiplex system that will lead to establish the equine stud book in the country. Creating a stud-book through DNA profiling would facilitate the seamless import and export of horses in Pakistan. Which would ultimately contribute to the economic advancement of the country.

METHODS

Sample collection: Blood samples of horses ranging in age approximately from 6 to 7 years and weight from 400 to 500 kg, were taken from healthy and active individuals from Horse shed UVAS Lahore Pakistan. Intravenously drawn

blood samples of 3 ml were taken from the jugular vein and placed in pre- labeled EDTA vacutainer vials with the horse's data like name, age and the date of collection. Following sample collection, the samples were properly delivered to the forensic laboratory CAMB for further proceedings. To prevent blood sample degradation, transport them immediately to the lab. To prevent blood sample degradation, samples were transported immediately to the lab. A cargo box with perforated sponge layers was used on the bottom and top of the samples, which were placed in securely closed zip-top bags. An unperforated sponge layer was added before sealing the box. The box temperature was maintained at 10°C during transport. Then samples were stored at 4°C. Organic Method of DNA Extraction: By following ethical guideline all the experiments like wet lab or Insilco labs were performed at Forensic DNA lab CAMB Lahore. The DNA was extracted using the organic method and purified with a microcon centrifugal device. The yield was estimated by 1% agarose gel electrophoresis and the gel was visualized using the BIO-RAD GelDoc system. The DNA was extracted by organic method and purified by microcon centrifugal device and estimation was done by 1% yield gel by using BIO-RAD Gel Doc system [15]. The primers were synthesized by ABI which were labeled with fluorescent dye as mentioned (Table1).

Table 1: Characteristic of Primers

S. No.	Gene/Marker	Primer	Dye	Size Range (bp)	Repeats
1	VHL20	F:CAAGTCCTCTTACT TGAAGACTAG	FAM- 6	87-105	30
		R:AACTCAGGGAGAAT CTTCCTCAG			
2	HMS7	F:TGTTGTTGAAACAT ACCTTGACTGT	FAM- 6	165-185	1
		R:CAGGAAACTCATGT TGATACCATC			
3	HMS6	F:GAAGCTGCCAGTAT TCAACCATTTG	VIC	151-169	4
		R:CTCCATCTTGTGAA GTGTAACCA			
4	ASB23	F:GAGGGCAGCAGGT TGGGAAGG	VIC	176-212	3
		R:ACATCCTGGTCAA ATCACAGTCC			
5	LEX14	F: CTTACTCACTG GGGAAT	VIC	204-206	5
		R: AGACTGAACACC TAATATGA			

After completing the gel electrophoresis, the stained gel was placed in a BIO-RAD GelDoc system connected to a computer. Using the Image Lab™ Software, the system was controlled to capture an image of the gel under UV light, making the stained bands visible. The software facilitated the analysis, such as measuring the intensity of the bands and comparing them with the 100 bp ladder. The optimal annealing temperature was determined using gradient PCR on BIO-RAD T100™ Thermal Cycler. The setup included 10ng DNA, 10uM primers, and a temperature range of 54°C to

64°C. The PCR protocol consisted of initial denaturation at 95°C (5min), denaturation at 95°C (30sec), annealing at 54°C to 64°C (75s), and final extension at 72°C (10min) in a 25uL reaction volume. Three sensitivity analyses were conducted to optimize PCR conditions using the Conventional PCR GeneAMP PCR System 9700. The analyses focused on determining the optimal lowest DNA concentration (ranging from 0.25ng to 10ng) (Table 2).

Table 2: Plan for DNA Sensitivity Analysis (8 Reactions)

S. No.	Chemical Reagents	Quantities of Volume
1	Primer Mix	80uL (10uL for Each Reaction)
2	Template DNA	24uL (24ng) (3ng for Each)
3	Taq DNA Polymerase	4uL (0.5uL for Each)
4	Master Mix	79.5uL
5	T.E Buffer	19.75uL

Primer sensitivity with concentrations from 2uM to 10uM, and volume quantities (25uL, 12.5uL, and 7.5uL) while maintaining consistent conditions and conserving reagents (Table 3). PCR products were genotyped using Capillary electrophoresis. A 96-well microtiter plate was prepared with the first well as a negative control containing 0.4 uL Liz (GS500) and 13 uL Hi-Di formamide. The other

Table 4: Genotyping Data (DNA Sensitivity Analysis)

Microsatellite Markers	Dye-Labelled	Peak Heights at different Concentration of DNA in Electropherogram								
		Amplicon Size	10ng	5ng	4ng	3ng	2ng	1ng	0.5ng	0.25ng
VHL20	FAM-6	91-104	2878-1752	2023-1246	1737-1029	2706-1612	1382-1895	1632-930	136-76	557-385
HMS7	FAM-6	172-174	783-509	958-651	473-344	926-946	205-159	391-308	97-80	-
HMS6	VIC	167	2185	1360	891	834	643	892	263	-
ASB23	VIC	192	2234	1141	536	1109	445	405	186	-
LEX14	VIC	206	2926	1631	763	1512	457	678	291	-

Similarly, the RFU values for primer sensitivity showed that there was a good amplification at 6uM to 10uM (Table 5).

Table 5: Genotyping Data of Primer Sensitivity Analysis

Microsatellite Markers	Dye-Labelled	Peak Heights at different Primer Concentrations in Electropherogram					
		Amplicon Size	10µM	8µM	6µM	4µM	2µM
VHL20	FAM-6	91-104	1456-970	1664-1083	867-685	69-<50	66-53
HMS7	FAM-6	172-174	787-489	1200-731	490-265	62-<50	<50
HMS6	VIC	167	2067	2267	1154	95	85
ASB23	VIC	192	969	1034	441	<50	227
LEX14	VIC	206	1083	1457	604	250	380

The genotyping data for primer sensitivity analysis was also represented graphically (Figure 8). Subsequently the peak height (RFU) suggested that there was good amplification at 25uL and 12.5uL. But at 7.5uL there was a decline in RFU values which may result in allelic drop out (Table 6).

Table 6: Genotyping Data of Primer Sensitivity Analysis

Microsatellite Markers	Dye-Labelled	Amplicon Size	Peak Heights of different Volumes of PCR Mix in Electropherogram		
			25µl	12.5µl	7.5µl
VHL20	FAM-6	91-104	1664-1083	1212-708	930-640
HMS7	FAM-6	172-174	1200-731	1271-742	897-552
HMS6	VIC	167	2267	2723	1766
ASB23	VIC	192	1034	469	202
LEX14	VIC	206	1457	569	296

wells contained 2 uL of PCR product in addition to Liz and formamide. After loading and spinning, the plate was incubated at 95°C for 5 minutes, followed by a 3-4-minute heat shock. After another spin, the plate was wrapped and sent for capillary electrophoresis on an ABI prism 3130XL Genetic analyzer. Genotyping data was then analyzed using Gene Mapper ID 3.2v software.

Table 3: Reaction mix for Sensitivity Analysis of Primer (5 Reactions)

S. No.	Chemical Reagents	Quantities of Volume
1	Master Mix	50uL (10uL Each Reaction)
2	Taq DNA Polymerase	2.5uL (0.5 for Each Reaction)
3	Primer Mix	30uL (2uL to 10uL) for 5 Reactions
4	T.E Buffer	27.5uL
5	Template DNA	3ng (3uL) for Each Reaction

RESULTS

Below these concentrations the amplification was not significant. The genotyping data analysis also revealed that the best RFU (Relative Fluorescence Units) values were observed within the DNA concentration range of 3ng to 10ng (Table 4).

In the examination of the 4% product gel, amplification was detected at temperatures of 56°C, 58°C and 60°C. Among these, the most robust amplification was consistently observed at 60°C (Figure 1).

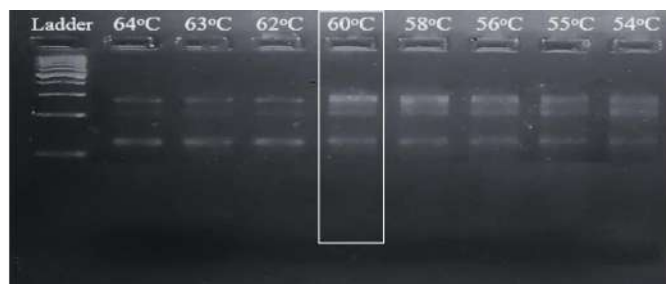


Figure 1: Product Gel of Gradient PCR

In figure 2 gel electrophoresis illustrating DNA sensitivity analysis, displaying bands corresponding to different DNA template concentrations, indicating successful amplification across a range of sensitivities."

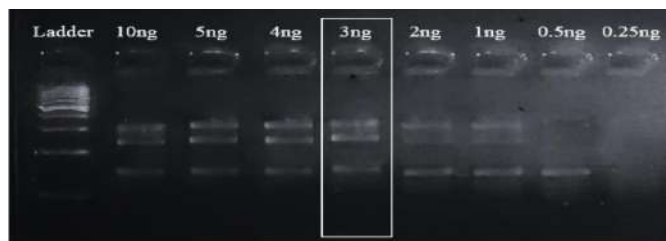


Figure 2: Product Gel of DNA Sensitivity Analysis

In figure 3 gel electrophoresis showing the results of primer sensitivity analysis, with distinct bands indicating successful amplification at varying primer concentrations (Figure 3).

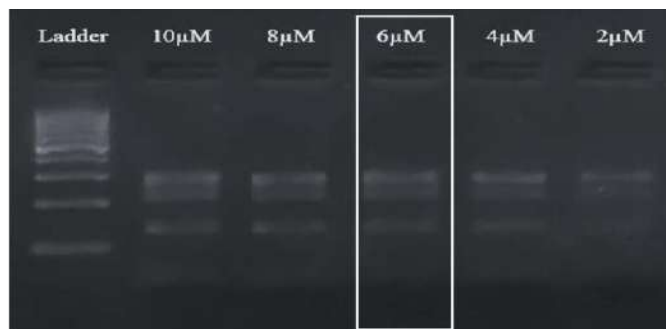


Figure 3: Product Gel of Primer Sensitivity Analysis

In figure 4 gel electrophoresis showing the results of optimal volume analysis, with bands representing varying reaction volumes to determine the ideal conditions for efficient amplification.

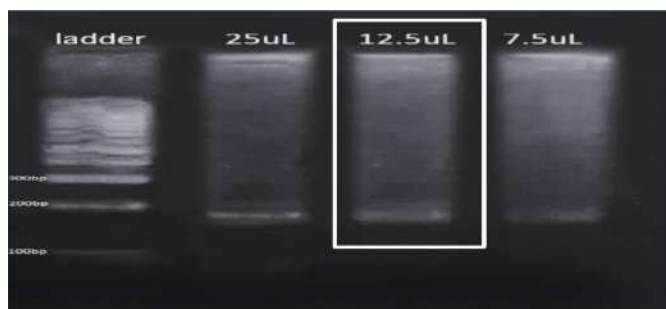


Figure 4: Product Gel of Optimal Volume Analysis

Notably, there was a decline in RFU values at the 2ng and 1ng DNA concentrations, heightening the risk of allelic dropout particularly in cases of heterozygosity. Moreover, the RFU values for the VHL20 and HMS7 loci resulted in allele dropout at 0.5ng. Additionally, at the 0.25ng DNA concentration, only the VHL20 locus exhibited amplification. In light of these findings, the DNA concentration of 3ng was identified as the optimal DNA concentration (Figure 5).



Figure 5: DNA Sensitivity Analysis (3ng)

The genotyping data for DNA sensitivity analysis was also represented graphically (Figure 6).

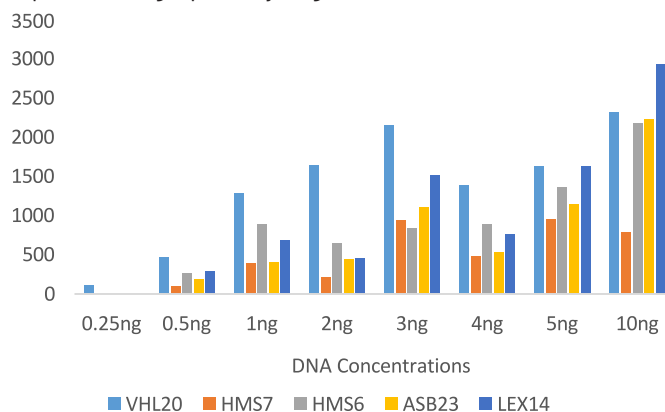


Figure 6: Graphical Representation of DNA Sensitivity Analysis (0.2 ng to 10ng)

While primer concentrations 4uM and 2 uM result in allelic drop out. So 6uM was reported as least primer concentration that give best amplification (Figure 7).

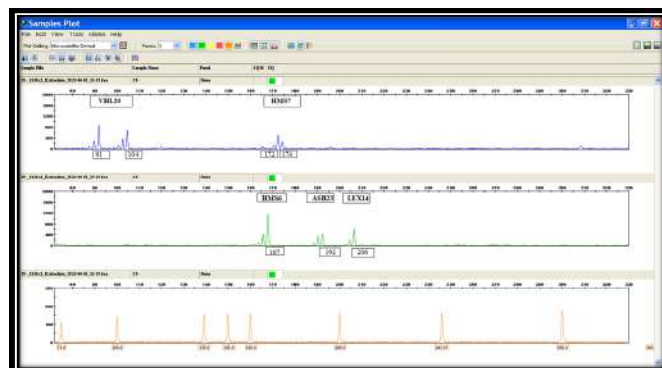


Figure 7: Primer Sensitivity Analysis (6uM)

A graph showing primer sensitivity analysis from 2 μ M to 10 μ M typically plots primer concentration on the x-axis and PCR efficiency or product yield on the y-axis. The curve helps determine the optimal primer concentration for maximum amplification success while minimizing nonspecific products (Figure 8).

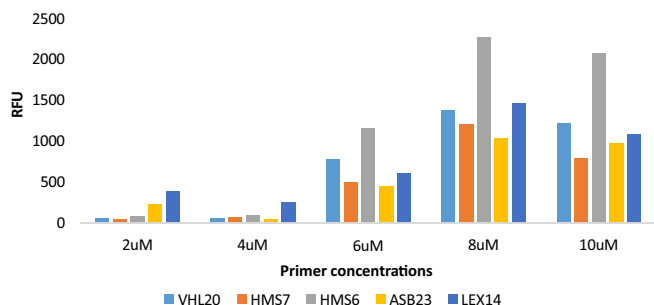


Figure 8: Graphical Representation of Primer Sensitivity Analysis (2uM to 10uM)

To prevent the wastage of costly reagents, it was recommended that a final PCR reaction volume of 12.5 would be optimal (Figure 9).

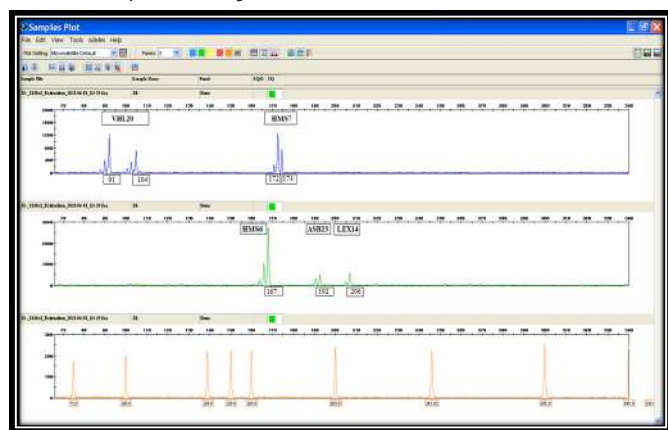


Figure 9: Volume sensitivity Analysis (12.5uL)

The genotyping data for primer sensitivity analysis was also represented graphically (Figure 10)

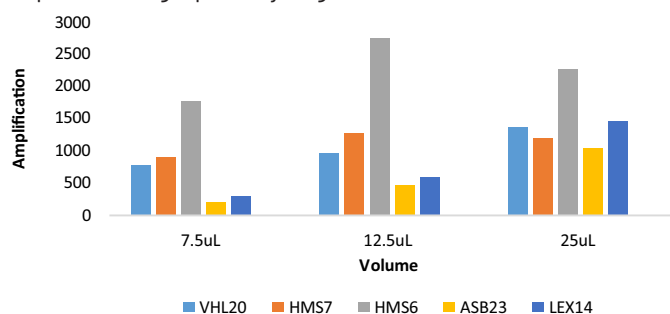


Figure 10: Graphical Representation of Volume Sensitivity Analysis

DISCUSSION

Besides other methods, which have been previously used, this study has been done to develop multiplex PCR of five Thoroughbred horses STR markers (VHL20, HMS6, HMS7, ASB23 and LEX 14). This study puts forward a novel idea to

create a cheaper local kit for accurately testing horse's parentage. IT considered several critical factors in a multiplex PCR setup for the recommended ISAG STR markers. These factors include the annealing temperature, minimum template DNA and primer concentrations, as well as the optimal PCR volume. The research conducted on Arabian horses and Caspian horses which coincided with the creation of multiplex PCR assays for 17 STR loci and 7 STR loci respectively, revealed a consistent identical annealing temperature with this study finding. In Korea, a multiplex analysis was conducted utilizing 14 STR markers, employing an annealing temperature of 60°C [16-18]. The DNA sensitivity analysis was found to be interconnected with related research, such as the advancement of a 19-plex PCR system. This study indicated that DNA concentrations ranging from 2ng to 20ng yielded successful amplification, while using 1ng of template DNA led to allelic dropouts. Consequently, utilizing 1ng or less of template DNA was not recommended based on these finding [19]. In the development of 13-plex PCR a primer concentration range of 5uM was used which was closely in line with this findings [19]. The finding of this research suggested 12.5uL as the optimum reaction volume. Research in Portugal however, employed 10uL of final PCR reaction volume to test the paternity of Portuguese autochthonous horse breeds [20]. To validate the paternity of the Syrian Arabian horse breed, a microsatellite analysis was conducted using a 12uL sample from the final volume, demonstrating alignment with this research outcomes [21]. This study will provide a platform to establish a mega multiplex system that will lead to establish the equine stud book in the country.

CONCLUSIONS

In this study, five autosomal STR markers HMS6, HMS7, ASB23, VHL20 and LEX14 have been optimized using multiplex PCR for equine genotyping analysis. The best annealing temperature for the multiplex PCR of HMS6, HMS7, ASB23, VHL20 and LEX14 primers was found as 60°C. The least DNA concentration that gave the amplification of all five primers in multiplex PCR was found as 3ng. The minimum primer concentration needed for successful amplification of this penta-plex was found to be 6uM. This study recommends the use of 12.5uL PCR reaction volume. To make the assay more economical. This study will provide a platform to establish a mega multiplex system for Equine genotyping which will lead to establish the equine stud book in the country. The establishment of stud-book on the basis of DNA profiling would ultimately aid in the import and export of horses into Pakistan.

Authors Contribution

Conceptualization: Z, MH

Methodology: Z, SS

Formal analysis: UM, J

Writing, review and editing: MH

All authors have read and agreed to the published version of the manuscript.

Conflicts of Interest

The authors declare no conflict of interest.

Source of Funding

The authors received no financial support for the research, authorship and/or publication of this article.

REFERENCES

- [1] Rook L, Bernor RL, Avilla LS, Cirilli O, Flynn L, Jukar A et al. Mammal biochronology (Land Mammal Ages) around the world from Late Miocene to Middle Pleistocene and major events in horse evolutionary history. *Frontiers in Ecology and Evolution*. 2019 Jul; 7: 278. doi: 10.3389/fevo.2019.00278.
- [2] Huntington PJ, Brown-Douglas CG, Pagan JD. Growth and development of Thoroughbred horses. *Animal Production Science*. 2020 Nov; 60(18): 2093-102. doi: 10.1071/AN19629.
- [3] Lebedeva LF, Atroshchenko MM, Naumenkova VA, Solodova EV. Comparative analysis of various technologies of breedings of horses. *In IOP Conference Series: Earth and Environmental Science* 2021 Jul; 624(1): 012035. doi: 10.1088/1755-1315/624/1/012035.
- [4] Cosenza M, La Rosa V, Rosati R, Chiofalo V. Genetic diversity of the Italian thoroughbred horse population. *Italian Journal of Animal Science*. 2019 Jan 2; 18(1): 538-45.
- [5] Bergmann IM. Towards Interspecies Sustainability: The Future for Thoroughbreds and Thoroughbred Racing [Doctoral dissertation]; 2020.
- [6] Petersen JL. Horse Breeding. *In Animal Breeding and Genetics* 2022 Nov: 279-295. doi: 10.1007/978-10716-2460-9_1120.
- [7] Flynn P, Morrin-O'Donnell R, Weld R, Gargan LM, Carlsson J, Daly S et al. Comparative analysis of single nucleotide polymorphisms and microsatellite markers for parentage verification and discovery within the equine Thoroughbred breed. *bioRxiv*. 2021 Jul: 2021-07. doi: 10.1101/2021.07.28.453868.
- [8] Zhu J, Lv M, Zhou N, Chen D, Jiang Y, Wang L et al. Genotyping polymorphic microhaplotype markers through the Illumina® MiSeq platform for forensics. *Forensic Science International: Genetics*. 2019 Mar; 39: 1-7. doi: 10.1016/j.fsigen.2018.11.005.
- [9] Khrabrova LA, Blohina NV, Suleymanov OI, Rozhdestvenskaya GA, Pustovoy VF. Assessment of line differentiation in the Thoroughbred horse breed using DNA microsatellite loci. *Вавиловский журнал генетики и селекции*. 2019; 23(5): 569-74. doi: 10.18699/VJ19.526.
- [10] Al-Shuhaib MB and Hashim HO. Mastering DNA chromatogram analysis in Sanger sequencing for reliable clinical analysis. *Journal of Genetic Engineering and Biotechnology*. 2023 Nov; 21(1): 115. doi: 10.1186/s43141-023-00587-6.
- [11] Park CS, Lee SY, Cho GJ. Evaluation of recent changes in genetic variability in Thoroughbred horses based on microsatellite markers parentage panel in Korea. *Animal Bioscience*. 2022 Apr; 35(4): 527. doi: 10.5713/ab.21.0272.
- [12] Atiq I, Zahoor I, Basheer A, Khan W. Genetic Diversity, Population Structure And Phylogenetic Relationship Of Race, Sports, Draft And Wild Type Horses. *Pakistan Journal of Agricultural Sciences*. 2018 Mar; 55(1). doi: 10.21162/PAKJAS/17.5087.
- [13] Pérez JR, Palacios DM, Garro JM. Genetic characterization of the Colombian Creole Horse population via STR markers used in filiation tests and equine certification. *Forensic Science International: Animals and Environments*. 2023 Dec; 3: 100065. doi: 10.1016/j.fsiae.2023.100065.
- [14] Machmoum M, Boujenane I, Azelhak R, Badaoui B, Petit D, Piro M. Genetic diversity and population structure of Arabian horse populations using microsatellite markers. *Journal of Equine Veterinary Science*. 2020 Oct; 93: 103200. doi: 10.1016/j.jevs.2020.103200.
- [15] Paul R, Ostermann E, Wei Q. Advances in point-of-care nucleic acid extraction technologies for rapid diagnosis of human and plant diseases. *Biosensors and Bioelectronics*. 2020 Dec; 169: 112592. doi: 10.1016/j.bios.2020.112592.
- [16] Ropka-Molik K, Stefaniuk-Szmukier M, Musiał AD, Velie BD. The genetics of racing performance in Arabian horses. *International Journal of Genomics*. 2019 Sep; 2019(1): 9013239. doi: 10.1155/2019/9013239.
- [17] Sadeghi R, Moradi-Shahrbabak M, Miraei Ashtiani SR, Schlamp F, Cosgrove EJ, Antczak DF. Genetic diversity of Persian Arabian horses and their relationship to other native Iranian horse breeds. *Journal of Heredity*. 2019 Mar; 110(2): 173-82. doi: 10.1093/jhered/esy061.
- [18] Yaralı C, Köseman A, Özşensoy Y, Şeker İ, Toprak B, Zengin K. Parentage verification and genetic diversity of the Arabian and Thoroughbred horse populations in Türkiye using microsatellite analysis. *Überprüfung der Abstammung und genetischen Vielfalt der Araber-und Vollblutpferde in der Türkei mittels Mikrosatellitenanalyse. Arch. Tierheilkd*. 2023 Nov; 165: 716-25. doi: 10.52973/rcfcv-e33262.
- [19] Shang S, Zhang M, Zhao Y, Dang W, Hua P, Zhang S et al. Development and validation of a novel 13-plex PCR system for commonly used short tandem repeats in

- horses (*Equus caballus*). *Equine Veterinary Journal*. 2019 Sep; 51(5): 688-95. doi: 10.1111/evj.13047.
- [20] Cozzi MC, Valiati P, Longeri M, Ferreira C, Abreu Ferreira S. Genetic variability trend of lusitano horse breed reared in Italy. *Animals*. 2022 Jan; 12(1): 98. doi: 10.3390/ani12010098.
- [21] Sargious MA, Ahmed HA, El-Shawarby RM, Bakery HH, Ramadan SI, Cothran EG *et al*. Genetic diversity and population assignment of Arabian horses. 2021 Nov: 1-9. doi: 10.17582/journal.pjz/20201013221026.

FUTURISTIC BIOTECHNOLOGY

<https://fbtjournal.com/index.php/fbt>

ISSN (E): 2959-0981, (P): 2959-0973

Volume 4, Issue 3 (July-Sep 2024)



Original Article



Ultraviolet and Ethyl Methanesulfonate-Induced Mutagenesis in *Aspergillus niger* and *Salmonella typhi* for Enhanced Azoreductase Production in Azo Dyes Bioremediation

Faiza Tariq¹, Dua Batool¹, Huda Rehman¹ and Manam Walait¹¹Faculty of Science and Technology, University of Central Punjab, Lahore, Pakistan

ARTICLE INFO

Keywords:

Azoreductase, Azo dye degradation, *Aspergillus niger*, *Salmonella typhi*, EMS mutagenesis, UV mutagenesis, Bioremediation, L-cysteine, Enzyme enhancement

How to Cite:

Tariq, F., Batool, D., Rehman, H., & Walait, M. (2024). Ultraviolet and Ethyl Methanesulfonate-Induced Mutagenesis in *Aspergillus niger* and *Salmonella typhi* for Enhanced Azoreductase Production in Azo Dyes Bioremediation: Mutagenesis in *Aspergillus niger* and *Salmonella typhi*. *Futuristic Biotechnology*, 4(03), 41-55. <https://doi.org/10.54393/fbt.v4i03.164>

*Corresponding Author:

Faiza Tariq
Faculty of Science and Technology, University of Central Punjab, Lahore, Pakistan
faiztariq16@gmail.com

Received date: 4th August, 2024Acceptance date: 22nd September, 2024Published date: 30th September, 2024

ABSTRACT

Azoreductase, an enzyme capable of degrading toxic industrial azo dyes, holds significant potential for environmental remediation. **Objective:** To enhance azoreductase production through innovative approaches, addressing the challenge of azo dye persistence in industrial wastewater. **Method:** Mutagenesis using EMS and UV irradiation was applied to *Aspergillus niger* and *Salmonella typhi*, followed by treatment with L-cysteine HCl to enhance azoreductase production. **Result:** Mutant strains showed significantly higher azoreductase activity and more efficient azo dye degradation than wild types. **Conclusions:** Mutagenesis is a promising strategy to boost azoreductase production for effective industrial dye bioremediation. Chemical mutagenesis using Ethyl Methane Sulfonate (EMS) (1-6 mM) and physical mutagenesis via UV irradiation (254 nm, 10-120 minutes) were applied to *Aspergillus niger* and *Salmonella typhi* to induce mutations. Further enhancement of enzyme production and strain resistance was achieved through treatment with L-cysteine HCl monohydrate. Comparative analysis using spectrophotometry and Fourier Transform Infrared (FTIR) spectroscopy demonstrated increase in azoreductase activity in mutant strains compared to wild strains. Additionally, textile dye degradation tests validated the enzyme's efficacy for bioremediation.

INTRODUCTION

The discharge of azo dyes from industrial sources poses significant environmental and health risks due to their persistence, toxicity, and mutagenic potential [1]. These synthetic dyes, extensively used in textiles, pharmaceuticals, food, and cosmetics, are resistant to natural degradation and can cause genetic mutations, cancer, and organ damage [2]. Traditional treatment methods such as adsorption, ion exchange, and advanced oxidation are often costly and generate toxic by-products [3]. Biological methods using microbial enzymes offer a more sustainable and cost-effective approach to degrading these compounds [4]. Among these, azoreductases play a central role in breaking azo bonds

under both aerobic and anaerobic conditions. These enzymes are known for their stability across a wide pH and temperature range and exhibit varied cofactor dependencies and electron donor preferences [5]. Several bacterial genera, including *Pseudomonas*, *Enterobacter*, *Bacillus*, and fungal species such as *Aspergillus niger*, are known to secrete azoreductases [6-8]. Enhancing enzyme yield through induced mutagenesis is a promising strategy [9]. Physical mutagens like ultraviolet (UV) radiation and chemical agents such as ethyl methanesulfonate (EMS) are commonly employed to increase microbial enzyme production [10]. UV primarily causes thymine dimers, while EMS induces GC-AT transitions via alkylation [11, 12].



Aspergillus niger is recognized for its metabolic versatility and capacity to produce enzymes like azoreductase [13]. Likewise, *Salmonella typhi*, despite its pathogenicity, shows potential for enzyme production due to its adaptable metabolism [14]. Mutagenesis in these organisms could enhance their ability to degrade azo dyes more efficiently [15]. Fermentation using low-cost substrates such as soybean meal has been reported to enhance enzyme production due to its rich nutrient content [16]. Additionally, spontaneous and induced mutations contribute to strain improvement and elevated enzyme yield [17]. This study investigated the effect of UV and EMS-induced mutations on *Aspergillus niger* and *Salmonella typhi* for enhanced azoreductase production. A comparative analysis of wild-type and mutant strains was conducted using FTIR and spectrophotometric assays to evaluate enzyme activity in the bioremediation of azo dyes [18]. Azoreductases are a diverse group of enzymes classified based on their cofactor dependency (FMN, FAD, or flavin-independent) and electron donor preference (NADH, NADPH-dependent or independent) [19]. Their ability to function under both aerobic and anaerobic conditions, coupled with their tolerance to a broad pH (5–9) and temperature (25–85°C) range, makes them particularly effective for industrial applications [20]. In addition to their role in azo dye degradation, azoreductases have applications in xenobiotic metabolism, biosensor development, and prodrug activation [21]. Many microorganisms harbor multiple azoreductase isoforms, complicating the understanding of their physiological roles [22]. The variation in their catalytic mechanisms further emphasizes the need to study organism-specific enzymes to identify high-efficiency candidates for industrial use. Moreover, comparative data on bacterial and fungal azoreductases remain limited, particularly regarding their activity levels, substrate specificities, and optimal production conditions under mutagenic enhancement. *Aspergillus niger*, a filamentous fungus widely used in biotechnology, is known for its robust enzyme secretion capabilities and metabolic adaptability. On the other hand, *Salmonella typhi*, though pathogenic, demonstrates metabolic versatility that could be exploited under controlled, inactivated conditions for biotechnological applications [23]. In recent years, omics-based approaches such as genomics, transcriptomics, and proteomics have emerged as powerful tools to elucidate the genetic and molecular basis of azoreductase expression and activity. These techniques enable the identification of regulatory genes, promoter regions, and metabolic pathways involved in dye degradation, offering potential targets for genetic engineering. Integrating mutagenesis with high-throughput screening and molecular characterization could accelerate the discovery

of hyper-producing strains. Additionally, immobilization of microbial cells or enzymes on suitable carriers has shown promise in enhancing enzyme stability and reusability, making the bioremediation process more economically viable. The development of bioreactors tailored for continuous dye degradation under optimized environmental conditions—such as pH, temperature, aeration, and nutrient supplementation—further supports the scalability of microbial azoreductase systems. Future research should focus on designing synthetic microbial consortia and engineering microbial communities capable of synergistic dye breakdown, thereby overcoming the limitations of single-strain systems. Furthermore, comprehensive risk assessments and containment strategies must be implemented when employing genetically modified or pathogenic organisms like *Salmonella typhi*, ensuring biosafety and regulatory compliance. By combining classical microbiological techniques with modern molecular and bioprocess engineering, the field of enzyme-based dye bioremediation can transition from laboratory-scale success to industrial-scale implementation. A systematic comparison between these two organisms under mutagenic stress could provide insight into strain-specific enzyme enhancement strategies. Despite advances in enzyme biotechnology, there remains a gap in optimizing physicochemical parameters and identifying the most productive microbial strains for azoreductase-mediated bioremediation [24]. Addressing this gap could enable more targeted and cost-effective strategies for large-scale treatment of dye-contaminated effluents.

METHODS

Microbial Strains and Culture Conditions

Aspergillus niger and *Salmonella typhi* were obtained from Forman Christian College University, Lahore. Fungi were cultured on Potato Dextrose Agar (PDA) at 30°C and bacteria on nutrient agar at 37°C. Morphological identifications were confirmed via lactophenol cotton blue staining for *A. niger* and Gram staining for *S. typhi*.

Induced Mutagenesis

Mutagenesis was carried out using Ultraviolet (UV) light and Ethyl Methanesulfonate (EMS) to enhance azoreductase production. EMS was applied at concentrations of 1–6 mM for 10–120 minutes, followed by neutralization with 0.05 mM sodium thiosulfate. UV exposure ranged from 10–140 minutes at 260 nm. Post-treatment, cultures were incubated (fungi at 30°C for 3 days; bacteria at 37°C for 24 hours) and the best-growing mutants were selected.

Fermentation and Enzyme Extraction

Selected strains were grown in 50 mL Potato Dextrose Broth (PDB) for *A. niger* and LB broth for *S. typhi*. After incubation (fungi: 3 days at 30°C; bacteria: 24 hours at

37°C), cultures were centrifuged at 4000 rpm for 25 min. Mycelial pellets (fungi) were ground and suspended in phosphate buffer (pH 7.4), incubated for 2 hours at 30°C, and centrifuged again to collect the supernatant. Bacterial pellets were processed similarly.

Azoreductase Isolation and Activity Assay

Mid-log phase cells were disrupted by sonication (40% power, 6 min). Enzyme was precipitated using 40% ammonium sulfate, incubated at 4°C for 24 hours, and desalted by dialysis. Azoreductase activity was measured spectrophotometrically at 540 nm using the formula:

$$\text{Enzyme Activity (U/mL)} = \Delta A \times V / (\epsilon \times l \times v \times t)$$

Where, ΔA is the absorbance change, V is total volume, ϵ is molar absorptivity, l is path length, v is sample volume, and t is time.

Dye Decolorization Assay

Dye solutions (0.2 g/100 mL) of Reactive Black, Congo Red, Methyl Orange, and Brilliant Blue were used. 400 μ L dye, 500 μ L enzyme supernatant, and 300 μ L phosphate buffer (pH 7.0) were mixed and incubated at 37°C for 72 hours. Absorbance was measured pre- and post-incubation to determine decolorization efficiency using: Decolorization (%) = [(Initial Abs - Final Abs) / Initial Abs] \times 100

FTIR Analysis

Pellets from the best mutants (wild, UV-treated, and EMS-treated) of each organism were dried at 30°C for 4 hours and submitted for FTIR analysis at Lahore College for Women University (LCWU), Lahore. This analysis was used to evaluate chemical structure differences among strains.

RESULTS

This figure showed the characteristic smooth, moist, beige colonies of *Salmonella typhi* grown on nutrient agar, confirming successful cultivation and typical morphological features.



Off-white colonies

Figure 1: Growth of *Salmonella typhi* on Nutrient Agar

Growth pattern of *Aspergillus niger* on malt extract media showing A) wild type, B) colony morphology after exposure to 3 mM EMS, and C) enhanced growth and sporulation after exposure to 6 mM EMS, indicating mutagenic impact.

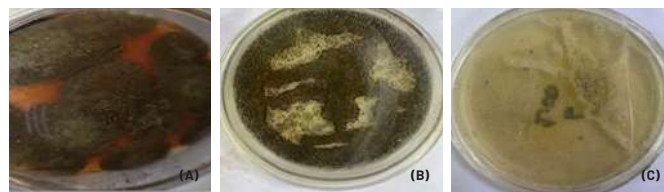


Figure 2: Growth of *Aspergillus niger* on wild and mutated strain on malt extract media. A) Wild type B) exposure to 3 mM concentration C) exposure to 6 mM concentration of EMS

Growth of *Salmonella typhi* on nutrient agar showing A) wild type, B) colony morphology after exposure to 3 mM EMS, and C) altered growth pattern following 6 mM EMS treatment, indicating successful chemical mutagenesis.

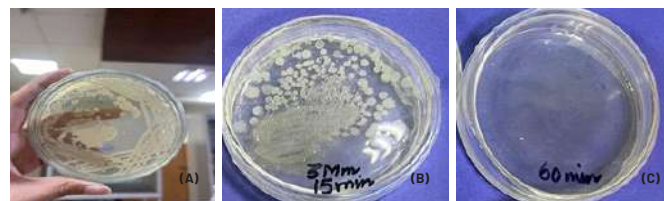


Figure 3: Growth of *Salmonella typhi* on Wild and Mutated Strain on Nutrient Agar. A) Wild Type B) Exposure to 3 mM Concentration C) Exposure to 6 mM Concentration of EMS

Azoreductase activity (U/mL) of *Aspergillus niger* comparing wild and mutant strains, highlighting enhanced enzyme production following EMS and UV mutagenesis.

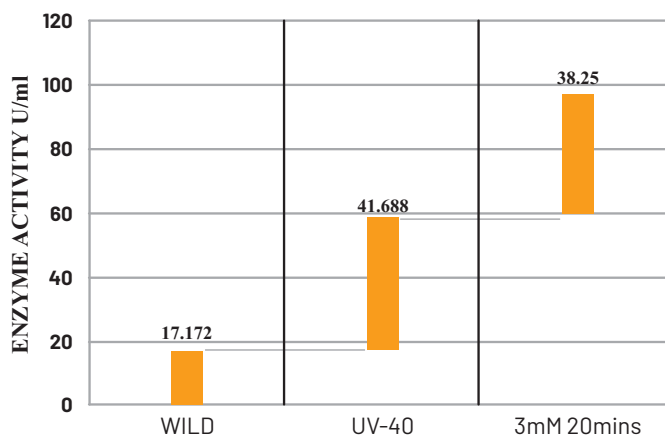


Figure 4: Enzyme Activity of *Aspergillus niger*

Azoreductase activity (U/mL) of *Salmonella typhi* in wild and mutated strains, showing increased enzyme production after EMS and UV-induced mutagenesis.

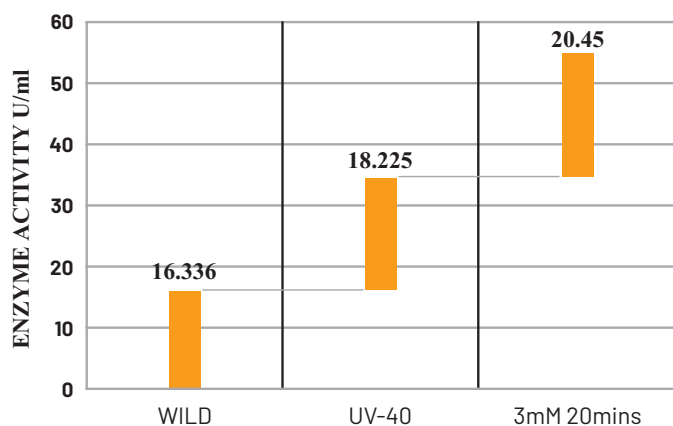


Figure 5: Enzyme Activity of *Salmonella typhi*

FTIR spectrum of UV40-mutated *Aspergillus niger* highlighting key peaks associated with enhanced azoreductase production, including amide I and II regions, polysaccharide, lipid, and hydrogen bonding signatures.

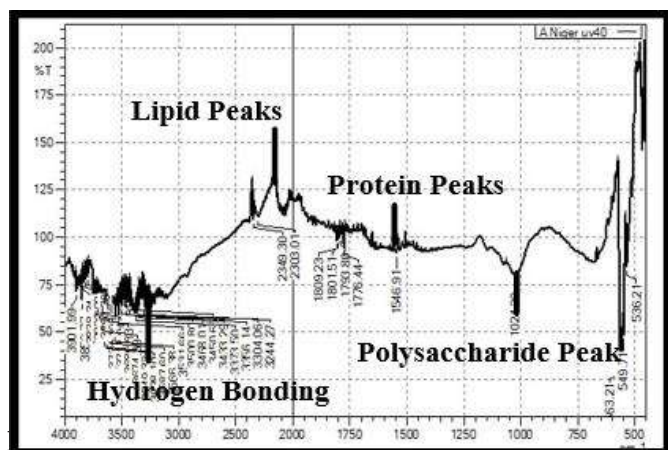


Figure 6: FTIR spectrum showing key peaks for azoreductase production in UV40-mutated *Aspergillus niger*

Based on peaks reported in the literature for azoreductase, the physically mutated strain of *Aspergillus niger* (UV40) exhibited higher intensities in key FTIR regions compared to both the wild strain and the chemically mutated strain (3mM EMS). The UV40 strain showed increased protein-related peaks ($\sim 1641 \text{ cm}^{-1}$ and $\sim 1549 \text{ cm}^{-1}$), indicating enhanced catalytic efficiency and enzyme stability [22]. Additionally, stronger lipid ($\sim 2875\text{--}2925 \text{ cm}^{-1}$) and polysaccharide ($\sim 1030 \text{ cm}^{-1}$) intensities suggest improved membrane stability and cell wall integrity, facilitating better enzyme secretion. Higher hydrogen bonding ($\sim 3317 \text{ cm}^{-1}$) further supports enhanced environmental resistance, making UV40 a more efficient azoreductase producer for azo dye degradation.

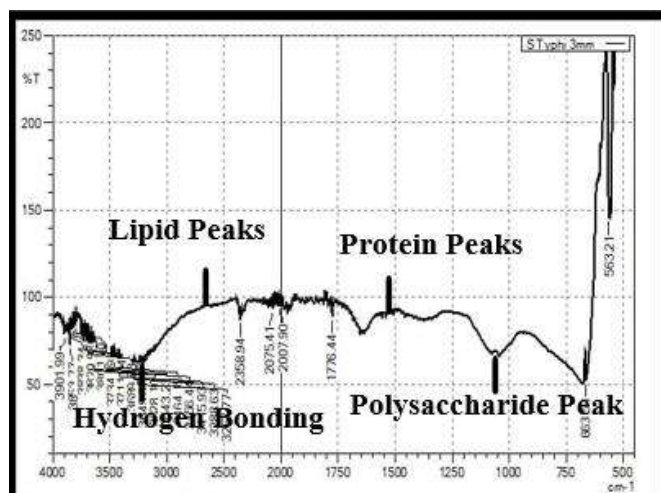


Figure 7: FTIR Spectrum Showing Key Peaks for Azoreductase Production in Chemically Mutated 3mM Strain of *Salmonella typhi*

Based on peaks reported in the literature for azoreductase, the chemically mutated strain of *Salmonella typhi* (3mM EMS) exhibited higher intensities in key FTIR regions compared to the wild strain. The 3mM EMS strain showed increased protein-related peaks ($\sim 1641 \text{ cm}^{-1}$ and $\sim 1549 \text{ cm}^{-1}$), indicating enhanced catalytic efficiency and enzyme stability. Additionally, stronger lipid ($\sim 2875\text{--}2925 \text{ cm}^{-1}$) and polysaccharide ($\sim 1030 \text{ cm}^{-1}$) intensities suggest improved membrane stability and cell wall integrity, facilitating better enzyme secretion. Higher hydrogen bonding ($\sim 3317 \text{ cm}^{-1}$) further supports enhanced environmental resistance, making the 3mM EMS strain a more efficient azoreductase producer for azo dye degradation [23].

FTIR Comparison of UV40 Mutated *Aspergillus niger* and Mutated 3mM Strains of *Salmonella typhi*:

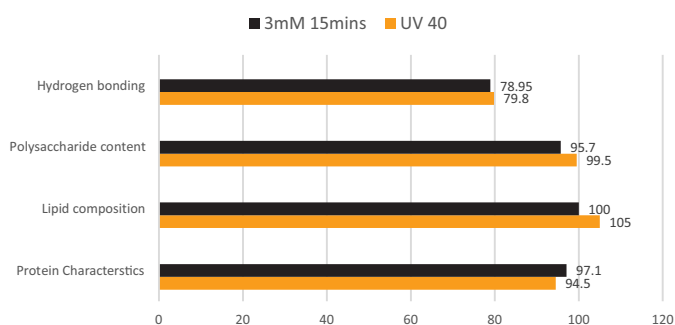


Figure 8: FTIR Comparison of UV40 Mutated *Aspergillus niger* and Chemically Mutated 3mM Strains of *Salmonella typhi*

Aspergillus niger UV40 demonstrated superior results compared to *Salmonella typhi* 3mM, exhibiting enhanced sustained secretion, higher enzyme stability, and improved long-term functionality, making it a more efficient azoreductase producer [15].

Biodegradation of Methyl Orange Textile Dye for *Salmonella typhi*



Figure 9: Before Incubation

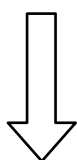


Figure 10: After Incubation for 72 Hours of Methyl Orange dye for *S. typhi*

Initial absorbance readings of Methyl Orange dye at 464 nm before incubation with wild and mutated *Salmonella typhi* strains, showing uniform baseline across all groups.

Table 1: Absorbance of Methyl Orange Dye at 464 nm before Incubation

Type of Strain	Absorbance at 464 nm
Wild	3.000
20 mins	3.000
40 mins	3.000
2mM 15 mins	3.000
3mM 15 mins	3.000

Absorbance of Methyl Orange dye at 464 nm after 72 hours of incubation with *Salmonella typhi*, showing significant dye

degradation by mutated strains compared to the wild type.

Table 2: Absorbance of Methyl Orange Dye at 464 nm after Incubation of 72hrs

Type of Strain	Absorbance at 464 nm
Wild	1.732
20 mins	0.189
40 mins	0.190
2mM 15 mins	0.189
3mM 15 mins	0.191

Wild dye degradation percentage

$$D\% = 100 \times (C_i - C_o) / C_i$$

$$D\% = 100 \times (3.000 - 1.7332) / 3.000$$

$$D\% = 42.2\%$$

Physically mutated strain 20 mins dye degradation percentage

$$D\% = 100 \times (C_i - C_o) / C_i$$

$$D\% = 100 \times (3.000 - 0.189) / 3.000$$

$$D\% = 93.7\%$$

Physically mutated strain 40 mins dye degradation percentage

$$D\% = 100 \times (C_i - C_o) / C_i$$

$$D\% = 100 \times (3.000 - 0.190) / 3.000$$

$$D\% = 93.6\%$$

Chemically mutated strain 2mM 15 mins dye degradation percentage

$$D\% = 100 \times (C_i - C_o) / C_i$$

$$D\% = 100 \times (3.000 - 0.189) / 3.000$$

$$D\% = 93.7\%$$

Chemically mutated strain 3mM 15 mins dye degradation percentage

$$D\% = 100 \times (C_i - C_o) / C_i$$

$$D\% = 100 \times (3.000 - 0.191) / 3.000$$

$$D\% = 93.7\%$$

Brilliant Blue Textile Dye for *Salmonella typhi*

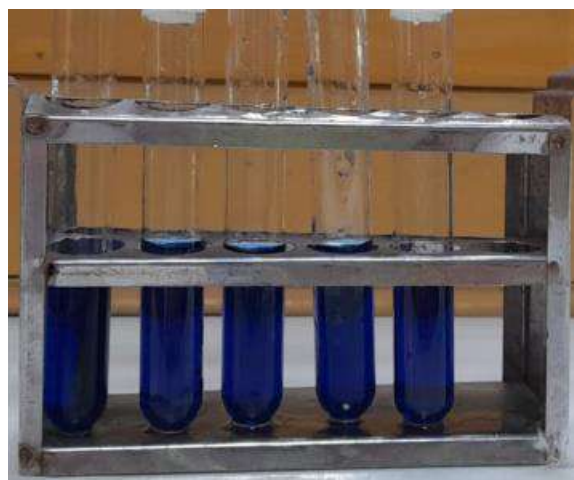


Figure 11: Before Incubation

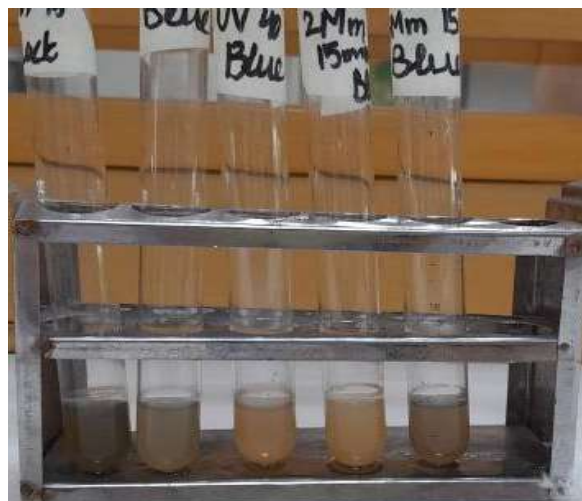


Figure 12: After incubating for 72 hours of brilliant blue dye for *S. typhi*

Baseline absorbance values of Brilliant Blue dye at 628 nm before incubation with wild and mutated *Salmonella typhi* strains, indicating no initial variation among groups.

Table 3: Absorbance of Brilliant Blue Dye at 628 nm before Incubation

Type of Strain	Absorbance at 628 nm
Wild	3.000
20 mins	3.000
40 mins	3.000
2mM 15 mins	3.000
3mM 15 mins	3.000

Absorbance of Brilliant Blue dye at 628 nm after 72 hours of incubation with *Salmonella typhi*, showing enhanced decolorization by EMS and UV-mutated strains compared to the wild type.

Table 4: Absorbance of Brilliant Blue Dye at 628 nm after Incubation of 72hrs

Type of Strain	Absorbance at 628 nm
Wild	0.523
20 mins	0.1926
40 mins	0.1926
2mM 15 mins	0.1927
3mM 15 mins	0.1927

Wild dye degradation percentage

$$D\% = 100 \times (C_i - C_o) / C_i$$

$$D\% = 100 \times (3.000 - 0.523) / 3.000$$

$$D\% = 82.56\%$$

Physically mutated strain 20 mins dye degradation percentage

$$D\% = 100 \times (C_i - C_o) / C_i$$

$$D\% = 100 \times (3.000 - 0.1926) / 3.000$$

$$D\% = 93.58\%$$

Physically mutated strain 40 mins dye degradation percentage

$$D\% = 100 \times (C_i - C_o) / C_i$$

$$D\% = 100 \times (3.000 - 0.1926) / 3.000$$

$$D\% = 93.58\%$$

Chemically mutated strain 2mM 15 mins dye degradation percentage

$$D\% = 100 \times (C_i - C_o) / C_i$$

$$D\% = 100 \times (3.000 - 0.1927) / 3.000$$

$$D\% = 93.57\%$$

Chemically mutated strain 3mM 15 mins dye degradation percentage

$$D\% = 100 \times (C_i - C_o) / C_i$$

$$D\% = 100 \times (3.000 - 0.1927) / 3.000$$

$$D\% = 93.57\%$$

The degradation of Congo Red dye by *Salmonella typhi* strains was assessed over a 72-hour incubation period. As shown in figure 13, all dye samples exhibited a uniform deep red color prior to incubation, confirming the consistency of initial dye concentration across all experimental groups. After 72 hours, notable differences in dye intensity were observed (Figure 14), where mutated strains, particularly those treated with EMS and UV exposure, demonstrated significant decolorization compared to the wild type. This visual observation supports the spectrophotometric data and highlights the enhanced azoreductase activity of the mutated strains in degrading complex dye structures.

Congo Red Textile Dye for *Salmonella typhi*



Figure 13: Before Incubation

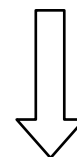




Figure 14: After incubating for 72 hours of Congo Red Dye for *S. typhi*

Baseline absorbance values of Congo Red dye at 497 nm before incubation with wild and mutated *Salmonella typhi* strains, confirming equal initial dye concentration.

Table 5: Absorbance of Congo red Dye at 497 nm before Incubation

Type of Strain	Absorbance at 497 nm
Wild	3.000
20 mins	3.000
40 mins	3.000
2mM 15 mins	3.000
3mM 15 mins	3.000

Absorbance values of Congo Red dye at 497 nm after 72 hours of incubation with *Salmonella typhi*, indicating greater dye degradation by mutated strains compared to the wild type.

Table 6: Absorbance of Congo red dye at 497 nm after incubation of 72hrs

Type of Strain	Absorbance at 497 nm
Wild	0.545
20 mins	0.512
40 mins	0.522
2mM 15 mins	0.525
3mM 15 mins	0.528

Wild dye degradation percentage

$$D\% = 100 \times (Ci - Co) / Ci$$

$$D\% = 100 \times (3.000 - 0.545) / 3.000$$

$$D\% = 81.8\%$$

Physically mutated strain 20 mins dye degradation percentage

$$D\% = 100 \times (Ci - Co) / Ci$$

$$D\% = 100 \times (3.000 - 0.512) / 3.000$$

$$D\% = 82.9\%$$

Physically mutated strain 40 mins dye degradation percentage

$$D\% = 100 \times (Ci - Co) / Ci$$

$$D\% = 100 \times (3.000 - 0.522) / 3.000$$

$$D\% = 82.6\%$$

Chemically mutated strain 2mM 15 mins dye degradation percentage

$$D\% = 100 \times (Ci - Co) / Ci$$

$$D\% = 100 \times (3.000 - 0.525) / 3.000$$

$$D\% = 82.5\%$$

Chemically mutated strain 3mM 15 mins dye degradation percentage

$$D\% = 100 \times (Ci - Co) / Ci$$

$$D\% = 100 \times (3.000 - 0.528) / 3.000$$

$$D\% = 82.4\%$$

The biodegradation potential of *Salmonella typhi* against Reactive Black dye was visually assessed before and after incubation. As shown in figure 15, all samples displayed uniform dark coloration prior to treatment, confirming consistent initial dye concentration. After 72 hours of incubation (Figure 16), notable fading of color was observed in the samples exposed to EMS and UV-mutated strains, indicating enhanced decolorization compared to the wild type. These visual findings align with spectrophotometric results, supporting the improved azoreductase activity in mutated strains for dye degradation.

Reactive Black Textile Dye for *Salmonella typhi*



Figure 15: Before Incubation

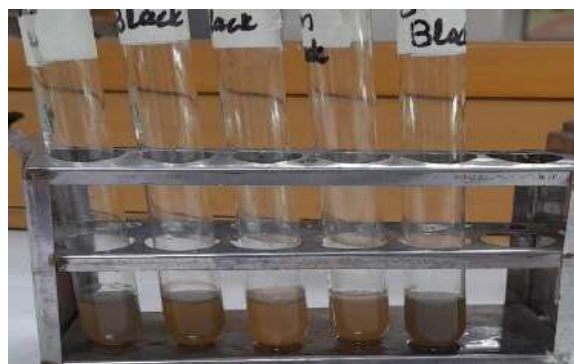


Figure 16: After incubation for 72 hours of reactive black dye for *S. typhi*

Initial absorbance readings of Reactive Black dye at 597 nm before incubation with wild and mutated *Salmonella typhi* strains, showing identical starting concentrations across all groups.

Table 7: Absorbance of Reactive black dye at 597 nm before incubation

Type of Strain	Absorbance at 597 nm
Wild	3.000
20 mins	3.000
40 mins	3.000
2mM 15 mins	3.000
3mM 15 mins	3.000

Absorbance of Reactive Black dye at 597 nm after 72 hours of incubation with *Salmonella typhi*, showing slightly enhanced dye degradation by EMS and UV-mutated strains compared to the wild type.

Absorbance values of Reactive Black dye at 597 nm after 72 hours of incubation with *Salmonella typhi*, indicating effective dye degradation across all mutated strains compared to the wild type.

Table 8: Absorbance of Reactive black dye at 597 nm before incubation

Type of Strain	Absorbance at 597 nm
Wild	0.539
20 mins	0.535
40 mins	0.537
2mM 15 mins	0.537
3mM 15 mins	0.536

Wild dye degradation percentage

$$D\% = 100 \times (C_i - C_o) / C_i$$

$$D\% = 100 \times (3.000 - 0.539) / 3.000$$

$$D\% = 82.03\%$$

Physically mutated strain 20 mins dye degradation percentage

$$D\% = 100 \times (C_i - C_o) / C_i$$

$$D\% = 100 \times (3.000 - 0.535) / 3.000$$

$$D\% = 82.16\%$$

Physically mutated strain 40 mins dye degradation percentage

$$D\% = 100 \times (C_i - C_o) / C_i$$

$$D\% = 100 \times (3.000 - 0.537) / 3.000$$

$$D\% = 82.1\%$$

Chemically mutated strain 2mM 15 mins dye degradation percentage

$$D\% = 100 \times (C_i - C_o) / C_i$$

$$D\% = 100 \times (3.000 - 0.537) / 3.000$$

$$D\% = 82.1\%$$

Chemically mutated strain 3mM 15 mins dye degradation percentage

$$D\% = 100 \times (C_i - C_o) / C_i$$

$$D\% = 100 \times (3.000 - 0.537) / 3.000$$

$$D\% = 82.1\%$$

The decolorization of Congo Red dye by *Aspergillus niger* strains was visually monitored before and after incubation. As shown in figure 17, all dye solutions appeared uniformly red before treatment, indicating consistent initial dye concentrations across wild and mutated strains. After 72 hours of incubation (Figure 18), significant color reduction was observed in samples treated with EMS and UV-mutated strains, highlighting the enhanced azoreductase activity of *A. niger* mutants in dye degradation.

Congo Red Textile Dye for *Aspergillus niger*

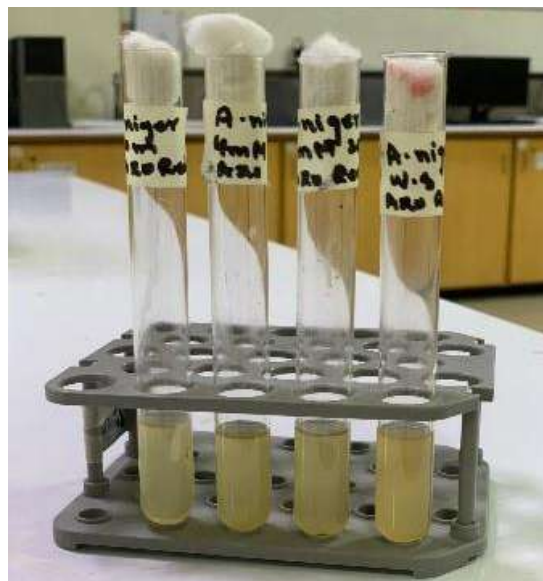


Figure 17: Before Incubation

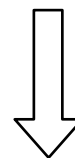


Figure 18: After incubation for 72 hours of Congo red dye for *A. niger* strains. Baseline absorbance of Congo Red dye at 497 nm before incubation with wild and mutated *Aspergillus niger* strains,

showing equal starting concentrations.

Table 9: Absorbance of Azo orange dye at 497 nm before incubation

Type of Strain	Absorbance at 497 nm
Wild	3.000
30 mins	3.000
3mM 20 mins	3.000
4mM 20 mins	3.000

Absorbance of Azo Orange dye at 520 nm after 72 hours of incubation with *Aspergillus niger*, showing enhanced dye degradation by EMS and UV-mutated strains compared to the wild type.

Table 10: Absorbance of Congo red textile dye at 520 nm after incubation of 72hrs

Type of Strain	Absorbance at 520 nm
Wild	0.195
30 mins	0.193
3mM 20 mins	0.190
4mM 20 mins	0.189

Wild dye degradation percentage

$$D\% = 100 \times (C_i - C_o) / C_i$$

$$D\% = 100 \times (3.000 - 0.195) / 3.000$$

$$D\% = 93.5\%$$

Physically mutated strain 30 mins dye degradation percentage

$$D\% = 100 \times (C_i - C_o) / C_i$$

$$D\% = 100 \times (3.000 - 0.193) / 3.000$$

$$D\% = 93.5\%$$

Chemically mutated strain 3mM 20 mins dye degradation percentage

$$D\% = 100 \times (C_i - C_o) / C_i$$

$$D\% = 100 \times (3.000 - 0.190) / 3.000$$

$$D\% = 93.66\%$$

Chemically mutated strain 4mM 20 mins dye degradation percentage

$$D\% = 100 \times (C_i - C_o) / C_i$$

$$D\% = 100 \times (3.000 - 0.189) / 3.000$$

$$D\% = 93.7\%$$

The decolorization of Reactive Black dye by *Aspergillus niger* was visually evaluated before and after treatment. As illustrated in Figure 19, all samples exhibited uniform dark coloration prior to incubation, confirming consistent initial dye levels across the strains. Following 72 hours of incubation (Figure 20), noticeable fading of the dye was observed in cultures exposed to EMS and UV-induced mutations, indicating improved azoreductase activity in the mutated *A. niger* strains.

Reactive Black Textile Dye for *Aspergillus niger*



Figure 19: Before Incubation

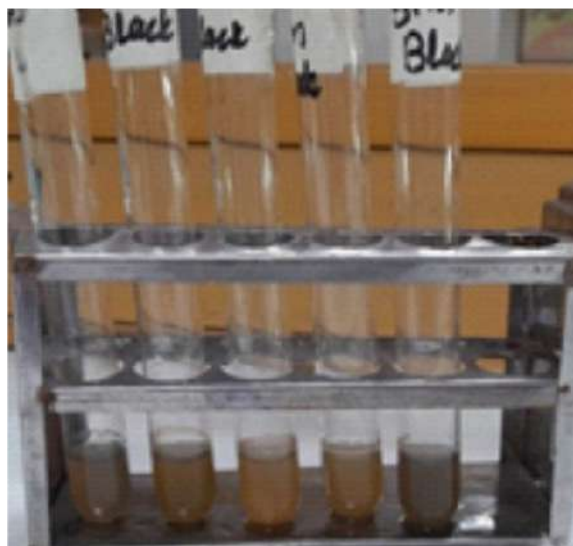


Figure 20: After incubation for 72 hours of reactive black dye for *A. Niger*

Initial absorbance values of Reactive Black dye at 597 nm before incubation with wild and mutated *Aspergillus niger* strains, confirming uniform starting concentrations.

Table 11: Absorbance of Reactive black dye at 597 nm before incubation

Type of Strain	Absorbance at 597 nm
Wild	3.000
30 mins	3.000
3mM 20 mins	3.000
4mM 20 mins	3.000

Absorbance of Reactive Black dye at 597 nm after 72 hours of incubation with *Aspergillus niger*, showing slightly enhanced dye degradation by mutated strains compared to the wild type.

Table 12: Absorbance of Reactive black dye at 597 nm before incubation

Type of Strain	Absorbance at 597 nm
Wild	0.537
30 mins	0.536
3mM 20 mins	0.536
4mM 20 mins	0.535

Wild dye degradation percentage

$$D\% = 100 \times (C_i - C_o) / C_i$$

$$D\% = 100 \times (3.000 - 0.537) / 3.000$$

$$D\% = 82.1$$

Physically mutated strain 30 mins dye degradation percentage

$$D\% = 100 \times (C_i - C_o) / C_i$$

$$D\% = 100 \times (3.000 - 0.536) / 3.000$$

$$D\% = 82.1\%$$

Chemically mutated strain 3mM 20 mins dye degradation percentage

$$D\% = 100 \times (C_i - C_o) / C_i$$

$$D\% = 100 \times (3.000 - 0.536) / 3.000$$

$$D\% = 82.1\%$$

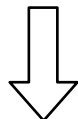
Chemically mutated strain 4mM 20 mins dye degradation percentage

$$D\% = 100 \times (C_i - C_o) / C_i$$

$$D\% = 100 \times (3.000 - 0.535) / 3.000$$

$$D\% = 82.2\%$$

The degradation of Methyl Orange dye by *Aspergillus niger* was visually assessed before and after incubation. As shown in figure 21, all samples exhibited the same deep orange hue prior to treatment, confirming equal initial dye concentrations. After 72 hours of incubation (Figure 22), minimal visual change was observed across all strains, indicating limited azoreductase activity and poor degradation efficiency of Methyl Orange by both wild and mutated *A. niger* strains.

Methyl Orange dye for *Aspergillus niger***Figure 21:** Before Incubation**Figure 22:** After incubation for 72 hours of methyl orange dye for *A. Niger*

Baseline absorbance values of Methyl Orange dye at 464 nm before incubation with wild and mutated *Aspergillus niger* strains, showing uniform initial concentrations across all samples.

Table 13: Absorbance of Reactive black dye at 597 nm before incubation

Type of Strain	Absorbance at 597 nm
Wild	3.000
30 mins	3.000
40 mins	3.000
3mM 20 mins	3.000
4mM 20 mins	3.000

Absorbance of Methyl Orange dye at 464 nm after 72 hours of incubation with *Aspergillus niger*, indicating minimal dye degradation by both wild and mutated strains.

Table 14: Absorbance of Methyl orange dye at 464 nm after incubation of 72hrs

Type of Strain	Absorbance at 464 nm
Wild	1.732
30 mins	1.818
40 mins	1.812
3mM 20 mins	1.819
4mM 20 mins	1.824

Wild dye degradation percentage

$$D\% = 100 \times (C_i - C_o) / C_i$$

$$D\% = 100 \times (3.000 - 1.7332) / 3.000$$

$$D\% = 42.9\%$$

Physically mutated strain 30 mins dye degradation percentage

$$D\% = 100 \times (C_i - C_o) / C_i$$

$$D\% = 100 \times (3.000 - 1.818) / 3.000$$

$$D\% = 39.4\%$$

Physically mutated strain 40 mins dye degradation percentage

$$D\% = 100 \times (C_i - C_o) / C_i$$

$$D\% = 100 \times (3.000 - 1.812) / 3.000$$

$$D\% = 39.6\%$$

Chemically mutated strain 3mM 20 mins dye degradation percentage

$$D\% = 100 \times (Ci - Co) / Ci$$

$$D\% = 100 \times (3.000 - 1.819) / 3.000$$

$$D\% = 39.36\%$$

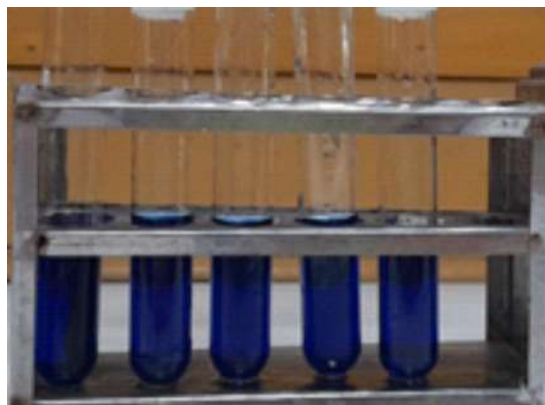
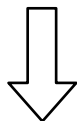
Chemically mutated strain 4mM 20 mins dye degradation percentage

$$D\% = 100 \times (Ci - Co) / Ci$$

$$D\% = 100 \times (3.000 - 1.824) / 3.000$$

$$D\% = 39.2\%$$

The results showed that *Aspergillus niger* did not degrade methyl orange dye when incubated for 72 hours. There was no significant reduction in dye concentration, indicating a lack of azoreductase activity against this particular dye.

Brilliant blue dye for *Aspergillus niger***Figure 23:** Before Incubation**Figure 24:** After incubation for 72hours of Brilliant Blue Dye for *A. Niger*

Initial absorbance values of Brilliant Blue dye at 628 nm before incubation with wild and mutated *Aspergillus niger* strains, confirming equal starting concentrations.

Table 15: Absorbance of Brilliant Blue Dye at 628 nm before Incubation

Type of Strain	Absorbance at 628 nm
Wild	3.000
30 mins	3.000
40 mins	3.000
3mM 20 mins	3.000
4mM 20 mins	3.000

Absorbance of Brilliant Blue dye at 628 nm after 72 hours of incubation with *Aspergillus niger*, indicating minimal decolorization and limited azoreductase activity across all strains.

Table 16: Absorbance of Brilliant Blue Dye at 628 nm after incubation of 72hrs

Type of Strain	Absorbance at 628 nm
Wild	1.825
30 mins	1.815
40 mins	1.848
3mM 20 mins	1.845
4mM 20 mins	1.844

Absorbance of Brilliant Blue dye at 628 nm after 72 hours of incubation with *Aspergillus niger*, indicating minimal decolorization and limited azoreductase activity across all strains.

Wild dye degradation percentage

$$D\% = 100 \times (Ci - Co) / Ci$$

$$D\% = 100 \times (3.000 - 1.825) / 3.000$$

$$D\% = 39.16\%$$

Physically mutated strain 30 mins dye degradation percentage

$$D\% = 100 \times (Ci - Co) / Ci$$

$$D\% = 100 \times (3.000 - 1.815) / 3.000$$

$$D\% = 39.5\%$$

Physically mutated strain 40 mins dye degradation percentage

$$D\% = 100 \times (Ci - Co) / Ci$$

$$D\% = 100 \times (3.000 - 1.848) / 3.000$$

$$D\% = 38.4\%$$

Chemically mutated strain 3mM 20 mins dye degradation percentage

$$D\% = 100 \times (Ci - Co) / Ci$$

$$D\% = 100 \times (3.000 - 1.845) / 3.000$$

$$D\% = 38.5\%$$

Chemically mutated strain 4mM 20 mins dye degradation percentage

$$D\% = 100 \times (Ci - Co) / Ci$$

$$D\% = 100 \times (3.000 - 1.844) / 3.000$$

$$D\% = 38.53\%$$

The results showed that *Aspergillus niger* did not degrade brilliant blue dye when incubated for 72 hours. There was no significant reduction in dye concentration, indicating a lack of azoreductase activity against this particular dye.

Aspergillus niger showed less OD value for brilliant blue compared to Congo Red and Reactive Black.

DISCUSSION

This study demonstrates the successful growth of *Aspergillus niger* and *Salmonella typhi*, both showing their characteristic features. *Aspergillus niger* appeared black, velvety with rough conidia and biseriate conidiophores, whereas *Salmonella typhi* showed smooth, moist, beige colonies under the microscope [24, 25]. The main objective of this study was to compare the azoreductases production capacity of wild and mutated strains of both organisms. *Aspergillus niger* was grown on PDA media, while *Salmonella typhi* on nutrient agar media that support effective growth. Both of the organisms proved to be producing azoreductases, the enzyme that has been of considerable interest in textile industries for azo dye degradation and decolorization capability [26, 27]. Azoreductases demonstrate remarkable efficiency in degrading azo dyes like Methyl Orange, Congo Red, Reactive Black, and Brilliant Blue by converting them into non-toxic amines under aerobic and anaerobic conditions, showing prospects for the bioremediation of industrial wastewaters [2]. Their wide range of pH stability and temperature (25–85°C) stability reinforces their significance in bioremediation [5–9, 28]. Complementary enzymes such as laccase and peroxidases work synergistically with azoreductases to enhance dye degradation, offering a holistic approach for tackling complex pollutants [29]. This combined enzymatic activity underlines the power of bioremediation technologies in mitigating environmental pollution [30]. This study aimed to enhance azoreductases production in *Aspergillus niger* and *Salmonella typhi* through physical and chemical mutagenesis. Mutation induction was performed using Ethyl Methane Sulphonate (EMS) and UV radiation with optimal conditions. EMS, a known ethylating agent that has been used in previous studies to induce GC-AT and AT-GC transitions as well as insertions and deletions [31]. EMS has been widely used to improve enzyme production in various microorganisms including bacteria and fungi with concentration ranging from 1mM to 6mM, as practiced in this research following previous literature [32]. EMS mutagenesis has been used successfully to enhance protein secretion in *Ashbya goossypoi* and increase Ethanol production and also been utilized to enhance the characteristics of other microbial strains like *Beauveria* which is a pest control agent [33, 34]. Similarly, physical mutagenesis methods including UV radiation, X-rays and Gamma rays showed improved enzyme production compared to parental strains [35]. In this research, the results revealed that production of azoreductases has been enhanced in *Aspergillus niger* (3 mM EMS for 20 min and 40 min UV exposure) and *Salmonella typhi* (3 mM EMS for 20 min and 40 min UV exposure). In case of *Aspergillus niger*, chemical mutation resulted in a production of 1.207 mg/ml, while that by physical mutation was 1.116 mg/ml, compared to the wild strain's production of 0.43 mg/ml. For *Salmonella typhi*, chemical mutation resulted in 0.185

mg/ml, and physical mutation to 0.121 mg/ml, both of which were higher than the wild strain. The use of physical and chemical mutagens holds promise for increasing enzyme production and improving enzyme and strain activity [36]. This mutagenic approach holds promise for applications such as textile dye decolorization and industrial enzyme production [37]. Mutated strains of *Aspergillus niger* and *Salmonella typhi* were treated with 1mM L-cysteine HCl for 15 mins, known for its antioxidants and reducing effects during enzyme production. The study revealed that the viability and resistance of the strains improved when treated with 1mM L-cysteine HCl for 15 mins, aligning with the results of [38]. The Quantitative analysis was evaluated through UV-VIS Spectrophotometer and FTIR. The production of azoreductase in both *Aspergillus niger* and *Salmonella typhi* was evaluated through Spectrophotometer at 540nm, which revealed that mutated strains had a higher level of enzyme compared to wild control strains. For *A. Niger*, the absorbance values of the supernatant from fermentation media were 1.158 for 3mM and 1.078 for UV40, which translates to enzyme concentration of 1.207 mg/ml and 1.116 mg/ml respectively, indicated that significant increase of azoreductase production. While in *Salmonella typhi* mutant strains showed 0.299 for 3mM and 0.235 for UV40, which means 0.185 mg/ml and 0.121 mg/ml of enzyme concentrations, respectively. These results have validated the role of spectrophotometric analysis in measuring azoreductase production and showed the influence of mutations in the increase of enzyme titer, which is also in line with the previous work of [39]. The FTIR results, based on specific intensities and peak positions, provide definitive evidence for azoreductase production, aligning with literature-reported. FTIR analysis revealed the structural changes responsible for strain improvements. Large shifts in amide I (~1650 cm⁻¹) and amide II (~1550 cm⁻¹) regions indicated a change in secondary structure of proteins, probably due to enhanced production of azoreductase. Increased carbohydrate peaks (1000–1200 cm⁻¹) and lipid associated vibrations (2850–2950 cm⁻¹), indicated upregulation of metabolic pathways and membrane restructuring, thus allowing better secretion of enzymes. These results are supported by earlier observation by and in which similar biochemical mechanisms were also exhibited in overexpression strains of modified enzymes [2, 8]. The stronger O-H and N-H stretching's around 3300 cm⁻¹ indicated dynamic functional group was improved by FTIR. The result was validated by matching with literature showed UV-induced mutants UV40 showed better growth and enzyme activity than EMS-induced mutants. The Qualitative Analysis was monitored by decolorization of azo dyes through azoreductase activity, an extensively studied enzymatic process. The decolorization was observed after 72 hours. The bacterial strains were incubated at 37 °C, while fungal strains at 30°C. The readings were taken according to the time interval in the UV-VIS

spectrophotometer. The % decolorization was measured by standard formula, indicated that mutated strains more efficiently decolorized dye compared to controls. These findings supported by studies that mutagenesis may boost microbial ability for azo dye degradation [40]. In addition, it has been widely reported that azoreductases can break complex dye structures under optimal conditions which supports the observed efficiency of the mutated strains in this study.

CONCLUSIONS

This study demonstrated that chemical and physical mutagenesis significantly enhances azoreductase production in *Aspergillus niger* and *Salmonella typhi*. The use of optimized substrates and mutagenic treatments led to increased enzyme activity, showcasing the potential of microbial strain improvement for biotechnological applications. Enhanced degradation of Azo dyes such as Methyl Orange, Brilliant Blue, Reactive Black, and Congo Red by mutated strains highlights a sustainable solution for industrial wastewater treatment. Quantitative analysis through UV-Vis Spectrophotometry and FTIR confirmed higher enzyme levels in mutated strains, while qualitative analysis showed improved dye decolorization compared to wild types. These results support the application of microbial azoreductases in bioremediation, with scalability for industrial use. The findings underscore the versatility of azoreductases in environmental and industrial biotechnology, encouraging future research into strain engineering and enzyme optimization. This work contributes to the development of eco-friendly alternatives to conventional chemical treatments. The authors declare no competing financial or personal interests that could have influenced the outcomes of this study.

Authors Contribution

Conceptualization: FT

Methodology: DB, HR, FT

Formal analysis: HR, DB, FT

Writing, review and editing: MW, HR, FT

All authors have read and agreed to the published version of the manuscript.

Conflicts of Interest

The authors declare no conflict of interest.

Source of Funding

The authors received no financial support for the research, authorship and/or publication of this article.

REFERENCES

- [1] Alzain H, Kalimugogo V, Hussein K, Karkadan M. A review of environmental impact of azo dyes. *International Journal of Research and Review*. 2023 Jun; 10(6): 673-89. doi: 10.52403/ijrr.20230682.
- [2] Singh GB, Vinayak A, Mudgal G, Kesari KK. Azo dye bioremediation: An interdisciplinary path to sustainable fashion. *Environmental Technology & Innovation*. 2024 Sep; 103832. doi: 10.1016/j.eti.2024.103832.
- [3] Chaudhary R, Nawaz A, Fouillaud M, Dufossé L, Haq IU, Mukhtar H. Microbial cell factories: biodiversity, pathway construction, robustness, and industrial applicability. *Microbiology Research*. 2024 Feb; 15(1): 247-72. doi: 10.3390/microbiolres15010018.
- [4] Bumpus JA. Biodegradation of azo dyes by fungi. *Mycology Series*. 2004 Mar; 21: 457-70. doi: 10.1201/9780203913369.ch38.
- [5] Bala S, Garg D, Thirumalesh BV, Sharma M, Sridhar K, Inbaraj BS et al. Recent strategies for bioremediation of emerging pollutants: a review for a green and sustainable environment. *Toxics*. 2022 Aug; 10(8): 484. doi: 10.3390/toxics10080484.
- [6] Wang R, Li H, Liu Y, Chen J, Peng F, Jiang Z et al. Efficient removal of azo dyes by *Enterococcus faecalis* R1107 and its application in simulated textile effluent treatment. *Ecotoxicology and Environmental Safety*. 2022 Jun; 238: 113577. doi: 10.1016/j.ecoenv.2022.113577.
- [7] Ikram M, Naeem M, Zahoor M, Rahim A, Hanafiah MM, Oyekanmi AA et al. Biodegradation of azo dye methyl red by *Pseudomonas aeruginosa*: optimization of process conditions. *International Journal of Environmental Research and Public Health*. 2022 Aug; 19(16): 9962. doi: 10.3390/ijerph19169962.
- [8] Ayed L, Bekir K, Jabeur C. Modeling and optimization of biodegradation of methylene blue by *Staphylococcus aureus* through a statistical optimization process: a sustainable approach for waste management. *Water Science and Technology*. 2022 Jul; 86(2): 380-94. doi: 10.2166/wst.2022.211.
- [9] Kumar Shri Guru A and Kumar Singh S. Biodegradation of azo dyes by *Bacillus subtilis* "RA29" 2018. Available from: <https://www.researchgate.net/publication/281959357>.
- [10] Kumar A, Chopra J, Singh SK, Khan A, Singh RN. Biodegradation of azo dyes by *Bacillus subtilis* 'RA29'. *Der Pharmacia Lettre*. 2015 Jan; 7(6): 234-8.
- [11] Philip I, Sarojini S, Biswas S, Jayaram S. Exploring the Potential of *Bacillus velezensis*, an Endophytic Bacteria Isolated from *Alternanthera philoxeroides* for Plant Growth Promotion and Bioremediation Properties. *Journal of Pure & Applied Microbiology*. 2023 Sep; 17(3). doi: 10.22207/JPAM.17.3.40.
- [12] Carruthers DN and Lee TS. Translating advances in microbial bioproduction to sustainable biotechnology. *Frontiers in Bioengineering and*

- Biotechnology. 2022 Aug; 10: 968437. doi: 10.3389/fbioe.2022.968437.
- [13] Basu S, Bose C, Ojha N, Das N, Das J, Pal M et al. Evolution of bacterial and fungal growth media. *Bioinformation*. 2015 Apr; 11(4): 182. doi: 10.6026/97320630011182.
- [14] Schroeder JW, Yeesin P, Simmons LA, Wang JD. Sources of spontaneous mutagenesis in bacteria. *Critical Reviews in Biochemistry and Molecular Biology*. 2018 Jan; 53(1): 29-48. doi: 10.1080/10409238.2017.1394262.
- [15] Wei W, Ho WC, Behringer MG, Miller SF, Bcharah G, Lynch M. Rapid evolution of mutation rate and spectrum in response to environmental and population-genetic challenges. *Nature Communications*. 2022 Aug; 13(1): 4752. doi: 10.1038/s41467-022-32353-6.
- [16] Tamano K. Enhancing microbial metabolite and enzyme production: current strategies and challenges. *Frontiers in Microbiology*. 2014 Dec; 5: 718. doi: 10.3389/fmicb.2014.00718.
- [17] Yuan L, Chang J, Yin Q, Lu M, Di Y, Wang P et al. Fermented soybean meal improves the growth performance, nutrient digestibility, and microbial flora in piglets. *Animal Nutrition*. 2017 Mar; 3(1): 19-24. doi: 10.1016/j.aninu.2016.11.003.
- [18] Brüsweiler BJ and Merlot C. Azo dyes in clothing textiles can be cleaved into a series of mutagenic aromatic amines which are not regulated yet. *Regulatory Toxicology and Pharmacology*. 2017 Aug; 88: 214-26. doi: 10.1016/j.yrtph.2017.06.012.
- [19] Leonard CA, Brown SD, Hayman JR. Random mutagenesis of the *Aspergillus oryzae* genome results in fungal antibacterial activity. *International Journal of Microbiology*. 2013; 2013(1): 901697. doi: 10.1155/2013/901697.
- [20] Chen H, Hopper SL, Cerniglia CE. Biochemical and molecular characterization of an azoreductase from *Staphylococcus aureus*, a tetrameric NADPH-dependent flavoprotein. *Microbiology*. 2005 May; 151(5): 1433-41. doi: 10.1099/mic.0.27805-0.
- [21] Saranraj P, Stella D, Sivasakthivelan P. Separation, purification and characterization of dye degrading enzyme azoreductase from bacterial isolates. *Central European Journal of Experimental Biology*. 2014; 3(2): 19-25.
- [22] Cong J, Xie X, Liu Y, Qin Y, Fan J, Fang Y et al. Biochemical characterization of a novel azo reductase named BVU5 from the bacterial flora DDMZ1: application for decolorization of azo dyes. *RSC advances*. 2022 Jan; 12(4): 1968-81. doi: 10.1039/D1RA08090C.
- [23] Liu S, Xu X, Kang Y, Xiao Y, Liu H. Degradation and detoxification of azo dyes with recombinant ligninolytic enzymes from *Aspergillus* sp. with secretory overexpression in *Pichia pastoris*. *Royal Society Open Science*. 2020 Sep; 7(9): 200688. doi: 10.1098/rsos.200688.
- [24] Diba K, Kordbacheh P, Mirhendi SH, Rezaie S, Mahmoudi M. Identification of *Aspergillus* species using morphological characteristics. 2007 Oct - Dec; 23(6): 867-872.
- [25] Afzal H, Shazad S, Qamar S, Nisa U. Morphological identification of *Aspergillus* species from the soil of Larkana District (Sindh, Pakistan). *Asian Journal of Agriculture and Biology*. 2013 Jan; 1(3): 105-17.
- [26] Baweja M, Nain L, Kawarabayasi Y, Shukla P. Current technological improvements in enzymes toward their biotechnological applications. *Frontiers in Microbiology*. 2016 Jun; 7: 965. doi: 10.3389/fmicb.2016.00965.
- [27] Pinheiro LR, Gradissimo DG, Xavier LP, Santos AV. Degradation of azo dyes: bacterial potential for bioremediation. *Sustainability*. 2022 Jan; 14(3): 1510. doi: 10.3390/su14031510.
- [28] Alabdraba W and Bayati M. Biodegradation of Azo dyes a review. *International Journal of Environmental Sciences & Natural Resources*. 2014 Oct; 1(4): 179-89.
- [29] Sudha M, Saranya A, Selvakumar G, Sivakumar N. Microbial degradation of azo dyes: a review. *International Journal of Current Microbiology and Applied Sciences*. 2014 Mar; 3(2): 670-90.
- [30] Pramanik S and Chaudhuri S. Laccase activity and azo dye decolorization potential of *Podoscypha elegans*. *Mycobiology*. 2018 Jan; 46(1): 79-83. doi: 10.1080/12298093.2018.1454006.
- [31] Sega GA. A review of the genetic effects of ethyl methanesulfonate. *Mutation Research/Reviews in Genetic Toxicology*. 1984 Sep; 134(2-3): 113-42. doi: 10.1016/0165-1110(84)90007-1.
- [32] Chen L, Duan L, Sun M, Yang Z, Li H, Hu K et al. Current trends and insights on EMS mutagenesis application to studies on plant abiotic stress tolerance and development. *Frontiers in Plant Science*. 2023 Jan; 13: 1052569. doi: 10.3389/fpls.2022.1052569.
- [33] Ribeiro O, Magalhães F, Aguiar TQ, Wiebe MG, Penttilä M, Domingues L. Random and direct mutagenesis to enhance protein secretion in *Ashbya gossypii*. *Bioengineered*. 2013 Sep; 4(5): 322-31. doi: 10.4161/bioe.24653.
- [34] Majumdar A. Molecular techniques for the improvement of microbial biocontrol agents against plant pathogens. *Egyptian Journal of Biological Pest Control*. 2023 Oct; 33(1): 103. doi: 10.1186/s41938-023-00746-4.

- [35] Ghazi S, Sepahy AA, Azin M, Khaje K, Khavarinejad R. UV mutagenesis for the overproduction of xylanase from *Bacillus mojavensis* PTCC 1723 and optimization of the production condition. *Iranian Journal of Basic Medical Sciences*. 2014 Nov; 17(11): 844–853.
- [36] Kaul P and Asano Y. Strategies for discovery and improvement of enzyme function: state of the art and opportunities. *Microbial Biotechnology*. 2012 Jan; 5(1): 18–33. doi: 10.1111/j.1751-7915.2011.00280.x.
- [37] Tripathi M, Singh S, Pathak S, Kasaudhan J, Mishra A, Bala S et al. Recent strategies for the remediation of textile dyes from wastewater: a systematic review. *Toxics*. 2023 Nov; 11(11): 940. doi: 10.3390/toxics11110940.
- [38] Hussein HA and Alshammari SO. Cysteine mitigates the effect of NaCl salt toxicity in flax (*Linum usitatissimum* L) plants by modulating antioxidant systems. *Scientific Reports*. 2022 Jul; 12(1): 11359. doi: 10.1038/s41598-022-14689-7.
- [39] Adeniyi AO, Boyro DE, Chindo IY, Mahmoud AA. Spectrophotometric and infra-red analyses of azo reactive dyes derived from 2-methyl-3-(2'-methylphenyl)-6-arylazo-4-oxoquinazoline. *Science World Journal*. 2023 Oct; 18(2): 231–9. doi: 10.4314/swj.v18i2.10.
- [40] El Awady ME, El-Shall FN, Mohamed GE, Abd-Elaziz AM, Abdel-Monem MO, Hassan MG. Exploring the decolorization efficiency and biodegradation mechanisms of different functional textile azo dyes by *Streptomyces albidoflavus* 3MGH. *BioMed Central Microbiology*. 2024 Jun; 24(1): 210. doi: 10.1186/s12866-024-03347-9.

FUTURISTIC BIOTECHNOLOGY

<https://fbtjournal.com/index.php/fbt>

ISSN (E): 2959-0981, (P): 2959-0973

Volume 4, Issue 3 (July–Sep 2024)



Original Article



Silver Nanoparticle–Integrated Nile Tilapia Skin Improves Healing of Skin Burn Wounds in Sprague Dawley Rats

Nadia Wajid¹, Sheheryar Ahmad Khan¹, Amna Bibi¹, Sumair Raza¹ and Fatima Ali^{1*}

¹Institute of Molecular Biology and Biotechnology, The University of Lahore, Lahore, Pakistan

ARTICLE INFO

Keywords:

Tilapia Fish, Silver Nanoparticles, Burn, Wound Healing, Collagen

How to Cite:

Wajid, N., Khan, S. A., Bibi, A., Raza, S., & Ali, F. (2024). Silver Nanoparticle–Integrated Nile Tilapia Skin Improves Healing of Skin Burn Wounds in Sprague Dawley Rats: Silver Nanoparticle–Integrated Nile Tilapia: Sprague Dawley Rats. *Futuristic Biotechnology*, 4(03), 56–61. <https://doi.org/10.54393/fbt.v4i03.205>

*Corresponding Author:

Fatima Ali

Institute of Molecular Biology and Biotechnology,
The University of Lahore, Lahore, Pakistan
fatima.ali@imbb.uol.edu.pk

Received Date: 22nd June, 2024

Acceptance Date: 10th September, 2024

Published Date: 30th September, 2024

ABSTRACT

In developing nations, skin burns create a significant economic and medical burden, given the lack of proper infection control, which leads to high morbidity and mortality. Tilapia fish skin and silver nanoparticles (AgNPs) have strong antibacterial and healing-promoting abilities as a traditional biological dressing and as a potent biological dressing, respectively. **Objectives:** To measure the wound-healing ability of AgNP-modified Tilapia fish skin on second-degree burns in Sprague Dawley rats. **Methods:** A total of 20 male rats were categorized into four groups, namely Group 1 (normal skin), Group 2 (burn), Group 3 (burn treated with Tilapia fish skin), and Group 4 (burn treated with Tilapia fish skin conjugated with AgNPs). The method applied to induce the second-degree burns involved a heated metal block, and treatments were done after 24 hours. Day 21, histological and biochemical samples of the skin were taken, and they underwent ELISA and hydroxyproline assays. **Results:** The concentration of the hydroxyproline levels was raised significantly ($375.67 \pm 42.16 \mu\text{g}/\text{mg}$) in comparison with Group II ($96.00 \pm 4.36 \mu\text{g}/\text{mg}$). There was an increase in VEGF and SDF-1 α , which means that angiogenesis and tissue repair were increased. Antioxidant parameters were found to restore GSH ($0.272 \pm 0.0157 \mu\text{mol}/\text{mg}$) and normalize SOD and CAT activities, and they reduced MDA ($0.024 \pm 0.0026 \text{ nmol}/\text{mg}$). Liver, kidney, and heart histology were normal. **Conclusions:** AgNPs impaired tilapia fish skin enhances the healing of the burn wound through the increased production of collagen, angiogenesis, and the antioxidant response without causing systemic toxicity and making it a safe, cost-effective biological dressing.

INTRODUCTION

Millions of people are affected by Skin Burns annually, with a severe burden on a global level [1], particularly in developing nations because of the lack of resources and proper facilities [2]. In Pakistan, the case is even more complicated by the late treatment and the ignorance of the population, which results in the high infection rate [3]. Tilapia fish with skin contains high collagen, moisture retention, and is biocompatible. In a Phase III randomized controlled trial, it significantly increased re-epithelialization, decreased pain, and lowered the treatment costs compared to silver sulfadiazine cream in patients with partial-thickness burns [4]. In Pakistan, infections in the burn wounds are a major cause of morbidity and mortality due to the multidrug-resistant

(MDR) bacteria [5]. Silver nanoparticles (AgNPs) have been reported to have antimicrobial activity against many MDR Gram-positive and Gram-negative bacteria. AgNPs in synergy with antibiotics improve the antibacterial efficacy, potentially reducing the side effects [6, 7]. AgNPs exhibit antibacterial, antioxidant, and anti-inflammatory properties owing to better wound healing [8–10]. The present study combines the healing potential of tilapia fish skin with the antibacterial properties of silver nanoparticles. We hypothesized that the synergistic combination of Tilapia skin and AgNPs would result in a composite dressing that significantly accelerates burn wound healing compared to either component alone, by concurrently enhancing collagen deposition,

angiogenesis, and antioxidant defense while preventing infection.

The objective of this study was to evaluate the efficacy and biosafety of this novel AgNP-integrated Tilapia skin dressing on second-degree burn wounds in a rat model.

METHODS

This experimental study was conducted at the University of Lahore from 1 December 2023 to 30 May 2024. Fresh Tilapia (*Oreochromis niloticus*) from the River Nile was procured from the Fisheries Research and Training Institute, Lahore. Skin was carefully separated from the muscle using a sharp and blunt dissection method. Isolated skin samples were washed with normal saline and cut into 2 × 2 cm patches. A starch solution was prepared in deionized water, and 100 mL of silver nitrate (Ag-NO₃) solution was added to it. The mixture was transferred to a dark glass bottle and autoclaved for 5 minutes. The yellow color indicated the formation of Ag-NPs, which were stored at room temperature away from direct sunlight. The initial yellowish-brown color observed indicated the preliminary reduction of Ag⁺ ions to Ag⁰ nanoparticles, attributed to surface plasmon resonance. However, the formation and stability of Ag-NPs were further confirmed through UV-Vis spectroscopy, TEM, DLS, and zeta potential analyses. UV-Visible spectroscopy confirmed the surface plasmon resonance peak at 420 nm, indicating Ag-NP formation. Transmission Electron Microscopy (TEM) images showed spherical particles averaging 25–35 nm in size. Dynamic Light Scattering (DLS) analysis confirmed a narrow size distribution (PDI = 0.21), while zeta potential measurements (−28.6 mV) indicated good colloidal stability. The concentration of silver nitrate used for nanoparticle synthesis was 1 mM, and after purification, the final colloidal Ag-NP concentration was approximately 0.85 mM, corresponding to an 85% yield. Concentration and yield were determined by gravimetric analysis following centrifugation and drying of Ag-NP pellets at 60°C for 12 hours. The sample size was justified with the following addition: A sample size of five rats per group (n=5) was determined to be adequate based on a power analysis conducted using G*Power software (version 3.1.9.7). The calculation assumed an effect size (f) of 0.4, an alpha error probability of 0.05, and a statistical power (1-β) of 0.8 for a one-way ANOVA design with four groups. This effect size is consistent with similar previously published studies on burn wound healing in rodent models. Twenty healthy male Sprague Dawley rats (200–250 g) were acclimatized at 22 ± 2°C for one week with free access to food and water. Rats were anesthetized with intraperitoneal injection of ketamine and xylazine. Second-degree burn was inflicted with a solid iron bar (2 × 2 cm) heated in boiling water (100°C),

leading to surgical debridement to remove necrotic tissue. Application of Tilapia skin on excisional burn Wounds was done. Animals were divided into four groups (n = 5 per group): Group I Normal (no burn); Group II Burn only; Group III Burn + Tilapia fish skin; Group IV Burn + Tilapia fish skin functionalized with Ag-NPs. For Group IV, each Tilapia skin patch (2 × 2 cm) was coated with 2 mL of Ag-NP colloidal solution (0.85 mM) and allowed to dry for 30 minutes under sterile laminar flow conditions before application. This ensured uniform nanoparticle adsorption and consistent dosing across treated wounds. Fish skins were applied after 24 hours of the wound. All rats were sacrificed on day 21 to evaluate tissue regeneration and biosafety. Guidelines of the American Veterinary Medical Association (AVMA) were followed for the Euthanasia (2020) [11]. Wound areas were traced on transparent sheets and photographed with a metric ruler for calibration. The images were coded, and the wound area (mm²) was measured by an investigator blinded to the experimental groups using ImageJ software (version 1.53t, NIH, USA). Wound areas were recorded on days 7, 14, and 21 by tracing the margins on transparent sheets. All rats were carefully monitored for any sign of infection, including fever and pus. Ibuprofen BP (100 mg/5 mL) was administered daily to all rats as an analgesic. Wound areas were traced on transparent sheets and photographed with a metric ruler for calibration. Images were analyzed using ImageJ software (version 1.53t, NIH, USA). Wound area (mm²) was measured at days 7, 14, and 21, and percentage wound contraction was calculated as: Wound contraction (%) = $\frac{A_0 - A_t}{A_0} \times 100$, where A₀ is the initial wound area and A_t is the wound area at each time point. Histopathological analysis of skin tissue was done. Skin samples were fixed in 10% neutral buffered formalin at room temperature overnight. The tissues were then dehydrated in ethanol (70%, 80%, 90%, and 100%), treated with xylene, and embedded in paraffin wax. Staining was performed as reported by our research group [5]. Estimation of hydroxyproline was done. Hydroxyproline is a key marker of collagen content and extracellular-matrix remodeling [12]. Skin was dried at 60°C for 24 hours, which was transferred to an Eppendorf tube and hydrolyzed with 6 N HCl for 12 hours. The acid was neutralized with 10 N NaOH, and the resulting lysate was diluted to 20 mg/mL of water. From this, 300 µL was transferred to a test tube, and 0.01 M CuSO₄, 2.5 N NaOH, and 6% H₂O₂ were added. After vigorously shaking for 5 minutes, the tubes were incubated at 80°C for 10 minutes. Samples were treated with 3 N H₂SO₄ and freshly prepared P-dimethylaminobenzaldehyde (PDMAB). This mixture was incubated at 75°C for 15 minutes, cooled, absorbance was taken at 540 nm. Indirect

ELISA was performed to quantify VEGF and SDF-1 levels using commercial ELISA kits (MyBioSource, USA; Cat. Nos. MBS723495 and MBS2508553). Protein extracts (50 μ L) from skin tissue were added to 96-well plates and incubated overnight for antigen adsorption. After washing with PBS-T, wells were incubated with rabbit anti-rat VEGF or rabbit anti-rat SDF-1 primary antibodies (1:1000 dilution), followed by HRP-conjugated goat anti-rabbit IgG secondary antibody (1:2000 dilution). The TMB substrate was added to initiate the enzyme-substrate reaction, and 2 M HCl was used to stop the reaction. Absorbance was measured at 450 nm (reference 650 nm) using a microplate reader (BioTek ELx808, USA). Each sample was measured in triplicate, and the mean value was used for analysis. A pooled control sample was included on each plate to calculate the inter-assay coefficient of variation (CV), which was maintained below 10%. The activity of antioxidant enzymes, including catalase (CAT), superoxide dismutase (SOD), glutathione (GSH), and malondialdehyde (MDA), was determined using standardized spectrophotometric protocols. Reagent concentrations and reaction volumes were standardized to maintain linear reaction kinetics and reproducibility. Activity of antioxidant enzymes (CAT, SOD, GSH, and reactive oxygen species MDA) were estimated from skin tissue homogenates according to our lab's standard protocols [13]. All spectrophotometric measurements for antioxidant enzymes and MDA were performed in duplicate for each sample. The intra-assay CV was consistently below 8% for all parameters. Glutathione (GSH) estimation: 50 μ L homogenate of the tissue and 50 μ L disodium hydrogen phosphate (0.3 M) were combined and centrifuged at 13,000 rpm for 10 minutes. 18.2 μ L of the supernatant was combined with 72.7 μ L disodium hydrogen phosphate (0.3 M) and 9 μ L of DTNB (0.001 M). Absorbance was taken at 520 nm. Estimation of CAT: 1 mL of the skin protein was combined with 1 mL of 10 mM PBS and centrifuged at 13,000 rpm at 4°C. 286 μ L supernatant was combined with 143 μ L 10 mM phosphate buffer and 57.1 μ L 0.2 M H₂O₂ and boiled for 10 minutes. Samples were left to cool, and the absorbance at 530 nm was taken. Superoxide Dismutase (SOD): 100 μ L of 50 percent TCA was added to 100 μ L of protein. The mixture was centrifuged at 13,000 rpm for 10 minutes, and 30 μ L supernatant was mixed with 300 μ L of 50 mM sodium phosphate buffer (pH 8.3), 30 μ L phenazine methosulfate, 90 μ L NBT, and 60 μ L NADH. After 10 minutes, acetic acid and n-butanol were added, and the samples were centrifuged at 2,000 rpm for 5 minutes. Absorbance of the upper layer was taken at 520 nm. Estimation of Malondialdehyde (MDA): Tissue homogenate was centrifuged at 13,000 rpm for 10 minutes at 4°C. 20 μ L of homogenate was mixed with 20 μ L of 8.1% SDS, 150 μ L (0.8%) TBA, and 150 μ L (20%) acetic acid (pH 3.5). Using

distilled water, the volume of the mixture was raised to 400 μ L, which was then boiled at 90°C for 60 minutes.

MDA was then cooled and extracted with 500 μ L of n-butanol and pyridine solution (15:1). The centrifugation absorbance of the top layer was measured at 532 nm. The hearts, livers, and kidneys of all study groups were removed and stained with the use of hematoxylin and eosin (H&E) as mentioned above. A microscope (Olympus, USA) was used to view the slides in order to evaluate any morphological changes. All data are in the form of mean \pm standard deviation (SD). The test of normality of data distribution was conducted with the aid of the Shapiro-Wilk test, and the homogeneity of the variances was tested with the assistance of the Brown-Forsythe test. GraphPad Prism software (version 9.5.0, GraphPad Software, USA) was used to statistically analyze the results. General comparisons between several groups were done using a one-way analysis of variance (ANOVA), and then, the post-hoc test was done using Tukey to establish specific group differences. There are specific p-values reported where significant post-hoc comparisons are present, and the probability value of $p < 0.05$ was deemed significant.

RESULTS

Measurement of wound areas was done on days 7, 14, and 21 with tracing paper and measured subsequently after calibration (1 cm = 10 pixels) in ImageJ software. The wound area was found to decrease progressively in all the treated groups where dressings were placed on the wounds. On day 21, near total epithelialization (about 95 percent wound contraction) was detected in rats in which the wounds were sprayed with Tilapia skin conjugated with Ag-NPs. There was no pus formation, tissue necrosis, or infection observed in either of the two experimental groups (A and B). Group II (burn only) skin of rats exhibited partial re-epithelialization and inflammatory-cell-infiltration, and necrotic debris. Conversely, Group IV (Tilapia fish skin + Ag-NPs) showed full re-epithelialization of tissues with distinct epidermal layers, a high number of fibroblasts, and thick deposits of collagen, which showed high tissue regeneration (C). On day 7, hydroxyproline levels were 675.33 ± 26.10 μ g/mg in Group I (normal), 20.67 ± 2.08 μ g/mg in Group II (burn), 31.33 ± 3.51 μ g/mg in Group III (Tilapia skin), and 49.33 ± 1.53 μ g/mg in Group IV (Tilapia + Ag-NPs). These results indicate a significant reduction of hydroxyproline in the burn group compared with the normal group and a marked recovery in Groups III and IV. On day 14, Group IV showed the highest hydroxyproline (102.33 ± 6.66 μ g/mg) compared with 67.40 ± 4.93 μ g/mg in Group II, indicating enhanced granulation-tissue development. By day 21, hydroxyproline further increased to 375.67 ± 42.16 μ g/mg in Group IV versus 96.00 ± 4.36 μ g/mg in Group II and 292.67 ± 11.93 μ g/mg in Group III (D). All values are expressed as mean

± SD (n=5). These results indicate a statistically significant reduction ($p < 0.001$) of hydroxyproline in the burn group compared with the normal group and a significant recovery ($p < 0.01$ for Group III; $p < 0.001$ for Group IV) in the treated groups (Figure 1).

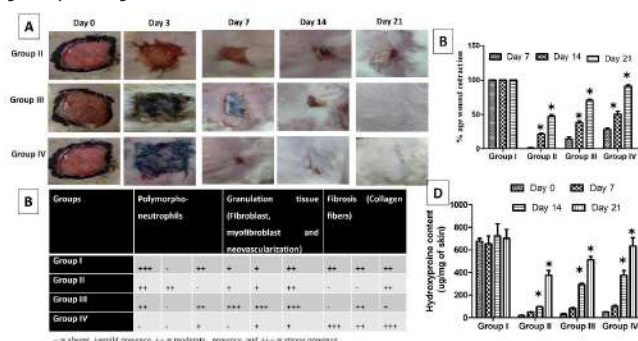


Figure 1: Wound Contraction, Histopathological Evaluation, Hydroxyproline Content (µg Hydroxyproline Per mg Dry Tissue)

VEGF (ng per mg protein) VEGF levels were highest in Group IV (0.364 ± 0.0230) compared with 0.132 ± 0.0097 in Group I, 0.153 ± 0.0039 in Group II, and 0.261 ± 0.0083 in Group III. These findings indicate that Tilapia skin conjugated with AgNPs markedly promoted neovascularization and granulation-tissue formation. Indicating significantly improved ($p < 0.001$) recruitment of progenitor/stem cells to the wound site. SDF-1 (ng per mg protein) SDF-1 levels were significantly reduced in Group II (0.259 ± 0.0059) compared with Group I (0.668 ± 0.0416), consistent with burn-induced depletion of stem-cell signaling. They were partially restored in Group III (0.534 ± 0.0286) and fully restored in Group IV (0.650 ± 0.0217), indicating improved recruitment of progenitor/stem cells to the wound site. (Corrected trend and unit clarified; previous numerical inconsistency resolved). Glutathione (GSH; µmol/g tissue). Group II had a considerable depletion of GSH than Group I (0.203 ± 0.0098 vs 0.287 ± 0.0253), which showed the existence of oxidative stress. Group III and Group IV had an improved GSH level of 0.275 and 0.272, respectively. Catalase (CAT; U/mg protein). Group I and Group II had CAT activity of 0.144 ± 0.0033 U/mg and Group II respectively, which was significantly higher 0.978 ± 0.0103 , as a compensatory response to the antioxidant. Activity also rose in Group III (1.263 ± 0.0258), and returned to normal in Group IV (1.137 ± 0.0226), which is good evidence of a redox balance restoration. Superoxide Dismutase (SOD; U/ mg protein) SOD levels shot up in the Group II (1.170 ± 0.0067) relative to Group I (0.106 ± 0.0141), which indicates an oxidative injury. They stabilized in Group III (0.984 ± 0.0571) and reverted to baseline in Group IV (0.963 ± 0.0031), and this indicates successful mitigation of superoxide stress by AgNP-conjugated Tilapia skin. Malondialdehyde (MDA; nmol/mg protein). The MDA level rose to 1.126 ± 0.0065 nmol/mg in Group II and 0.045 ± 0.0427 nmol/mg in Group I, which

means that lipid peroxidation was more effective in Group II compared to Group I after burn injury. Values went up to 0.979 ± 0.0418 nmol/mg in Group III and even less (0.024 ± 0.0026) in Group IV. These results indicate the existence of antioxidative and cytoprotective properties of Ag-NPs and Tilapia skin, which reduced the occurrence of lipid peroxidation and enhanced tissue regeneration (Figure 2).

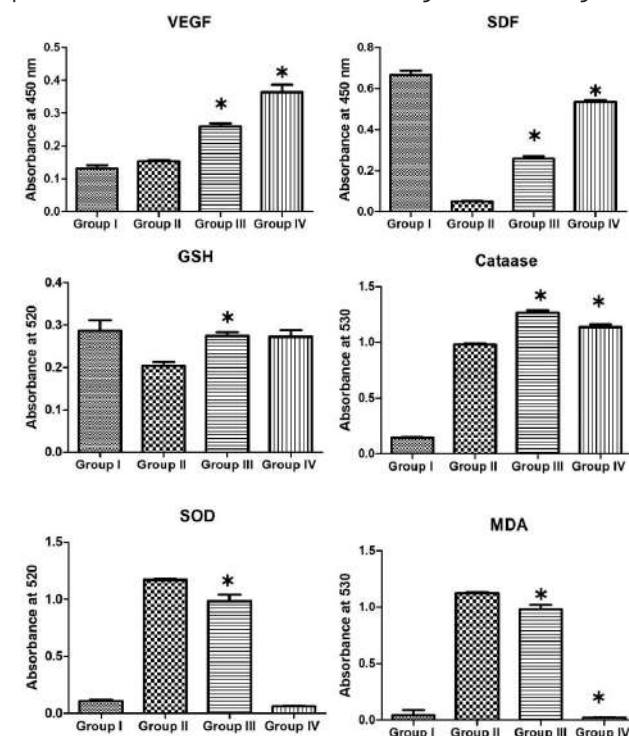


Figure 2: Growth Factors and Oxidative-Stress Markers

All the groups of rats studied using histological methods showed no pathological lesions, necrosis, or hemorrhage of the liver, kidney, or heart. There were normal hepatic cords and the architecture of the central vein in the liver. Kidney sections revealed normal glomeruli, tubular epithelium, and no interstitial inflammation and necrosis. Equally, the heart tissue showed normal myocardial fibers with distinct striation, intact nuclei, and devoid of edema, degeneration, or inflammatory infiltration (Figure 3).

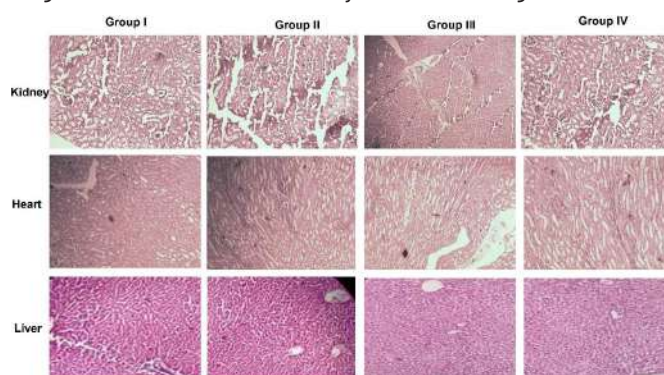


Figure 3: Biological Safety

DISCUSSION

The current research aims at exploiting the wound healing ability of the skin of Tilapia fish as well as the antibacterial properties of silver nanoparticles (AgNPs). Our results show that the combination of Tilapia–AgNPs treatment greatly increased the wound closure, collagen deposition, and tissue regeneration in comparison with the individual treatments, showing a synergistic effect. The Tilapia fish skin will serve as an inherent scaffold of collagen with high antimicrobial and anti-inflammatory properties (AgNPs) that prevent infection and facilitate re-epithelialization, which is structurally comparable to mammalian type I collagen and promotes fibroblast migration, keratinocyte proliferation, and angiogenesis [14, 15]. This two-fold action improves structural repair as well as biological defense at the wound site, developing an ideal microenvironment in which tissue can recover [16, 17]. Simultaneous increase in VEGF and SDF-1 in this experiment indicates the stimulation of angiogenic and progenitor-cell recruitment signaling linking neovascularization [18–20]. This kind of upregulation of the growth factors indicates increased cellular activation of endothelial and vascular remodeling, which is essential to deliver oxygen to regenerating tissue and nourishment. Additionally, the recovery of antioxidant enzyme activities (CAT, SOD, and GSH) and MDA decrease suggests suppression of oxidative stress and cellular redox signaling, which is in line with the established evidence of the ROS-scavenging capabilities of AgNPs and regenerative activity of collagen peptides [21–23]. AgNPs may act by suppressing NF- κ B, inhibiting ROS-mediated inflammation, and mechanically, Tilapia collagen peptides can activate TGF- β and FGF-2 signaling and stimulate fibroblast growth and organization of the extracellular matrix. Such complementary measures have most probably the effect of reducing the inflammatory process and hastening the development to the proliferative one, leading to accelerated granulation and re-epithelialization. More recent findings have also revealed that fish-skin collagen scaffolds that are combined with nanoparticles increase wound healing through the promotion of angiogenesis, matrix remodeling, and collagen fiber orientation [10, 24]. Thus, the synergized effect of Tilapia collagen and AgNPs must have reduced the inflammatory period and accelerated the process of tissue remodeling, which accounts for the better healing results in the combined treatment group. Both components were therapeutically safe as evidenced by histological analysis of liver, kidney, and heart, showing that there was no systemic toxicity or biocompatibility. On the whole, these results confirm that the Tilapia–AgNPs composite dressing can be considered both effective and biocompatible as a potential bioactive method of enhancing the healing of burn wounds faster and has a better clinical outcome.

CONCLUSIONS

Biosynthesized AgNPs impregnated on tilapia fish skin demonstrated a possibility of enhancing the healing process of burn wounds through collagen, angiogenesis, and antioxidant protection. The composite was cost-effective and biocompatible; hence, there was potential for the composite to be a high-quality topical therapeutic material. However, further preclinical and clinical studies are needed to validate its safety and efficacy.

Authors Contribution

Conceptualization: FA

Methodology: NW, SAK, AB, SR, FA

Formal analysis: FA

Writing review and editing: FA

All authors have read and agreed to the published version of the manuscript.

Conflicts of Interest

The authors declare no conflict of interest.

Source of Funding

The authors received no financial support for the research, authorship and/or publication of this article.

REFERENCES

- [1] Haruta A and Mandell SP. Assessment and Management of Acute Burn Injuries. *Physical Medicine and Rehabilitation Clinics*. 2023 Nov; 34(4): 701–16. doi: 10.1016/j.pmr.2023.06.019.
- [2] Fanstone R and Price P. Burn Contracture Risk Factors and Measurement in Low-Middle Income Countries: A Clinical Perspective. *Burns*. 2024 Mar; 50(2): 466–73. doi: 10.1016/j.burns.2023.09.007.
- [3] Ziauddin, Hussain T, Nazir A, Mahmood U, Hameed M, Ramakrishna S et al. Nano-engineered Therapeutic Scaffolds for Burn Wound Management. *Current Pharmaceutical Biotechnology*. 2022 Oct; 23(12): 1417–35. doi: 10.2174/1389201023666220329162910.
- [4] Júnior EM, De Moraes Filho MO, Costa BA, Fachine FV, Vale ML, De Loyola Diógenes AK et al. Nile Tilapia Fish Skin–Based Wound Dressing Improves Pain and Treatment-Related Costs of Superficial Partial-Thickness Burns: A Phase III Randomized Controlled Trial. *Plastic and Reconstructive Surgery*. 2021 May; 147(5): 1189–98. doi: 10.1097/PRS.00000000000007895.
- [5] Wali N, Wajid N, Shabbir A, Ali F, Shamim S, Abbas N et al. Safety Considerations for Lyophilized Human Amniotic Membrane Impregnated with Colistin and Silver Nanoparticles. *Applied Biochemistry and Biotechnology*. 2024 Mar; 196(3): 1419–34. doi: 10.1007/s12010-023-04618-3.

- [6] Francisco P, Neves Amaral M, Neves A, Ferreira-Gonçalves T, Viana AS, Catarino J et al. Pluronic® F127 Hydrogel Containing Silver Nanoparticles in Skin Burn Regeneration: An Experimental Approach from Fundamental to Translational Research. *Gels*. 2023 Mar; 9(3): 200. doi: 10.3390/gels9030200.
- [7] Bruna T, Maldonado-Bravo F, Jara P, Caro N. Silver Nanoparticles and Their Antibacterial Applications. *International Journal of Molecular Sciences*. 2021 Jul; 22(13): 7202. doi: 10.3390/ijms22137202.
- [8] Bold BE, Urnukhsaikhan E, Mishig-Ochir T. Biosynthesis of Silver Nanoparticles with Antibacterial, Antioxidant, Anti-Inflammatory Properties and Their Burn Wound Healing Efficacy. *Frontiers in Chemistry*. 2022 Aug; 10: 972534. doi: 10.3389/fchem.2022.972534.
- [9] Cheng L, Zhang S, Zhang Q, Gao W, Mu S, Wang B. Wound Healing Potential of Silver Nanoparticles from *Hybanthus enneaspermus* on Rats. *Heliyon*. 2024 Sep; 10(17). doi: 10.1016/j.heliyon.2024.e36118.
- [10] Adhikari SP, Paudel A, Sharma A, Thapa B, Khanal N, Shastri N et al. Development of Decellularized Fish Skin Scaffold Decorated with Biosynthesized Silver Nanoparticles for Accelerated Burn Wound Healing. *International Journal of Biomaterials*. 2023; 2023(1): 8541621. doi: 10.1155/2023/8541621.
- [11] American Veterinary Medical Association (AVMA). AVMA Guidelines for the Euthanasia of Animals. Schaumburg(IL): AVMA. 2020.
- [12] Orieshyina A, Puetzer JL, Amdursky N. Proton Transport Across Collagen Fibrils and Scaffolds: The Role of Hydroxyproline. *Biomacromolecules*. 2023 Sep; 24(11): 4653–62. doi: 10.1021/acs.biomac.3c00326.
- [13] Pudlarz AM, Czechowska E, S Karbownik M, Ranozek-Soliwoda K, Tomaszewska E, Celichowski G et al. The Effect of Immobilized Antioxidant Enzymes on the Oxidative Stress in UV-Irradiated Rat Skin. *Nanomedicine*. 2020 Jan; 15(1): 23–39. doi: 10.217/nnm-2019-0166.
- [14] Bustaman AL, Soekmadji PN, Sanjaya A. Nile Tilapia Skin in Burn Wound Healing: A Scoping Review. *Burns*. 2025 Apr; 107503. doi: 10.1016/j.burns.2025.107503.
- [15] Garrity C, Garcia-Rovetta C, Rivas I, Delatorre U, Wong A, Kültz D et al. Tilapia Fish Skin Treatment of Third-Degree Skin Burns in Murine Model. *Journal of Functional Biomaterials*. 2023 Oct; 14(10): 512. doi: 10.3390/jfb14100512.
- [16] Abdelnaby A, Assar DH, Salah A, Atiba A, El-Nokrashy AM, Elshafey AE et al. Extracted Marine Collagen from Nile Tilapia (*Oreochromis niloticus* L.) Skin Accelerates Burn Healing: Histopathological, Immunohistochemical and Gene Expression Analysis. *Egyptian Journal of Veterinary Sciences*. 2025 Jul; 56(8): 1849–65. doi: 10.21608/ejvs.2024.290709.2100.
- [17] Kaya M, Akdaşçi E, Eker F, Bechelany M, Karav S. Recent Advances of Silver Nanoparticles in Wound Healing: Evaluation of in Vivo and in Vitro Studies. *International Journal of Molecular Sciences*. 2025 Oct; 26(20): 9889. doi: 10.3390/ijms26209889.
- [18] Huang X, Liang P, Jiang B, Zhang P, Yu W, Duan M et al. Hyperbaric Oxygen Potentiates Diabetic Wound Healing by Promoting Fibroblast Cell Proliferation And Endothelial Cell Angiogenesis. *Life sciences*. 2020 Oct; 259: 118246. doi: 10.1016/j.lfs.2020.118246.
- [19] Barrera JA, Trotsyuk AA, Maan ZN, Bonham CA, Larson MR, Mittermiller PA et al. Adipose-Derived Stromal Cells Seeded in Pullulan–Collagen Hydrogels Improve Healing in Murine Burns. *Tissue Engineering Part A*. 2021 Jun; 27(11–12): 844–56. doi: 10.1089/ten.tea.2020.0320.
- [20] Tang D, Lin Q, Li PW, Wang S, Xu K, Huang YS et al. FG-4592 Combined with PRP Significantly Accelerates the Healing of Refractory Diabetic Wounds by Upregulating HIF-1 α . *Scientific Reports*. 2025 Apr; 15(1): 14292. doi: 10.1038/s41598-025-99356-3.
- [21] Chen R, Xu H, Li X, Dong J, Wang S, Hao J et al. Role of Oxidative Stress in Post-Burn Wound Healing. *Burns and Trauma*. 2025 Jun; tkaf040. doi: 10.1093/burnst/tkaf040.
- [22] Moreno DA, Saladini MS, Viroel FJ, Dini MM, Pickler TB, Amaral Filho J et al. Are Silver Nanoparticles Useful for Treating Second-Degree Burns? An Experimental Study in Rats. *Advanced Pharmaceutical Bulletin*. 2020 Nov; 11(1): 130. doi: 10.34172/apb.2021.014.
- [23] Matysiak-Kucharek M, Sawicki K, Kapka-Skrzypczak L. Effect of Silver Nanoparticles on Cytotoxicity, Oxidative Stress and Pro-Inflammatory Proteins Profile in Lung Adenocarcinoma A549 Cells. *Annals of Agricultural and Environmental Medicine*. 2023; 30(3): 566–9. doi: 10.26444/aaem/169214.
- [24] You C, Li Q, Wang X, Wu P, Ho JK, Jin R et al. Silver Nanoparticle Loaded Collagen/Chitosan Scaffolds Promote Wound Healing Via Regulating Fibroblast Migration and Macrophage Activation. *Scientific Reports*. 2017 Sep; 7(1): 10489. doi: 10.1038/s41598-017-10481-0.

FUTURISTIC BIOTECHNOLOGY

<https://fbtjournal.com/index.php/fbt>

ISSN (E): 2959-0981, (P): 2959-0973

Volume 4, Issue 3 (July-Sep 2024)



Original Article



Antibacterial Activity of Transition Metal Complexes of 2-(2-Hydroxybenzylidene) Hydrazinecarbothioamide

Hafiz Muhammad Ghuffran Qamar¹, Tehmina Bashir², Usman Ibrahim³, Adnan Mehmood⁴, Waiza Ansar⁵, Noor Muhammad⁵ and Aysun Baghirova Alazova⁶¹Department of Chemistry, Government College University, Lahore, Pakistan²Department of Botany, Government Graduate College, Lahore, Pakistan³Department of Chemistry, University of Agriculture Faisalabad, Faisalabad, Pakistan⁴Department of Microbiology, Gulab Devi Educational Complex, Lahore, Pakistan⁵Department of Zoology, Government College University, Lahore, Pakistan⁶Institute of Botany, Ministry of Science and Education of the Republic of Azerbaijan, Azerbaijan

ARTICLE INFO

Keywords:

Thiosemicarbazone Complex, Metal Coordination, Antibacterial Activity, *Bacillus licheniformis*, Minimum Inhibitory Concentration, Minimum Bactericidal Concentration

How to Cite:

Qamar, H. M. G., Bashir, T., Ibrahim, U., Mehmood, A., Ansar, W., Muhammad, N., & Alazova, A. B. (2024). Antibacterial Activity of Transition Metal Complexes of 2-(2-Hydroxybenzylidene) Hydrazinecarbothioamide: Antibacterial Activity of Transition Metal Complexes of Thiosemicarbazone Derivative. *Futuristic Biotechnology*, 4(03), 62-67. <https://doi.org/10.54393/fbt.v4i03.212>

*Corresponding Author:

Noor Muhammad
Department of Zoology, Government College University, Lahore, Pakistan
noormhd@gcu.edu.pkReceived Date: 22nd July, 2024Acceptance Date: 16th September, 2024Published Date: 30th September, 2024

ABSTRACT

Thiosemicarbazone derivatives in the form of metal complexes have been sought after superior antibacterial effects than free ligands. **Objectives:** To prepare new Cu(II), Co(II), Mn(II), and Cd(II) complexes of 2-(2-hydroxybenzylidene) hydrazinecarbothioamide and assess their antimicrobial characteristics against some pathogenic microorganisms. **Methods:** This was a laboratory-based experimental study, which synthesized and characterized complexes by means of standard analytical and spectroscopic methods. Against *Bacillus licheniformis*, *Escherichia coli*, and *Pseudomonas aeruginosa*, the agar well diffusion method was evaluated at 12.5, 25, and 50 mg/mL. The values of MIC and MBC were calculated by the broth dilution method. The results were provided in the form of mean and SD, and statistical analysis was carried out by one-way ANOVA ($p < 0.05$). **Results:** All the metal complexes showed concentration-dependent antibacterial activity. *B. licheniformis* was the most sensitive strain, in comparison to *E. coli* and *P. aeruginosa*. The Cu(II) and Mn(II) complexes had the strongest inhibitory effect, with the value of MIC and MBC, respectively, between 10 and 20 mg/mL against *B. licheniformis*. Co(II) and Cd(II) complexes were moderately active depending on the strain of bacteria. **Conclusions:** Coordination of 2-(2-hydroxybenzylidene) hydrazinecarbothioamide with transition metals enhances antibacterial activity in a metal- and dose-dependent manner. Cu(II) and Mn(II) complexes displayed the most promising antibacterial properties, supporting the potential of metal-thiosemicarbazone complexes as candidates for developing new antimicrobial agents. Further mechanistic and toxicity studies are warranted.

INTRODUCTION

The history of coordination compounds, also known as coordination complexes, dates back to the era of early chemical phenomena, including the bright pigment Prussian blue, which is now known as $KFe(Fe(CN)_6)$ [1]. In the 19th century, the theoretical knowledge about such complexes changed significantly. Christian Wilhelm Blomstrand proposed the chain-theory model in 1869, and

it is assumed that ammonia molecules bind with polymeric chains consisting of the NH_3 group bound to metal ions (which are called chains) [2]. This principle was later extended by Sophus Mads Jorgensen, who proposed that there are ligands that bind to the metal itself and those that do not get bound at all, but exist in chains outside of the coordination sphere. The main paradigm shift came in 1893

with the coordination theory by Alfred Werner, who introduced the concepts of primary valency (oxidation state), secondary valency (number of connections), and stated that the isomerism of cobalt ammine complexes was determined by specific spatial geometries [3, 4]. In current nomenclature, a coordination complex is composed of a central metal atom or ion and ligands, atoms, ions, or molecules that provide lone-pair electrons to become coordinate covalently bonded to the metal. These species are most often due to the partially filled d-orbitals of transition metals, which have variable oxidation states, have large melting and boiling points, and have colored complexes as a result of d-d transitions. These properties form the basis of their usefulness in catalysis, material science, and bioinorganic chemistry. Chelation multi-detects ligands create ring-structures with a metal ion to form stable complexes and increase their lipophilicity, which is a significant approach in medicinal inorganic chemistry [5, 6]. In the 21st century, coordination chemistry has reached the synthesis of metal-organic frameworks (MOFs) -crystalline assemblies of metal ions, linked by organic ligands, which have ultrahigh porosity, excellent thermal/chemical stability, and have broad applications in gas storage, catalysis, drug delivery, and environmental remediation [7, 8]. It is based on this that the ligands that include donor atoms like oxygen, nitrogen, and sulfur are of specific interest because of their capability to form stable coordination complexes with transition metals and possible bioactivity. Thiosemicarbazone derivatives, including 2-(2-hydroxybenzylidene) hydrazine-carbothioamide, contain the functional groups of -OH, -NH, and -C=S, so that they can chelate the metals and are an antibacterial agent [9, 10]. Past investigations have indicated that these ligands are able to create metal complexes with greater stability, lipophilicity, and biological activity. Thus, we are planning to synthesize, characterize, and analyze the anti-browning activity of 2-(2-hydroxybenzylidene)-hydrazinecarbothioamide complexes in this research. We hypothesize that complexation with these transition metals will enhance the antibacterial efficacy of the ligand as compared to the free ligand because of the increased lipophilicity and the enhanced interaction between the bacterial cell membranes and the ligand.

This study aimed to synthesize novel Cu (II), Co (II), Mn (II), and Cd (II) complexes of 2-(2-hydroxybenzylidene) hydrazinecarbothioamide and evaluate their antibacterial activity against selected pathogenic bacteria.

METHODS

This experimental laboratory-based study was conducted at Government College University Lahore over six months from March 2022 to January 2023. This ligand 2 (2-

hydroxybenzylidene) hydrazinecarbothioamide (C₈H₉O₃S) was obtained by condensing salicylaldehyde with thiosemicarbazide under controlled pH and reflux conditions. The yellow product was filtered, washed, dried, and had a melting point of 216°C, which verified its purity. The complexation of the metal ions was done by reacting 0.97 g of the ligand (0.00497 mol) with a 1:2 solution of the metal salts (CoCl₂, Cu(CH₃COO)₂, CdCl₂, and MnCl₂) in a 1:2 metal-ligand ratio. All reaction mixtures were allowed to heat at 75–80°C under constant stirring until they precipitated. The resulting solid complexes were washed using cold distilled water and dried under a desiccator, and stored. The yields of the purified complexes were as follows: Co (II) complex (72%), Cu (II) complex (85%), Cd (II) complex (68%), and Mn (II) complex (78%). The melting points of the synthesized complexes were 219°C (Co), 218°C (Cu), 220°C (Cd), and 222°C (Mn). The products were characterized by CHNS elemental analysis and FTIR spectroscopy, where the disappearance or shifting of the hydroxyl (-OH) and carbonyl (C=O) stretching bands confirmed coordination of the ligand to the metal through phenolic oxygen. Antibacterial activity of the ligand and its metal complexes was evaluated using the agar well diffusion method against *Escherichia coli*, *Pseudomonas aeruginosa*, and *Bacillus licheniformis*. The ligand was obtained as a yellow precipitate (melting point 216°C) with confirmed purity by CHNS analysis and FTIR; yield was X% (Supplementary Figure S1). Standardized bacterial suspensions (10⁸ CFU/mL) were spread on nutrient agar plates, and wells were loaded with compound solutions at concentrations of 12.5, 25, and 50 mg/mL prepared in ethanol. Rifampicin (50 µg/mL) was used as a positive control and ethanol-water (1:1) as a negative control to validate the agar well diffusion and MIC/MBC assays. Assays were performed according to standard published protocols (CLSI guidelines). Plates were incubated at 37°C for 24 hours, and the zones of inhibition (mm) were measured. For each bacterium and test compound, the assay was performed on three separate agar plates per experiment (technical replicates), and the entire experiment was repeated three times on different days with freshly prepared cultures (biological replicates), yielding a total of nine measurements per data point. All the antibacterial tests (agar well diffusion, MIC, and MBC) were performed using this scheme of replication: three independent experimental runs, and each run contained three replicated plates of the organism-compound combination. Each of the antibacterial assays was conducted in three independent experiments. None had the formal sample size calculation: results reliability and reproducibility were guaranteed by replicating. The inhibition zone diameters and MIC values were the dependent variables used in the

one-way ANOVA. Each of the antibacterial assays was conducted in three independent experiments. None had the formal sample size calculation: results reliability and reproducibility were guaranteed by replicating. The coefficient of variation (CV%) was used to measure the reproducibility of the assay and quantify the intra-assay variation by determining the measurements of the inhibition areas of the technical replicates. A low value of CV% (which was always less than 10) was an indicator that there were good reproducibility and high reliability of the data. The inhibition zone diameters and MIC values were the dependent variables used in the one-way ANOVA. Analysis was pre-tested by checking data normality and homogeneity of variance. Tukey test, where applicable, was used to make post-hoc comparisons. Every single outcome is expressed in the form of the mean standard deviation (SD). Descriptive analysis has been conducted, and an inferential analysis of the data was done using one-way ANOVA to test the statistical significance of the data in SPSS version 27.0, with the level of significance at $p < 0.05$.

RESULTS

The agar well diffusion method was used to determine the antibacterial activity of the synthesized Cu(II), Co(II), Mn(II), and Cd(II) complexes (Four Complexes) of 2-(2-hydroxybenzylidene) hydrazinecarbothioamide against *Bacillus licheniformis*, *Escherichia coli*, and *Pseudomonas aeruginosa* at 12.5, 25, and 50 mg/mL. The positive control (P.C.) was Rifampicin (50 µg/mL), and ethanol-water (1:1) was the negative control (N.C.). Obvious areas of inhibition were observed, which verify the antibacterial nature of the complexes. The most sensitive strain was *B. licheniformis*, with moderate to low sensitivity of *E. coli* and *P. aeruginosa*. The most active complexes were the Mn(II) and Cd(II), especially in the case of *B. licheniformis*, and the weakest activity was of the Cu(II) complex and the Co(II) complex. Antibacterial activity was found to be concentration-dependent, meaning that it was dose-dependent. The zones of inhibition of complexes with *B. licheniformis*. The greatest zones were obtained with Mn(II) and Cu(II) complexes at 50 mg/mL, and Cd(II) and Co(II) complexes were also moderately inhibited (Figure 1).



Figure 1: Agar Well Diffusion Assay Showing Antibacterial Activity of Four Complexes Against *B. licheniformis*

Antibacterial activity against *E. coli*. Mn(II) and Cu(II) complexes were most active at higher concentrations, forming clear inhibition zones, while Co(II) and Cd(II) were moderately active. No inhibition was observed in the negative control. Agar well diffusion assay showing

antibacterial activity of Cu(II), Co(II), Mn(II), and Cd(II) complexes against *E. coli* at 12.5, 25, and 50 mg/mL. P.C., Rifampicin; N.C., and ethanol-water. Mn(II) and Cu(II) complexes exhibit the strongest inhibition (Figure 2).

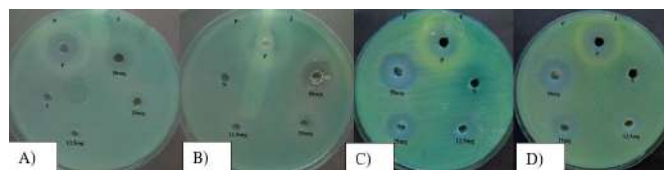


Figure 2: Agar Well Diffusion Assay Showing Antibacterial Activity of Four Complexes Against *E. coli*

Activity against *P. aeruginosa*, where Mn(II) and Cd(II) complexes showed moderate inhibition, Cu(II) exhibited low activity, and Co(II) displayed minimal activity. Agar well diffusion assay showing antibacterial activity of Cu(II), Co(II), Mn(II), and Cd(II) complexes against *P. aeruginosa* at 12.5, 25, and 50 mg/mL. P.C. Rifampicin; N.C. ethanol-water. Mn(II) and Cd(II) complexes show moderate activity (Figure 3).

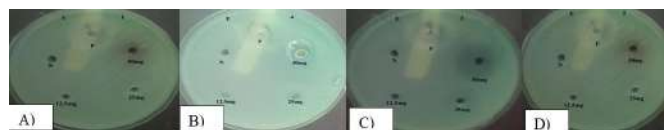


Figure 3: Agar Well Diffusion Assay Showing Antibacterial Activity of Four Complexes Against *P. aeruginosa*

The zones of inhibition (mm) for all complexes and bacterial strains. Mn(II) and Cd(II) complexes produced the largest zones against *B. licheniformis* (up to 10 mm), followed by Cu(II) (8 mm), and Co(II) (6 mm). Against *E. coli* and *P. aeruginosa*, inhibition zones were smaller but increased in size with increasing concentration. The zones of inhibition (mm, mean \pm SD) for all complexes and bacterial strains are detailed in the study. Against *B. licheniformis*, the Mn(II) and Cd(II) complexes produced the largest zones at 50 mg/mL (10.2 ± 0.4 mm and 10.1 ± 0.3 mm, respectively), which were significantly larger than those of the Co(II) complex (6.0 ± 0.5 mm, $p < 0.01$). The Cu(II) complex showed an intermediate zone of 8.1 ± 0.2 mm. The same trend was also noted at lower levels. Inhibition zones with *E. coli* and *P. aeruginosa* showed a smaller and usually dose-dependent increase. ANOVA at the one-way level confirmed that there were significant differences in overall activity of the complexes ($p < 0.05$), and post hoc, the test of Tukey confirmed the better activity of the complexes of Mn(II) and Cd(II) against the most susceptible strain, *B. licheniformis* (Table 1).

Table 1: Zone of Inhibition (mm) of Metal Complexes Against Pathogenic Bacteria Using Agar Well Diffusion Assay

Sr. No.	Complex	Bacterial Strain	50 mg/mL	25 mg/mL	12.5 mg/mL	Positive Control (Rifampicin 50 µg/mL)
1	Cu(C ₈ H ₉ ON ₃ S) ₂	<i>E. coli</i>	6 ± 0	S.G	NO	6
		<i>P. aeruginosa</i>	6 ± 0	S.G	NO	6
		<i>B. licheniformis</i>	8 ± 0	6 ± 0	6 ± 0	8
2	Co(C ₈ H ₉ ON ₃ S) ₂	<i>E. coli</i>	2 ± 0	NO	NO	6
		<i>P. aeruginosa</i>	6 ± 0	3 ± 0	NO	6
		<i>B. licheniformis</i>	8 ± 0	6 ± 0	4 ± 0	9
3	Mn(C ₈ H ₉ ON ₃ S) ₂	<i>E. coli</i>	6 ± 0	4 ± 0	NO	6
		<i>P. aeruginosa</i>	10 ± 0	6 ± 0	2 ± 0	10
		<i>B. licheniformis</i>	10 ± 0	8 ± 0	6 ± 0	10
4	Cd(C ₈ H ₉ ON ₃ S) ₂	<i>E. coli</i>	6 ± 0	NO	NO	6
		<i>P. aeruginosa</i>	6 ± 0	3 ± 0	3 ± 0	6
		<i>B. licheniformis</i>	10 ± 0	8 ± 0	6 ± 0	9

The minimum inhibitory concentration (MIC) and minimum bactericidal concentration (MBC) values of each of the complexes are summarized. The one-way ANOVA was used to make statistical comparisons of the potency of various metal complexes to compare the MIC values of each bacterial strain. It was found that the complexes of *B. licheniformis* (F (3,8) = (Insert F-value], p<0.01) and *P. aeruginosa* (F (3,8) Post-hoc Tukey's test confirmed that against *B. licheniformis*, the complexes of Mn(II) and Cd(II) (MIC = 10 mg/mL) were not only more potent than Co(II) complex (MIC = 20 mg/mL, p<0.05). The complex of Mn(II) (MIC = 15 mg/mL) was found to have lower values than the Co(II) complex (MIC = 30 mg/mL, p<0.05) against *P. aeruginosa*. No significant differences were found among the complexes for *E. coli* (p>0.05), which aligns with the overall lower susceptibility of this strain. These results provide statistical rigor to the conclusion that activity is metal-dependent and underscore the superior efficacy of the Mn(II) and Cd(II) complexes, particularly against *B. licheniformis* (Table 2).

Table 2: MIC and MBC of Metal Complexes Against Pathogenic Bacteria

Sr. No.	Compound	Bacterial Strain	MIC (mg/mL)	MBC (mg/mL)
1	Cu(C ₈ H ₉ ON ₃ S) ₂	<i>E. coli</i>	Not Observed	Not Observed
		<i>P. aeruginosa</i>	15	25
		<i>B. licheniformis</i>	Not Observed	Not Observed
2	Co(C ₈ H ₉ ON ₃ S) ₂	<i>E. coli</i>	60	Not Observed
		<i>P. aeruginosa</i>	20	30
		<i>B. licheniformis</i>	30	45
3	Mn(C ₈ H ₉ ON ₃ S) ₂	<i>E. coli</i>	50	60
		<i>P. aeruginosa</i>	10	20
		<i>B. licheniformis</i>	15	25
4	Cd(C ₈ H ₉ ON ₃ S) ₂	<i>E. coli</i>	45	60
		<i>P. aeruginosa</i>	10	20

	<i>B. licheniformis</i>	15	30
--	-------------------------	----	----

Not Observed(no inhibition)

DISCUSSION

The present study demonstrated that the ligand 2-(2-hydroxybenzylidene) hydrazinecarbothioamide has a better antibacterial activity than the free ligand after coordinating with its transition metals (Cu(II), Co(II), Mn(II), and Cd(II)) [11, 12]. Diffusion assays on agar wells and determinations of MIC and MBC demonstrated a concentration-dependent growth in the inhibition zone and bacteriostatic and bactericidal activity [13, 14]. The most susceptible bacterium, *Bacillus licheniformis* (Gram-positive), had the lowest MICs (10 mg/ml) and the lowest MBCs (20 mg/ml) of the tested bacteria. Comparatively, *Escherichia coli* and *Pseudomonas aeruginosa* (Gram-negative) were less susceptible, showing higher MICs and the absence of observable inhibition in some instances [15, 16]. These results can be compared with earlier studies on thiosemicarbazone and other hydrazones, which show the increase of the antibacterial activity when the metal is complexed [17, 18]. The observed variability in antibacterial efficacy, which is strongly metal-dependent, is classically explained by the chelation theory and its impact on cell permeability (Tweedy's hypothesis, Overton's rule). The loss of metal ion polarity upon chelation enhances electron delocalization and increases lipophilicity, thereby facilitating penetration of bacterial membranes. Our statistical findings provide robust support for this theory. The significantly larger inhibition zones and lower MIC values of the Mn(II) and Cd(II) complexes (p<0.05 compared to Co(II)), particularly against the Gram-positive *B. licheniformis*, are consistent with enhanced lipophilicity leading to superior membrane penetration in the absence of a complex outer membrane. Furthermore, the significant differences in potency revealed by the ANOVA of MIC values (p<0.05 for *B. licheniformis* and *P. aeruginosa*) underscore that metal choice is a critical determinant of activity. These variations can be attributed to metal-specific effects, including coordination geometry, redox potential, and ligand field stabilization energy, which influence membrane interaction, reactive oxygen species generation, and intracellular target binding [19, 20]. The MIC/MBC values observed in this experiment are quantitatively similar to those observed in other thiosemicarbazone metal complexes: Mn and Cd complexes (MIC 10 mg/mL against *B. licheniformis*), whereas the Cu(II) and Co(II) complexes had higher MICs, as is seen by literature trends of selective or moderate activity [21]. Although Cd(II) complexes were shown to have very strong antibacterial in vitro effects, the cytotoxicity and environmental risks of cadmium inhibit its use in biomedicine. Copper and manganese complexes display

more desirable toxicological profiles, but full cytotoxicity and cellular compatibility in mammalian cells have to be conducted and assessed before usage in translational studies.

CONCLUSIONS

Coordination of 2-(2-hydroxybenzylidene) hydrazinecarbothioamide with transition metals enhances antibacterial activity in a metal- and dose-dependent manner. Mn (II) and Cd (II) complexes were most potent against *Bacillus licheniformis* (MIC 10 mg/mL; MBC 20 mg/mL), while Cu (II) was selective and Co (II) moderately active. These results highlight that metal choice strongly influences efficacy, supporting chelation-based enhancement of lipophilicity and membrane penetration. Toxicity concerns, especially with Cd (II), indicate that further mechanistic and safety studies are needed before biomedical applications.

Authors Contribution

Conceptualization: NM

Methodology: HMGQ, TB, NM

Formal analysis: HMGQ

Writing review and editing: HMGQ, TB, UI, AM, WA, NM, ABA

All authors have read and agreed to the published version of the manuscript.

Conflicts of Interest

The authors declare no conflict of interest.

Source of Funding

The authors received no financial support for the research, authorship and/or publication of this article.

REFERENCES

- [1] Aziz KN, Ahmed KM, Omer RA, Qader AF, Abdulkareem EI. A Review of Coordination Compounds: Structure, Stability, and Biological Significance. *Reviews in Inorganic Chemistry*. 2025 Mar; 45(1): 1-9. doi: 10.1515/revic-2024-0035.
- [2] Constable EC. What's In a Name? A Short History of Coordination Chemistry from Then to Now. *Chemistry*. 2019 Aug; 1(1): 126-63. doi: 10.3390/chemistry1010010.
- [3] Verma DK, Aslam J, editors. *Organometallic Compounds: Synthesis, Reactions, and Applications*. John Wiley and Sons. 2023 Feb. doi: 10.1002/9783527840946.
- [4] Ornelas C and Astruc D. *Organometallic Science: From Fundamental Chemistry to a Cornerstone of Modern Innovations and Technological Advances*. Organometallic Science. 2025 Apr: 1-.
- [5] León IE. Transition Metal Complexes: A New Generation of Anticancer Drugs. *Future Medicinal Chemistry*. 2024 Sep; 16(17): 1727-30. doi: 10.1080/17568919.2024.2383166.
- [6] Mosher M, Kelter P. Coordination Complexes. In *An Introduction to Chemistry*. Cham: Springer International Publishing. 2023 Mar: 903-937. doi: 10.1007/978-3-030-90267-4_19.
- [7] Ramesh M, Kuppuswamy N, Praveen S. Metal-Organic Framework for Batteries and Supercapacitors. In *Metal-Organic Frameworks for Chemical Reactions*. 2021 Jan: 19-35. doi: 10.1016/B978-0-12-822099-3.00002-2.
- [8] Sales MB, Neto JG, De Sousa Braz AK, De Sousa Junior PG, Melo RL, Valério RB et al. Trends and Opportunities in Enzyme Biosensors Coupled to Metal-Organic Frameworks (MOFs): An Advanced Bibliometric Analysis. *Electrochemical*. 2023 Apr; 4(2): 181-211. doi: 10.3390/electrochem4020014.
- [9] Gupta S, Singh N, Khan T, Joshi S. Thiosemicarbazone Derivatives of Transition Metals as Multi-Target Drugs: A Review. *Results in Chemistry*. 2022 Jan; 4: 100459. doi: 10.1016/j.rechem.2022.100459.
- [10] Garbuz O, Ceban E, Istrati D, Railean N, Toderas I, Gulea A. Thiosemicarbazone-Based Compounds: Cancer Cell Inhibitors with Antioxidant Properties. *Molecules*. 2025 May; 30(9): 2077. doi: 10.3390/molecules30092077.
- [11] Gulea AP, Usataia IS, Graur VO, Chumakov YM, Petrenko PA, Balan GG et al. Synthesis, Structure and Biological Activity of Coordination Compounds of Copper, Nickel, Cobalt, and Iron with Ethyl N'-(2-hydroxybenzylidene)-N-prop-2-en-1-ylcarbamohydrazonothioate. *Russian Journal of General Chemistry*. 2020 Apr; 90(4): 630-9. doi: 10.1134/S107036322004012X.
- [12] Alshater H, Al-Sulami AI, Aly SA, Abdalla EM, Sakr MA, Hassan SS. Antitumor and Antibacterial Activity of Ni (II), Cu (II), Ag (I), and Hg (II) complexes with Ligand Derived from Thiosemicarbazones: Characterization and Theoretical Studies. *Molecules*. 2023 Mar; 28(6): 2590. doi: 10.3390/molecules28062590.
- [13] Chikezie IO. Determination of Minimum Inhibitory Concentration (MIC) and Minimum Bactericidal Concentration (MBC) Using A Novel Dilution Tube Method. *African Journal of Microbiology Research*. 2017 Jun; 11(23): 977-80. doi: 10.5897/AJMR2017.8545.
- [14] Parvekar P, Palaskar J, Metgud S, Maria R, Dutta S. The Minimum Inhibitory Concentration (MIC) and Minimum Bactericidal Concentration (MBC) of Silver Nanoparticles Against *Staphylococcus Aureus*. *Biomaterial Investigations in Dentistry*. 2020 Jan 1; 7(1): 105-9. doi: 10.1080/26415275.2020.1796674.

- [15] Nussbaumer-Pröll A, Eberl S, Kurdina E, Schmidt L, Zeitlinger M. Challenging T> MIC Using Meropenem vs. *Escherichia coli* and *Pseudomonas aeruginosa*. *Frontiers in Pharmacology*. 2022 Apr; 13: 840692. doi: 10.3389/fphar.2022.840692.
- [16] Falagas ME, Tansarli GS, Rafailidis PI, Kapaskelis A, Vardakas KZ. Impact of Antibiotic MIC on Infection Outcome in Patients with Susceptible Gram-Negative Bacteria: A Systematic Review and Meta-Analysis. *Antimicrobial Agents and Chemotherapy*. 2012 Aug; 56(8): 4214-22. doi: 10.1128/AAC.00663-12.
- [17] Alam M, Abser MN, Kumer A, Bhuiyan MM, Akter P, Hossain ME, Chakma U. Synthesis, Characterization, Antibacterial Activity of Thiosemicarbazones Derivatives and Their Computational Approaches: Quantum Calculation, Molecular Docking, Molecular Dynamics, ADMET, QSAR. *Heliyon*. 2023 Jun; 9(6). doi: 10.1016/j.heliyon.2023.e16222.
- [18] Korkmaz G. A Review of Recent Research on the Antimicrobial Activities of Thiosemicarbazone-Based Compounds. *Journal of New Results in Science*. 2024; 13(1): 61-83. doi: 10.54187/jnrs.1464723.
- [19] Sumrra SH, Habiba U, Zafar W, Imran M, Chohan ZH. A Review on the Efficacy and Medicinal Applications of Metal-Based Triazole Derivatives. *Journal of Coordination Chemistry*. 2020 Oct; 73(20-22): 2838-77. doi: 10.1080/00958972.2020.1839751.
- [20] Sharma B, Shukla S, Rattan R, Fatima M, Goel M, Bhat M et al. Antimicrobial Agents Based on Metal Complexes: Present Situation and Future Prospects. *International Journal of Biomaterials*. 2022; 2022(1): 6819080. doi: 10.1155/2022/6819080.
- [21] Singh K, Kumari B, Sharma A. Copper (II), Nickel (II), Zinc(II) and Cadmium(II) Complexes of 1, 2, 4-Triazole Based Schiff Base Ligand: Synthesis, Comparative Spectroscopic, Thermal, Biological and Molecular Docking Studies. *Spectroscopy Letters*. 2021 Nov; 54(10): 742-62. doi: 10.1080/00387010.2021.1996395.